

OPTICAL BRIGHTNESS VARIATIONS IN A SAMPLE OF
NINETEEN RADIO-QUIET QUASI-STELLAR OBJECTS

BY

PATRICIA LOUISE EDWARDS

A DISSERTATION PRESENTED TO THE GRADUATE COUNCIL
OF THE UNIVERSITY OF FLORIDA IN
PARTIAL FULFILLMENT OF THE REQUIREMENTS
FOR THE DEGREE OF DOCTOR OF PHILOSOPHY

UNIVERSITY OF FLORIDA

1981

ACKNOWLEDGMENTS

The author is grateful to her advisor, Dr. Alex G. Smith, without whom the quasar monitoring program would not have existed, and to the other members of her graduate committee: Drs. Thomas D. Carr, H. L. Cohen, Guy C. Omer, Jr., Billy S. Thomas and Robert E. Wilson. Robert Leacock, Richard and Karen Hackney, Roger Scott, Ben McGimsey, Joe Pollock, and Andy Pica have contributed to the observations of quasars or related objects which provide a basis for comparisons. The quasar monitoring program has been supported by grants from the National Science Foundation. The current grant number is AST8000246.

The author benefited greatly from improvement in photographic procedures resulting from research by A. G. Smith, R. L. Scott, and Hans Schrader, and from the development of a microcomputer data reduction system by Joe Pollock and Larry Twigg. Drs. S. T. Gottesmann, H. L. Cohen, and H. K. Eichhorn provided most helpful discussions of least squares curve fitting. The use of a computer program written by Dr. H. L. Cohen is greatly appreciated.

During her enrollment at the University of Florida, the author has received support from the Graduate School, the Department of Physics and Astronomy, and the National Science Foundation. The financial and moral support of her parents, Dr. Leslie Edwards and Dr. Carolyn Edwards, and her sister, Dr. Lucy Edwards, is greatly appreciated. The author also wishes to thank Mrs. Jeanne Kerrick for her advice and encouragement and Mrs. Edna Larrick for typing this manuscript.

TABLE OF CONTENTS

	Page
ACKNOWLEDGMENTS	ii
LIST OF TABLES	v
LIST OF FIGURES	vii
KEY TO SYMBOLS AND ABBREVIATIONS	x
ABSTRACTxiii
CHAPTER	
1 INTRODUCTION	1
Quasars	1
RQSOs	2
Characteristics	4
Questions	5
Samples Chosen for the Present Study	6
2 DATA ACQUISITION	11
Florida Monitoring Program	11
Photographic Techniques	12
3 DATA REDUCTION AND ANALYSIS	13
Comparison	13
Iris Photometry	14
Programs	14
Errors	15
Curve Fitting	17
4 FIELD AT $1^h +6^o$	32
SA 94	32
PHL 938	35
PHL 3375	40
PHL 1027	45
PHL 3632	45
PHL 1186	54
PHL 1194	59
PHL 1222	64
PHL 1226	64
Summary	73

TABLE OF CONTENTS (continued)

CHAPTER		Page
5	FIELD AT $13^h +36^o$	75
	M 3	75
	ESO 1	75
	B 46	83
	ESO 2	88
	B 114	93
	B 154	98
	B 194	98
	B 201	107
	ESO 6	112
	B 234	117
	B 312	122
	ESO 11	122
	Summary	131
6	CONCLUSIONS	134
	Florida RQSO Results	134
	Other Studies of RQSOs	145
	Comparison with QSRs Variability	148
	Comparison with Quasar Models	151
	Summary	153
	BIBLIOGRAPHY	155
	BIOGRAPHICAL SKETCH	158

LIST OF TABLES

Table		Page
1	Sample of Radio-Quiet Quasi-Stellar Objects	8
2	Functional Forms Tested for Curve Fitting Procedure . .	27
3	Standard Stars in SA 94	33
4	Comparison Stars for PHL 938	36
5	B Magnitudes of PHL 938	38
6	Comparison Stars for PHL 3375	41
7	B Magnitudes of PHL 3375	43
8	Comparison Stars for PHL 1027	46
9	B Magnitudes of PHL 1027	48
10	Comparison Stars for PHL 3632	50
11	B Magnitudes of PHL 3632	52
12	Comparison Stars for PHL 1186	55
13	B Magnitudes of PHL 1186	57
14	Comparison Stars for PHL 1194	60
15	B Magnitudes of PHL 1194	62
16	Comparison Stars for PHL 1222	65
17	B Magnitudes of PHL 1222	67
18	Comparison Stars for PHL 1226	69
19	B Magnitudes of PHL 1226	71
20	Standard Stars in M 3	76
21	Comparison Stars for BSO 1	79
22	B Magnitudes of BSO 1	81
23	Comparison Stars for B 46	84

LIST OF TABLES (continued)

Table		Page
24	B Magnitudes of B 46	86
25	Comparison Stars for BSO 2	89
26	B Magnitudes for BSO 2	91
27	Comparison Stars for B 114	94
28	B Magnitudes of B 114	96
29	Comparison Stars for B 154	99
30	B Magnitudes of B 154	101
31	Comparison Stars for B 194	103
32	B Magnitudes of B 194	105
33	Comparison Stars for B 201	108
34	B Magnitudes of B 201	110
35	Comparison Stars for BSO 6	113
36	B Magnitudes of BSO 6	115
37	Comparison Stars for B 234	118
38	B Magnitudes of B 234	120
39	Comparison Stars for B 312	123
40	B Magnitudes of B 312	125
41	Comparison Stars for BSO 11	127
42	B Magnitudes of BSO 11	129
43	Variability of the Sample of Radio-Quiet Quasi-Stellar Objects	132
44	Linear Correlation Coefficients	137

LIST OF FIGURES

Figure		Page
1	Color-Color Diagram for PHL, BSO, B Objects	10
2	Average Rms of the Comparison Stars versus Magnitude.	18
3	Second Order Polynomial Fit in Magnitude	21
4	Second Order Polynomial Fit in Iris Reading	22
5	Third Order Polynomial Fit in Iris Reading	23
6	Fourth Order Polynomial Fit in Iris Reading	24
7	Fifth Order Polynomial Fit in Iris Reading	25
8	Line Plus Hyperbola	26
9	K and σ Values for Curves	29
10	SA 94 Field	34
11	PHL 938 Field	37
12	Variation with Time of PHL 938	39
13	PHL 3375 Field	42
14	Variation with Time of PHL 3375	44
15	PHL 1027 Field	47
16	Variation with Time of PHL 1027	49
17	PHL 3632 Field	51
18	Variation with Time of PHL 3632	53
19	PHL 1186 Field	56
20	Variation with Time of PHL 1186	58
21	PHL 1194 Field	61
22	Variation with Time of PHL 1194	63
23	PHL 1222 Field	66

LIST OF FIGURES (continued)

Figure		Page
24	Variation with Time of PHL 1222	68
25	PHL 1226 Field	70
26	Variation with Time of PHL 1226	72
27	M 3 Field	78
28	BSO 1 Field	80
29	Variation with Time of BSO 1	82
30	B 46 Field	85
31	Variation with Time of B 46	87
32	BSO 2 Field	90
33	Variation with Time of BSO 2	92
34	B 114 Field	95
35	Variation with Time of B 114	97
36	B 154 Field100
37	Variation with Time of B 154102
38	B 194 Field104
39	Variation with Time of B 194106
40	B 201 Field109
41	Variation with Time of B 201111
42	BSO 6 Field114
43	Variation with Time of BSO 6116
44	B 234 Field119
45	Variation with Time of B 234121

LIST OF FIGURES (continued)

Figure		Page
46	B 312 Field	124
47	Variation with Time of B 312	126
48	BSO 11 Field	128
49	Variation with Time of BSO 11	130
50	Variability Index versus U - B	139
51	Variability Index versus B - V	140
52	Variability Index versus U - V	141
53	Variability Index versus I _{ex}	142
54	Variability Index versus v - i	143
55	Variability Index versus Redshift for the RQOSO Sample .	144
56	Variability Index versus Relative Intrinsic Brightness .	146
57	Variability Index versus Redshift for QSRs and RQOSOs .	150

KEY TO SYMBOLS AND ABBREVIATIONS

AB #	Objects in the list of Bracessi <u>et al.</u> (1970, 1973)
B	Magnitude in the blue wavelength range
B #	Object in the list of Bracessi <u>et al.</u> (1968)
BSO #	Object in the list of Sandage and Veron (1965)
B - V	Color difference, blue magnitude minus visual
C.L.	Confidence level of variability - $P(\chi^2)$
cm	centimeter
DEC	Declination, angular position in the sky measured north or south of the celestial equator
df	Degrees of freedom in the χ^2 test
fu	Flux unit = jan = Watt/m ² /cycle per second
f/4	Focal ratio of the Newtonian focus of the 76cm telescope at the Rosemary Hill Observatory of the University of Florida
GHZ	Gigahertz = 10 ⁹ cycles per second
Hz	Hertz = cycle per second
Iex	Infrared excess as used by Braccesi <u>et al.</u> (1968)
IRIS	Iris reading on the Cuffey iris astrophotometer
K	$\frac{\sum_{i=1}^n \sigma_i^2}{(n - N)}$
Ly _α	Lyman alpha, spectral line resulting from loss of electron from the first shell of the hydrogen atom
m	Meter

KEY TO SYMBOLS AND ABBREVIATIONS (continued)

M 3	Third object in the Messier list, a globular cluster at $13^{\text{h}}40^{\text{m}}+28.6^{\circ}$
Mag.	Magnitude
mfu	Milliflux unit = 10^{-3} fu
MHz	Megahertz = 10^6 cycles per second
mm	Millimeter = $10^{-3}\text{m} = 10^{-1}\text{cm}$
MWP-2	Developer (Difley, 1968)
n	Number of standard stars
N	Number of unknowns in least squares curve fitting procedure
OVV	Optically Violent Variable, a subset of QSOs which show variations in brightness greater than one magnitude on a time scale of days
PET	Microcomputer manufactured by Commodore
PHL #	Object in the catalog of faint blue objects with small proper motion
Quasar	Acronym for "Quasi-Stellar Radio Source" now used for quasi-stellar objects with or without radio emission
QSRS	Quasi-Stellar Radio Source
QSO	Quasi-Stellar Object, an object whose optical image is "star-like" and whose redshift is extragalactic
R.I.B.	Relative Intrinsic Brightness = $B - 5 \log z$
RA	Right Ascension, angular position measured in hours, minutes and seconds of time, measured eastward from the Vernal Equinox
rms	Root mean square, average deviation of the comparison stars from the curve
RQQSO	Radio-Quiet Quasi-Stellar Objects
SA 94	Mt. Wilson Selected Area number 94, at $2^{\text{h}}53.3^{\text{m}}+0^{\circ}20'$

KEY TO SYMBOLS AND ABBREVIATIONS (continued)

U	Magnitude in the ultraviolet wavelength range
U - B	Color difference, ultraviolet magnitude minus blue magnitude
U - V	Color difference, ultraviolet magnitude minus visual magnitude
V	Magnitude in the visual wavelength range
V.I.	Variability index = χ^2/df normalized to 30 df
z	Redshift = $\Delta\lambda/\lambda_0$
3C	Third Cambridge catalog of radio sources
λ	Wavelength
$\Delta\lambda$	Difference in wavelength
λ_0	Wavelength measured in rest frame
σ	Average deviation of the standard stars from the curve
χ^2	Chi Square

Abstract of Dissertation Presented to the Graduate Council
of the University of Florida in Partial Fulfillment of the
Requirements for the Degree of Doctor of Philosophy

OPTICAL BRIGHTNESS VARIATIONS IN A SAMPLE OF
NINETEEN RADIO-QUIET QUASI-STELLAR OBJECTS

By

Patricia Louise Edwards

March 1981

Chairman: Dr. Alex G. Smith
Major Department: Astronomy

A photographic program, monitoring changes in the optical brightnesses of nineteen radio-quiet quasi-stellar objects (RQQSOs), was carried out at the Rosemary Hill Observatory of the University of Florida. This study was done in conjunction with continuing variability studies of quasi-stellar radio sources (QSRs) and related objects. The RQQSO observations cover the years 1974-1978.

The RQQSOs in this sample are located in two 6° fields, one centered at $1^{\text{h}} 36^{\text{m}} +6^{\circ}$ and the other at $13^{\text{h}} +36^{\circ}$. They had optical spectra and U - B and B - V colors similar to those of the QSRs, but had no radio flux above the detection limits of the early radio surveys. One object, B 194, has subsequently been detected in the radio. Another, B 234, was suggested as a possible detection.

Monitoring of the optical brightnesses was done to study the characteristics of the variability of the RQQSOs for comparison with the much larger sample of the QSRs. A variability index (V.I.) was computed to facilitate numerical comparisons and to check for correlation between the extent of variability and other properties of the quasi-stellar objects (QSOs).

Observations of each QSO and a sequence of nearby comparison stars were taken on hypersensitized Kodak 103-a-0 photographic plates in sealed cassettes with B filters at the f/4 Newtonian focus of the 76-cm Tinsley reflector of the Rosemary Hill Observatory.

Of the nineteen RQOSOs studied, eight did not show evidence of variability at a confidence level of at least 95 percent. Eight objects (PHL 3632, PHL 1186, PHL 1226, BSO 1, B 154, B 234, B 312, and BSO 11) were variable at a confidence level greater than 95 percent. An additional three objects showed variability at a confidence level greater than 99.9 percent. These strongly varying objects were PHL 1194, B 46, and B 114. The proportion of RQOSOs which show variability is similar to that of the QSRSS.

Sharp drops in magnitude seemed to be more common in RQOSOs than were sudden brightenings. Such drops occur less frequently in QSRSS.

No correlation between variability indices and $U - B$, $B - V$, $U - V$ or Iex colors was found. A slight correlation between variability and the $v - i$ given by Braccesi et al. (1970) for the B, BSO sample may suggest that variability is enhanced for objects which are brighter in the infrared.

There is a correlation between V.I. and magnitude and between V.I. and redshift, in the sense that fainter and closer objects are more variable. These two properties are coupled through a selection effect due to the cut-off in apparent B magnitude, since the fainter RQOSOs can only be seen at low redshift. Thus, it is difficult to determine whether the increased variability is due to greater age or lower luminosity.

CHAPTER 1

INTRODUCTION

Quasars

In the 1950's, as radio telescopes became more sensitive, several radio surveys were made of large areas of the sky. Positions of radio sources were published in various lists, denoted as MSN, 3C, PKS, NRAO, AO, Bl, CTA or CTD. Since radio telescopes operate at much longer wavelengths than optical telescopes, their spatial resolution is much less precise. Therefore, the radio position actually gives an area on the sky, usually referred to as the "radio error box," in which the source is located. Identifying the optical object corresponding to the radio source can be quite difficult, since there may be many objects within the radio error box. Many of the radio sources showed extended distributions and corresponded to nebulae in our galaxy or to external galaxies. However, some of the radio sources were "star-like," unresolved at radio wavelengths. These sources were called "quasi-stellar radio sources," which was often shortened to "quasars."

In order to identify the optical image of the radio sources, much more precise radio positions were needed. For some sources near the ecliptic, this was accomplished by timing lunar occultations, which gives very precise positions. In other cases, two radio telescopes were used together as a radio interferometer. At some of the improved

positions the only optical object was a faint star-like object. One of these radio sources, 3C48, was shown by Matthews and Sandage (1963) to correspond to a 16th-magnitude object with a stellar appearance. Spectra of this object showed that it did not have the spectrum of a normal galactic star. At some wavelengths, there were broad emission lines whose presence could not immediately be explained. A precise position for 3C273 was obtained by Hazard *et al.* (1963) by means of lunar occultation. At this position was a 13th-magnitude star-like object, showing similar broad emission lines, some of which Schmidt (1963) identified as the Balmer lines of hydrogen and a line due to ionized magnesium, all redshifted by the factor $z = \Delta\lambda/\lambda_0 = 0.158$. It was then shown by Greenstein and Matthews (1963) that these same lines appeared in 3C48 at a redshift of $z = 0.367$. Following this, many more star-like objects were identified with radio sources. However, many sources remained for which the radio error boxes were still quite large.

RQSOs

By studying the photometric properties of the quasars, Sandage and Veron (1965) hoped to learn to make better guesses at the optical identifications, which would still have to be confirmed by obtaining spectra. They realized that the quasars were bluer than most stars, and in particular that they occupied an area of the U - B, B - V color-color diagram near the black body line, and separated from the main-sequence stars (Fig. 1). Sandage and Veron (1965) used a double-exposure, two-filter photographic method, producing ultraviolet and blue images

separated by a small displacement. Any object with a brighter-than-normal ultraviolet image would be noticeable and would be a good candidate for spectral confirmation as the quasar. When they applied this technique to several fields in which the quasar had not yet been identified optically, they were surprised to find extra objects, "interlopers," with ultraviolet excesses but not near the radio position. Realizing that these objects were probably related to the faint blue objects at high galactic latitudes found in earlier surveys by Iriarte and Chavira (1957), Haro and Luyten (1962), Humason and Zwicky (1947), and Feige (1958), Sandage (1965) studied the space density of these objects with respect to their apparent magnitudes. These results led him to suggest that while the brighter of these blue objects were galactic stars, most of the fainter ones were extragalactic and could be expected to show large redshifts. When spectra were taken of several of these objects, three showed extragalactic redshifts (Sandage, 1965). The spectrum of BSO 1 was indistinguishable from those of the quasi-stellar radio sources (QSRs) and had a redshift of $z = 1.241$. These extragalactic objects not associated with radio sources are usually referred to as radio-quiet quasi-stellar objects or RQSOs.

In order to obtain a larger sample with which to study the space density of these objects, Sandage and Luyten (1967) carried out photometric studies on some of the blue objects found earlier in the Palomar field at $1^{\text{h}}36^{\text{m}} +6^{\circ}$ by Haro and Luyten (1962) using a U, V offset

method. These objects are referred to by their PHL numbers. Spectra by Sandage and Luyten (1967), and by Burbidge (1968) confirmed many of these as QSOs. Others proved to be galactic subdwarf stars. Braccesi (1967) suggested that QSOs should also be brighter than the subdwarfs in the infrared and that this could be used to weed the subdwarfs out of the sample. The U, B offset plates taken of the field at $13^{\text{h}}+36^{\circ}$ by Sandage and Veron (1965) were used to locate the objects which had ultraviolet excess. This plate was then compared by Braccesi, Lynds and Sandage (1968) with an infrared plate of the same field. Of those objects with a strong ultraviolet image, those which also showed strong infrared images were predominately QSOs, as confirmed by their spectra. These objects were listed as BSO or B objects. The more complete list, covering the same area, by Braccesi, Formigini and Gandolfi (1970) has later been referred to by AB numbers. These surveys suggest that the RQQSOs are much more numerous than the QSRs. Since "radio quiet" simply means not yet detected in the radio, some of these RQQSOs may be detected at radio frequencies as the sensitivity of radio telescopes is increased.

Characteristics

As more and more QSOs were identified and studied, it became easier to describe them as a class. They are star-like objects often coincident with a radio source. The spectra show broad emission lines redshifted by large amounts. Absorption lines may also be present. These two properties are enough to identify a candidate as a QSO, but

there appear to be other common attributes. QSRs are strong sources in the ultraviolet (Sandage, 1965) and in the infrared (Braccisi et al., 1968). These characteristics were useful in choosing candidates for spectra to confirm their extragalactic nature.

A fourth property possessed by many of the quasars is a variability in optical and/or radio output. This possibility was recognized when the magnitude of 3C48 was found to be different on a subsequent observation (Matthews and Sandage, 1963).

Questions

There are two different directions in which QSO studies have been aimed, based on the second and fourth properties. Because of the large redshifts, QSOs were suspected to be the most distant objects observable at the time. Therefore, they might be used to extend our baseline for the investigation of cosmology--for example, determination of the Hubble constant and the age of the universe (Sandage, 1972).

In cosmological studies the variability of QSOs proved to be a nuisance because of the resulting uncertainty in absolute magnitude and energy output. In other researches variability provided valuable information because the radius of the active region is limited to the distance that light can travel during the time scale of the variation. Results of variability investigations imply that these sources are quite small by galactic standards, which makes their tremendous energy output even harder to explain. In addition, their relative energy output across a wide spectrum, and relative changes in this energy

distribution, should contain information on the energy generation and transformation mechanisms in the immediate vicinity. In particular, two classes which have very different spectral energy distribution might show different types or degrees of variability. Quasars typically have their energy peak in the short radio range while RQSOs have no detectable emission in this range. If the source of the QSRs' variability were in the radio range, with much of the energy then being transferred to optical wavelengths through various physical processes, it might be expected that RQSOs having little or no radio output would be less likely to vary.

Samples Chosen for the Present Study

In order to study the optical behavior of RQSOs, one or more consistent samples with well-defined optical properties were needed. A spectrum showing the object to be a quasar was the second requirement. The existence of readily available photographic finding charts was another major consideration. Two groups of objects, conveniently 12 hours apart and accessible during different times of the year, fit these criteria. Eight objects in the PHL field $1^{\text{h}} +6^{\circ}$ studied by Sandage and Luyten (1967) had spectra and finders given by Kinman (1966), Burbidge (1968), and Burbidge et al. (1968). Redshifts were available for 11 of the objects in the $13^{\text{h}} +36^{\circ}$ field whose finders were published by Braccisi et al. (1968).

In the first of these fields the selection was based on ultraviolet excesses only. In the second field infrared excess was also

considered in choosing which spectra should be taken. There was probably also a preference toward the brighter objects. The limiting magnitude is approximately 1 mag. fainter for the objects in the second field. Positions and colors are given in Table 1 for the RQSO sample, which includes objects from both fields. These objects occupy a region in the U-B, B-V color-color diagram shown in Fig. 1.

TABLE 1

Sample of Radio-Quiet Quasi-Stellar Objects

Object	Alternate Designations	RA (1950)	DEC (1950)
PHL 938		0 ^h 58 ^m 12 ^s .0	1 ^o 56' 00"
PHL 3375		1 28 24.0	7 28 00
PHL 1027		1 30 30.0	3 22 00
PHL 3632		1 39 54.0	6 10 00
PHL 1186		1 47 36.0	9 01 00
PHL 1194		1 48 42.0	9 02 00
PHL 1222		1 51 12.0	4 48 00
PHL 1226		1 51 48.0	4 34 00
BSO 1	AB 9	12 46 28.7	37 46 50
B 46	AB 11	12 46 29.6	34 40 49
BSO 2	AB 17, B 87	12 48 17.7	33 47 11
B 114	AB 47	12 52 57.9	35 55 24
B 154	AB 64	12 55 2.1	35 21 21
B 194	AB 69	12 56 7.8	35 44 54
B 201	AB 78	12 57 26.7	34 39 31
BSO 6	AB 90, B 243	12 59 30.9	34 27 19
B 234	AB 100	13 0 42.5	36 07 34
B 312	AB 134	13 4 52.1	37 28 38
BSO 11	AB 168, B 416	13 11 19.5	36 15 40

TABLE 1 - extended

V	B-V	U-B	Z	Refs.
17.16	0.32	-0.88	1.930	a
18.02	0.29	-0.51	0.390	b, c
17.04	-0.03	-0.77	0.363	b, c
18.15	0.13	-0.75	1.479	b, c
17.4	-0.02	-0.83	0.270	b, d
17.50	-0.07	-0.85	0.298	b, c
17.63	0.41	-0.78	1.910	b, d
17.5	0.04	-0.72	0.404	b, d
16.98	0.31	-0.78	1.241	e, f, g, h
17.83	0.36	-0.87	0.271	e, h
18.64	0.28	-0.98	0.186	e, h
17.92	0.08	-0.90	0.221	e, h
18.56	0.32	-0.70	0.183	e, h
17.96	0.46	-0.76	1.864	e, h
16.79	0.26	-0.82	1.374	e, h
17.67	0.05	-1.01	1.956	e, h
17.52	0.86	-0.43	0.060	e, h
19.08	0.14	-0.67	0.450	e, h
18.41	0.06	-0.85	2.084	e, h

a Kinman, 1966.

b Burbidge, 1968.

c Sandage and Luyten, 1967.

d Burbidge, 1967.

e Braccesi et al., 1968.

f Sandage and Veron, 1965.

g Sandage, 1965.

h Braccesi et al., 1970, 1973.

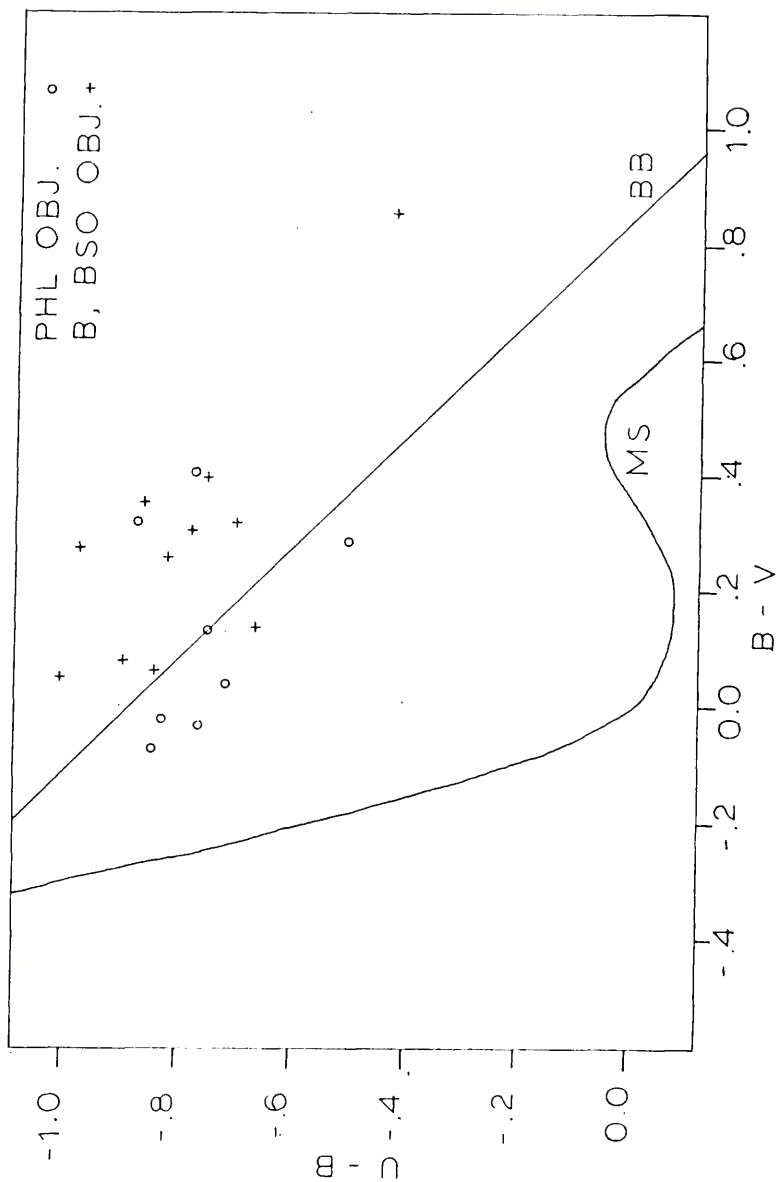


Fig. 1. Color-Color Diagram for PHL, BSO, B Objects.

CHAPTER 2

DATA ACQUISITION

Florida Monitoring Program

A photographic program monitoring the optical brightness of quasars and related objects has continued since 1968 at the University of Florida's Rosemary Hill Observatory located near Bronson, Florida. Four-inch by five-inch photographic plates are exposed in a camera located at the f/4 Newtonian focus of the 76-cm Tinsley reflecting telescope. Summaries of the results of this monitoring program have been published by Folsom et al. (1971), McGimsey et al. (1975), Scott et al. (1976), Pollock et al. (1979), and Pica et al. (1980).

Photographic Techniques

Since the telescope is rather small for use on such faint objects, special efforts are made to maintain the quality and improve the speed of the photographic plates. The plates are exposed in sealed cassettes filled with dry nitrogen gas to prevent differences in the plate responses due to oxygen and excessive humidity in the Florida air. The plates are hypersensitized to provide an increase in speed without an unacceptable increase in background density. Scott and Smith (1976) showed that baking Kodak 103a-0 plates in an atmosphere of dry nitrogen

increases their speed. Subsequent evacuation and soaking the plate in hydrogen gives an additional gain in speed. The plates are then kept in a dry nitrogen atmosphere during storage, use and exposure. The plates are developed 9^m in MWP-2 (Difley, 1968) with mechanical agitation to insure evenness of development.

For the RQQSO monitoring program the Kodak 103a-0 plates were exposed through a Schott GG 385 filter which restricted their sensitivity to the blue (B) region of the spectrum. This helped to minimize possible color effects due to atmospheric extinction. The RQQSO and an approximately one-half-degree field of stars surrounding it were recorded on the photographic plate.

CHAPTER 3

DATA REDUCTION AND ANALYSIS

Comparison

A preliminary estimate of the brightness of the RQSO can be made almost immediately by comparing the image with a pair of neighboring stars of similar magnitude, one of which is usually slightly brighter than the object and the other slightly dimmer. Pairs of plates suspected of showing variation can be studied using a blink comparator.

For numerical comparison a group of twelve or more stars is chosen near the RQSO covering a range of 3-4 magnitudes around that of the object. The magnitudes of these comparison stars are obtained by photographic transfer (equal-length exposures of the two fields on different areas of one plate) from a nearby area for which photographic or photoelectric magnitude sequences have been published. Since the two RQSO fields are very far apart, two calibration fields were needed. Photographic determinations for the stars in SA 94 (Purgathofer, 1969) near the $1^{\text{h}} +6^{\circ}$ field and a photoelectric sequence of the stars in M 3 (Sandage, 1970) near the $13^{\text{h}} +36^{\circ}$ field were conveniently placed. The transfer process involved at least one exposure of the calibration field for each RQSO in the nearby field. Since a number of exposures of these fields were made it was possible to smooth the published magnitude sequences for each of the two calibration fields to correct for any

secular changes since publication for any field effects in the telescope.

Iris Photometry

The prime reduction tool is the Astro-Mechanics Cuffey Iris Astrophotometer, which measures how much light is blocked out by the photographic image. An iris reading reflects the size of the iris opening required so that the light passing through the iris and then through the image on the plate is equal to that in a reference beam. When these readings are made with the iris centered first on the object and then on the stars of the comparison sequence, a curve is obtained that represents the relation between iris readings and the magnitudes of the comparison sequence. An example of such a curve is shown in Fig. 3. The crosses represent the iris reading-magnitude points of the standard stars in M 3 on a plate taken on June 6, 1977. The circles show the parabolic curve fitted to the points using a least squares routine.

Programs

A least squares program of Pollock et al. (1979) fitting a parabola to the iris reading-magnitude curve is run on a Commodore PET microcomputer. This program also displays the curve and the data points on a screen to allow a visual check of the fit. The rms scatter of the comparison star magnitudes is used as a measure of the precision of the RQSO magnitude determined. An expanded version of this program, run on the Amdahl 470/V6 computer of the North East Regional Data Center

located on the University of Florida campus, provides cumulative data reduction and allows for iterative smoothing of the comparison sequence.

Further statistical treatment of the first RQSO magnitudes is done on the PET, using a program which combines observations made during a short interval on one night into a single magnitude, and then computes the weighted Chi Square (see statistics texts such as Aitken, 1952, or Brownlee, 1960). Chi Square tables then give a confidence level reflecting how poorly the data fit an assumption that the object has no intrinsic variation but only reflects the same plate scatter as the comparison stars. In order to facilitate numerical comparisons between strongly varying objects, the program uses a mathematical approximation to Chi Square (χ^2) function for a given number of degrees of freedom (df) to compute a variability index (V.I.), which is χ^2/df normalized to 30 degrees of freedom. A confidence level of 95 percent corresponds to a V.I. of 1.46; 98 percent to a V.I. of 1.60; 99 percent to a V.I. of 1.70 and 99.9 percent to a V.I. of 2.00. Thus, variability indices greater than 1.5 indicate real variability. Variability indices greater than 2.0 reflect not only greater confidence but also greater variation of the object.

Errors

Like any experimental or observational measurements, photographic photometry is subject to error. There are three types, requiring different treatments, involved in the data reduction described here.

The first type is a zero point shift occurring due to the photographic transfer method of calibration. This error affects all of the comparison stars in a field and so does not affect the variability determination. It can be ignored except when comparing magnitudes with those of other observers, measured photoelectrically or on a different photographic system. No attempt is made at this time to convert the photographic blue magnitudes of this photographic plate filter combination to photoelectric magnitudes. A discussion of the relation between these photographic blue magnitudes and the Johnson B photoelectric magnitudes is given in Hackney (1973).

A second source of error, inherent in the photographic process, is caused by granularity of the photographic emulsion and its response to incident light. The size of these errors can be affected by observing conditions (camera focus, atmospheric seeing and sky brightness) and by the plate hypersensitization process. These random errors cannot be removed, but it is very important to know the amplitude of the random error since it is this with which the observed variation of the object must be compared in order to evaluate whether the observed variation is mainly inherent in the object or could have been entirely due to the random errors. For this reason it is necessary to remove the third type of error which, if allowed to remain, will increase the estimate of the random error.

This third type of error acts like an error in magnitude of the comparison stars. On the calibration plate, the effective magnitude of the stars as seen by the plate may differ from the photoelectric magnitude published, due to field effects in the telescope, adjacency

and sky background effects in the photographic emulsion and color terms due to the difference in wavelength bandpass in the photoelectric and photographic systems. Since each of the two calibration fields is used for a number of sources, the constant terms can be separated from the random terms and then smoothed out of the calibration sequence. An iterative smoothing is also performed on the comparison stars in each RQSO field to prevent the random deviations in the calibration exposure from contributing to each of the other observations. This also reduces the effective weight of the calibration plate to its proper level.

The mean rms deviation of the comparison stars is used to approximate the expected random error of the QSO in the χ^2 test. Since the QSO may be somewhat brighter or fainter than the average comparison star, this approximation might be expected to underestimate slightly or to overestimate the random error of the QSO if the slope of the iris reading-magnitude curve is not constant. The distribution of rms deviation of the comparison stars in the combined RQSO, quasar sample was examined (see Fig. 2). The linear correlation coefficient is only 0.17, with a slope of $0^m.02$ rms per one magnitude change in brightness, which is equivalent to $0^m.09$ over the range of magnitudes covered in this sample; thus, this is not an important source of error in this monitoring program.

Curve Fitting

Since the form of the mathematical equation used in the least squares curve fitted to the iris reading magnitude points may have an effect on the magnitudes and associated error so determined, an

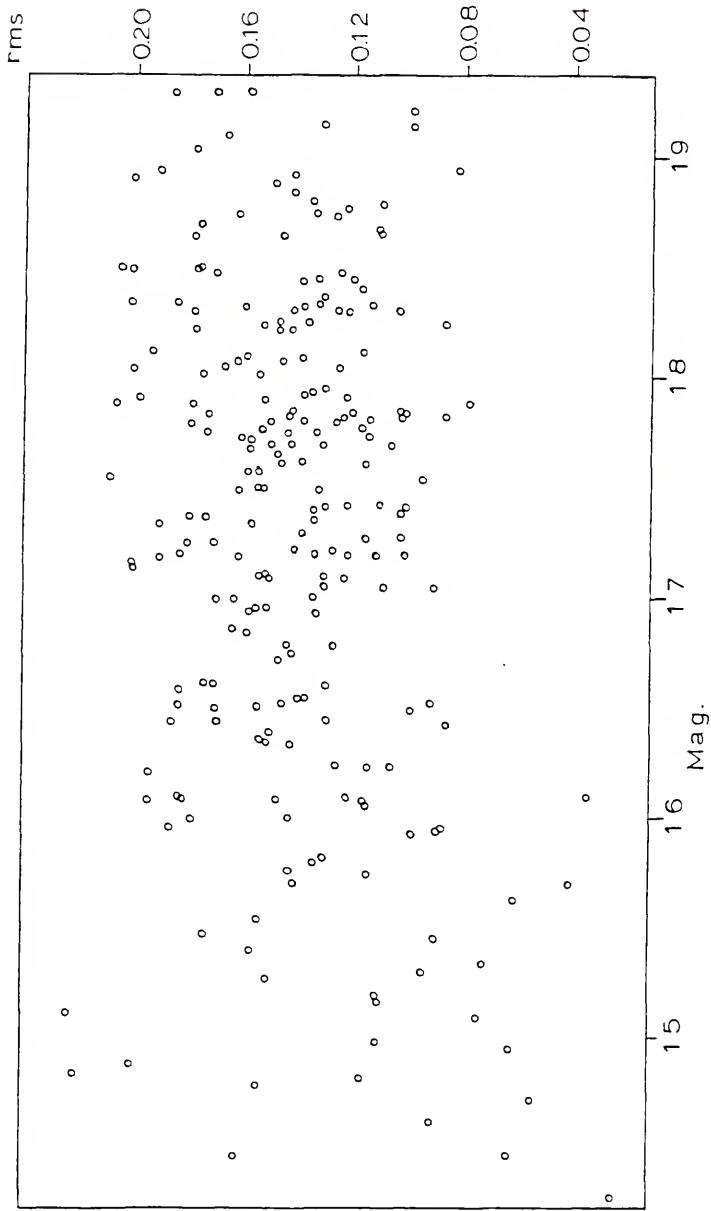


Fig. 2. Average Rms of the Comparison Stars versus Magnitude.

investigation was made of the various forms and methods used for curve fitting in iris astrophotometry programs.

In order to derive a magnitude from the iris reading of the object, a curve is fitted to the iris reading magnitude points for the comparison stars using a least squares procedure. A variety of systems have been used. When the magnitudes of the comparison stars are not known, a scale in terms of average iris reading is often used. Such a procedure is described in Penston and Cannon (1970). It is difficult to compare the amplitude of variability expressed in this way with results of any other studies. In addition, variability thus determined is suspect unless plate exposure, treatment, and sky conditions are sufficiently uniform that the slope of the iris curve is essentially the same on all plates.

Even when the magnitudes of the comparison stars are known or can be determined, many different forms and methods have been used to fit the iris curve, including a line fitted graphically by eye, a least squares line, a smooth curve of unspecified shape fitted by eye, and polynomials of varying degrees fitted by computer least squares programs, some of which use iris reading as the independent variable and some using magnitude. The RQSO observations were reduced using the same program as the Rosemary Hill Observatory quasar observations to facilitate comparison between these two classes of object. The computer program used in the data reduction to fit a parabola to the magnitudes and iris readings of the comparison stars (for an example see Fig. 3) assumes that all random errors occur in iris readings. The smoothing

technique assumes that constant terms are errors in magnitude and smooths them out iteratively.

The analytical form of the iris reading-magnitude relation produced by the Cuffey Iris Astrophotometer is not known. Empirically the curve is essentially linear over most of the range of interest, but the magnitude should increase asymptotically as the sky background makes an increasing contribution to the photographic image.

In order to compare the different curve fitting methods and to investigate the possible effects on variability determinations, a calibration plate of the M 3 field taken on the night of June 6, 1977, was reduced using a variety of analytical forms for the iris reading-magnitude relation. A least squares curve fitting computer program written by Dr. H. L. Cohen (1980) was used for polynomial forms and a modified version to fit a line plus hyperbola. The resulting curves are shown in Figs. 3 - 8. Results and comments are given in Table 2. In these figures crosses represent the iris reading-magnitude point of the standard stars in M 3. The circles show the least squares curve fitted to the crosses in each case.

In Fig. 3 it is assumed that all of the random errors are in iris reading and that iris reading may be expressed as a second order polynomial in magnitude. This is the form used in the RQQSO and quasar studies done at the Rosemary Hill Observatory of the University of Florida. Three unknown coefficients are determined in the least squares procedure. In order to determine the magnitude of the QSO from a known iris reading, this form must be inverted and the correct root chosen.

PARABOLA $IR = A + B \cdot M + C \cdot M^2$

M 3 6/19/77

+ stars

o curve

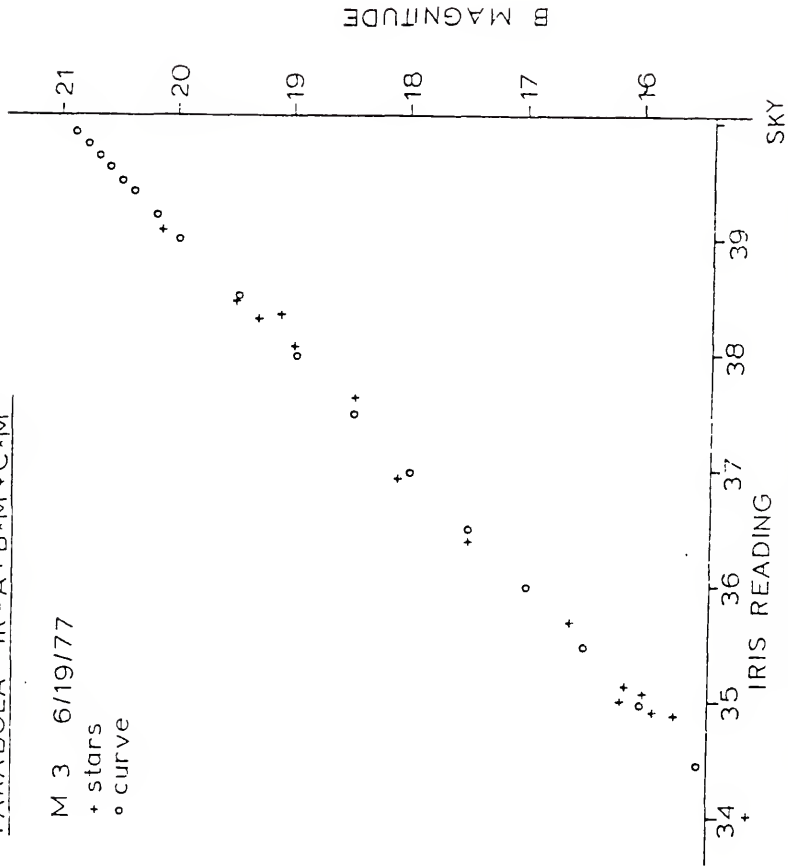


Fig. 3. Second Order Polynomial Fit in Magnitude.

PARABOLA $M = A + B \cdot IR + C \cdot IR^2$

M 3 6/19/77

+ stars

o curve

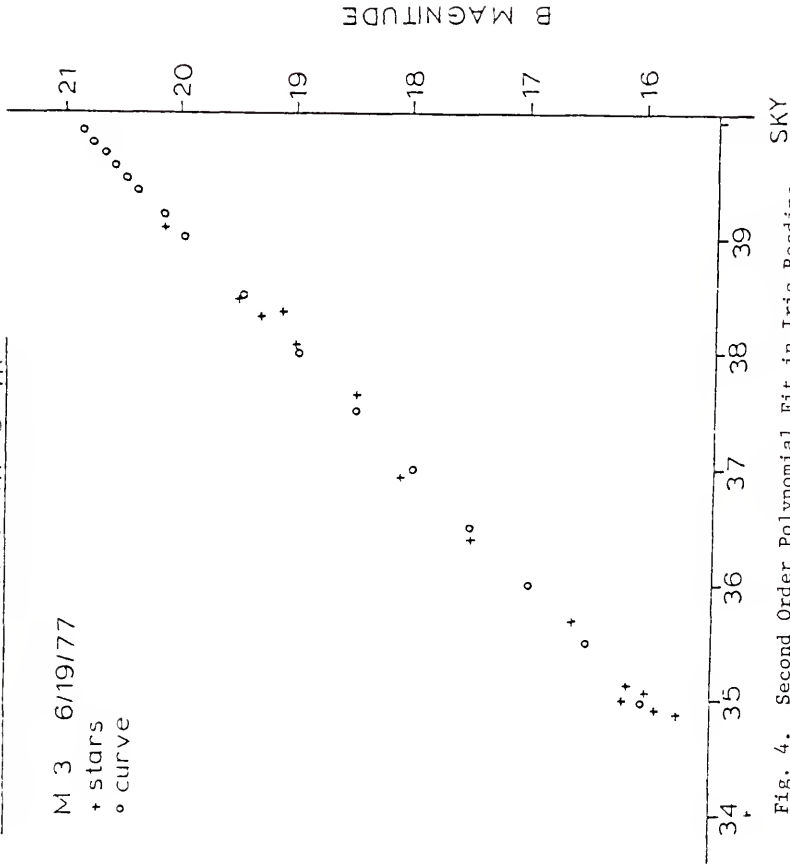


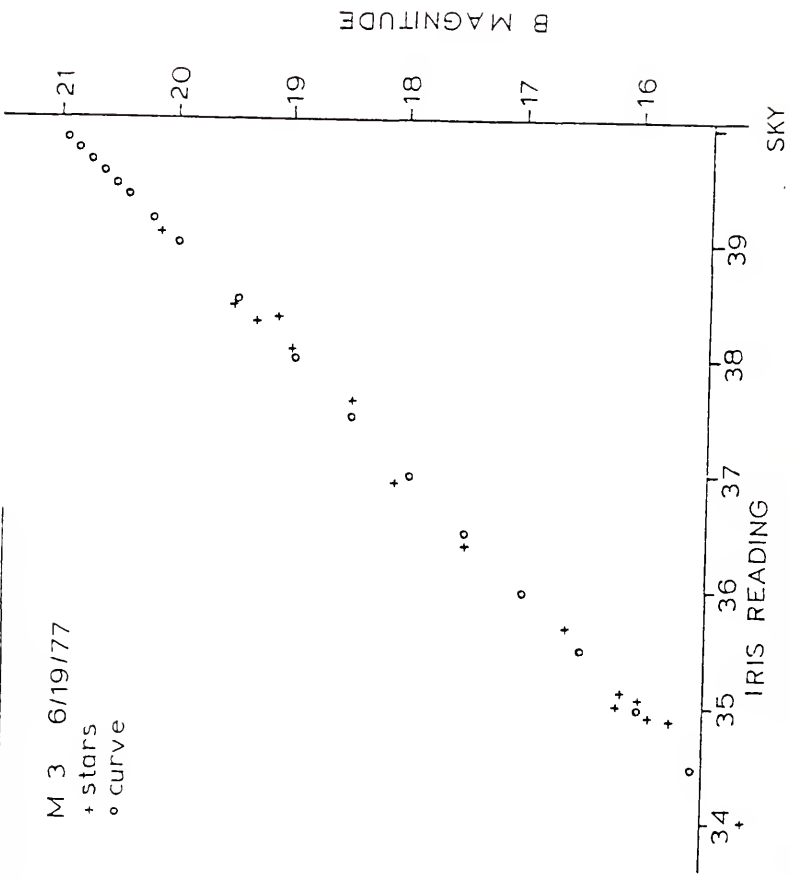
Fig. 4. Second Order Polynomial Fit in Iris Reading. SKY

$$M = A + B \cdot IR + C \cdot IR^2 + D \cdot IR^3$$

M 3 6/19/77

+ stars

o curve



$$M = A + B \cdot IR + C \cdot IR^2 + D \cdot IR^3 + E \cdot IR^4$$

M 3 6/19/77

+ stars
o curve

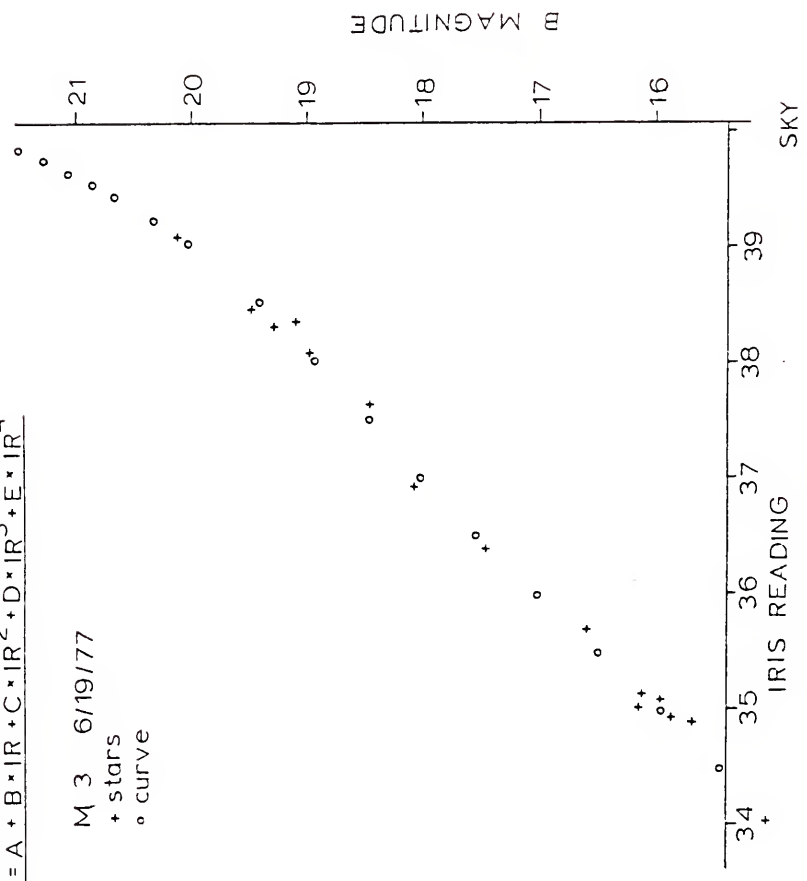


Fig. 6. Fourth Order Polynomial Fit in Iris Reading.

LINE PLUS HYPERBOLA

M 3 6/19/77

+ stars

o curve

$$M = A + B(IR - SKY) + C/(IR - SKY)$$

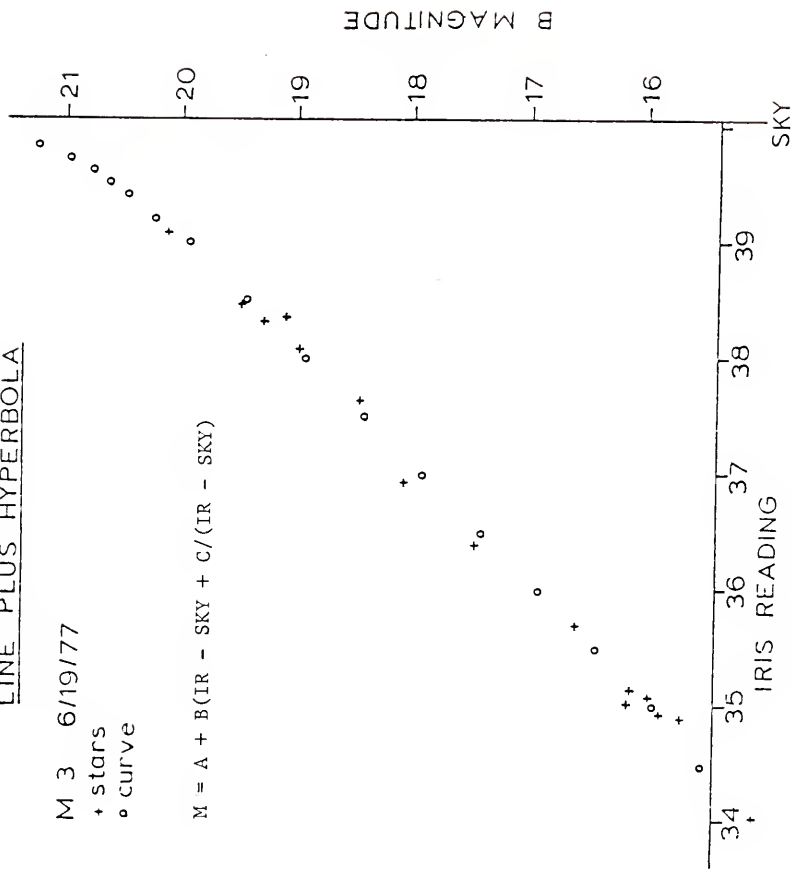


Fig. 8. Line Plus Hyperbola.

TABLE 2
Functional Forms Tested for Curve Fitting Procedure

N	σ	K	Functional Form	Comments
4	.1203	.01524	$IR=A(1)+A(2)M+A(3)M^2+A(4)M^3$	Hard to solve for M(IR).
3	.1174	.01389	$IR=A(1)+A(2)M+A(3)M^2$	Can approach sky background but curves elsewhere.
2	.1129	.01286	$IR=A(1)+A(2)M$	Curve should be nonlinear at sky.
3	.1156	.01364	$M=A(1)+A(2)IR+A(3)(IR-SKY)$	Good shape but assumes error is in magnitude. Sky reading must be known.
2	.1131	.01278	$M=A(1)+A(2)IR$	Curve should be nonlinear at sky. Assumes error is in magnitude.
3	.1177	.01383	$M=A(1)+A(2)IR+A(3)IR^2$	Assumes error is in magnitudes. Used by Penston and Cannon (1970).
4	.1221	.01531	$M=A(1)+A(2)IR+A(3)IR^2+A(4)IR^3$	Assumes error is in magnitude. Used by Burkhead and Seeds (1971) with fewer stars, and by Braccesi <u>et al.</u> (1970).
5	.1115	.01463	$M = \sum_{i=1}^5 A(i)IR^{i-1}$	Assumes error is in magnitude.
6	.1168	.01723	$M = \sum_{i=1}^6 A(i)IR^{i-1}$	Assumes error is in magnitude. Best fit found by Burkhead and Seeds (1971) for M 67 with a large number of stars.

$$K = \sum_{i=1}^n \sigma_i^2 / (n - N) \quad n = \text{number of standard stars} = 15$$

Higher order polynomials of this type become quite difficult to invert to determine the magnitude of the QSO.

Other observers, Penston and Cannon (1970), Braccesi et al. (1970), Burkhead and Seeds (1971) and Bonoli et al. (1979) use computer least squares fits expressing magnitude as a polynomial in iris reading. This form does not require inversion to determine the magnitude of the QSO, but this form assumes that all of the random errors occur in magnitude. This seems unrealistic since the magnitudes of the standard stars are usually determined photoelectrically with quite high precision while the iris reading is subject to the noise in the photographic emulsion. Figures 3 - 6 show magnitude expressed as second through fifth order polynomials in iris reading (3 - 6 unknowns).

Penston and Cannon (1970) use a second order polynomial in iris reading and many observers have followed their method. Burkhead and Seeds (1971) investigated computer fitted polynomials in iris reading for a field with more than one hundred stars. They found the best computer fit (minimum $K = \sum_{i=1}^n \sigma_i^2 / (n-N)$) with a fifth order polynomial, but they usually used a third order polynomial for cases with a small number of stars or fit a smooth curve by eye. Braccesi et al. (1970), also with a very large number of standard stars, found a minimum at third order although the third order terms were small. The M 3 field studied here had minimum K at first order (a line). A linear form does not fit near the sky background causing the magnitude to be underestimated. With only 15 standard stars, high order terms are susceptible to unreasonable curvature in the range where the curve should be linear.

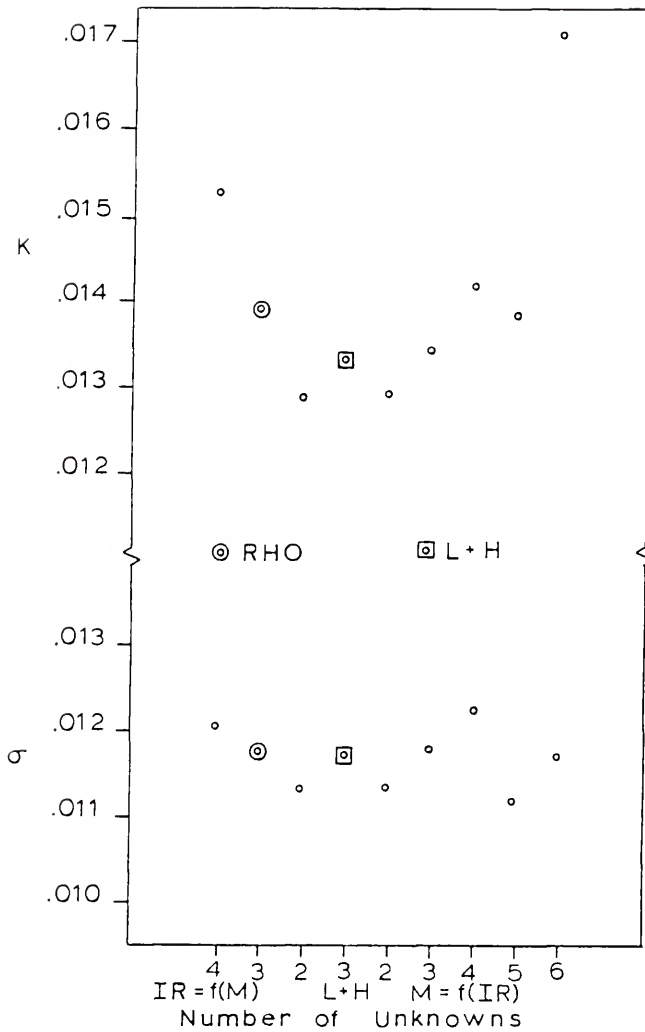


Fig. 9. K and σ Values for Curves.

In a search for a relatively simple mathematical form which would be linear over most of the range but would increase asymptotically as the sky background was reached, one such form was found: a line plus hyperbola (Fig. 8, L + H in Fig. 9). It has three unknown coefficients and an equation: $M = A(1) + A(2) \times (IR - SKY) + A(3)/(IR - SKY)$. It fits slightly better than the second order polynomial curves and has the proper behavior at the sky background. It does not require inversion to determine the object magnitude. It does have two disadvantages. The iris reading of the sky background must be known. This quantity was not measured on many of the old plates. Also, the line plus hyperbola has magnitude as a function of iris reading. In a linear least squares curve fitting program, this assumes that the random errors are in magnitude. The line plus hyperbola may be promising for future data reduction of the total RQSO and quasar samples if combined with a curve fitting program which will minimize residuals in both variables simultaneously.

Numerical comparison of the goodness of fit of the various mathematical forms tested on the M 3 field is shown in Table 2 and Fig. 9. Two quantities are calculated σ , the average rms scatter of the points about the curve (expressed in magnitude units), and K, which is $\frac{\sum_{i=1}^n \sigma_i^2}{(n-N)}$, where N is the number of unknown coefficients and n is the number of standard stars (in this case n = 15).

Where the minimum K value occurs seems to depend on the particular field and on how many comparison stars there are. A linear form is too simple and has the wrong behavior at the sky limit. A parabola in iris reading also does not approach the sky background properly. Most quasar

monitoring fields have only 10-15 comparison stars, in which case high order polynomials allow too much curvature in the middle range. The line plus hyperbola would allow a better shape than a parabola in magnitude, but requires a more complex least squares curve fitting procedure.

All of the RQSO data described in the following chapters were reduced using a parabola in iris reading, in order to be consistent with the reduction of the larger sample of quasars observed at Rosemary Hill Observatory and given in Pollock et al. (1979) and Pica et al. (1980). Use of the line plus hyperbola form will require re-reading of many older plates and development of a new curve-fitting program which will minimize the residuals in both variables simultaneously.

CHAPTER 4

FIELD AT $1^{\text{h}} +6^{\circ}$

SA 94

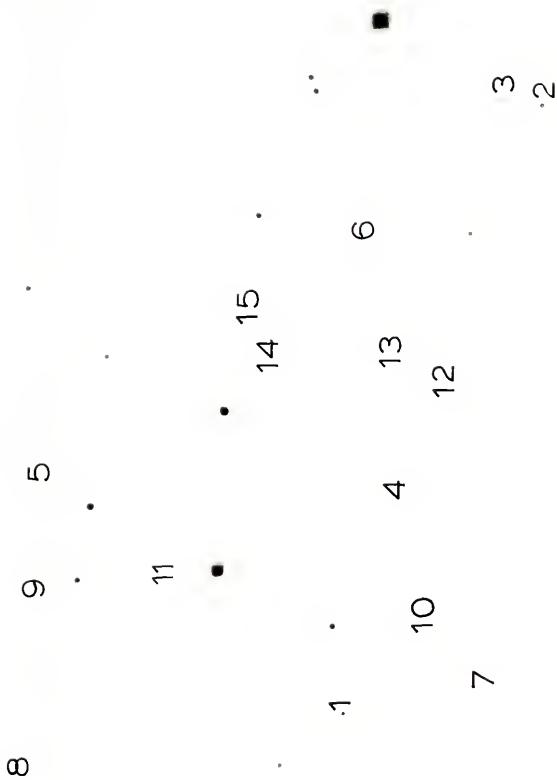
The comparison stars for the RQOSOs in the PHL field at $1^{\text{h}} +6^{\circ}$ were calibrated using stars in SA 94 centered at $2^{\text{h}} 53.3^{\text{m}} +0^{\circ} 20'$. A photoelectric sequence giving V magnitudes and B - V colors for 54 stars in SA 94 was published by Purgathofer in 1969. This information allows calculation of the B magnitudes of these stars. Eight observations of this field were made in calibrating the PHL objects. A sequence of 15 stars was used in each case. The magnitudes of these stars were iteratively smoothed to accommodate the field response of the telescope. The stars are identified in Fig. 10. Their designations and old and new magnitudes are listed in Table 3. Some random zero-point offset in the magnitudes in a RQOSO field may occur in the photographic transfer method, but this should be small and has no effect on the amount of variability measured. It would be relevant only when comparing particular Rosemary Hill Observatory magnitudes with magnitudes measured elsewhere. A photographic B magnitude is not exactly the same as a photoelectric Johnson B magnitude, but it is the same for most photographic observers (Hackney, 1973).

TABLE 3
Standard Stars in SA 94

Number	Designation*	Old B Mag.*	Smoothed B Mag.
1	37	14.86	14.86
2	39	15.08	15.13
3	40	15.30	15.33
4	41	15.94	16.01
5	42	15.73	15.78
6	44	15.87	15.82
7	46	16.28	16.30
8	47	16.22	16.29
9	48	16.65	16.71
10	49	16.80	16.88
11	50	16.96	16.96
12	51	16.87	16.78
13	52	17.41	17.49
14	53	17.90	17.83
15	54	18.15	17.68

*Purgathofer, 1969.

Fig. 10. SA 94 Field (facing page). This photograph was reproduced from a plate taken at Rosemary Hill Observatory on the night of December 31, 1975. North is at the top and east is to the left. One minute of arc equals 7 mm. The magnitudes of the standard stars are given in TABLE 3 (above).



PHL 938

PHL 938 is a blue star-like object found at $0^{\text{h}} 58^{\text{m}} 12^{\text{s}}$ and $+1^{\circ} 56'$ by Haro and Luyten (1962). Spectra (Kinman, 1966) based on oxygen, carbon and hydrogen lines gave a redshift of 1.93 with some absorption lines suggested. Kinman photographically determined a visual (V) magnitude of $17^{\text{m}}16$, B - V color of $0^{\text{m}}32$ and $U - B = -0^{\text{m}}88$. Since no radio source was known at this position, a special search was made by Bolton (Kinman, 1966), who could not find any radio emission at 11 cm down to a detection limit of 0.1 fu. Because of the absorption lines, Burbidge et al. (1968) took more spectra, finding an emission redshift of 1.955, an absorption in the Lyman alpha (Ly_{α}) hydrogen line at 1.906 and a series of absorption lines due to iron and magnesium at a redshift of 0.613.

The comparison stars for the PHL 938 field were calibrated by photographic transfer from the sequence in SA 94 on a plate taken the night of January 4, 1976. These stars are identified in Fig. 11 and their magnitudes are given in Table 4. The Florida results were based on 13 observations, which include two pairs of exposures taken close together in time. The magnitudes of PHL 938 are given in Table 5 and plotted versus time in Fig. 12. They do not show any evidence of variability. The mean magnitude is $B = 16^{\text{m}}85$ with a range of $0^{\text{m}}25$ compared to an rms scatter of the comparison stars of $0^{\text{m}}08$ (Table 43).

TABLE 4
Comparison Stars for PHL 938

Star	1	2	3	4	5	6	7	8	9	10	11	12
Mag.	17.00	16.97	16.08	17.81	16.71	16.54	17.39	16.35	15.47	14.98	17.75	16.84

Fig. 11. PHL 938 Field (facing page). This photograph was reproduced from a plate taken at Rosemary Hill Observatory on the night of October 27, 1975. North is at the top and east is to the left. One minute of arc equals 7mm. The object is identified by two short perpendicular lines. The magnitudes of the comparison stars are given in TABLE 4 (above).

12

6

10

9

7

11

5

43

L

1

2

TABLE 5
B Magnitudes of PHL 938

Date	EST	JD	Mag.	rms
12/17/74	2138	42399.610	16.75	0.07
8/14/75	0238	42638.818	16.74	0.07
9/ 4/75	0229	42659.812	16.86	0.12
10/27/75	2211	42713.633	16.88	0.07
11/ 1/75	2035	42718.566	16.99	0.08
12/24/75	1920	42771.514	16.81	0.07
1/ 4/76	2110	42782.590	16.84	0.06
2/ 2/76	1950	42811.535	16.91	0.11
10/21/76	2319	43073.680	16.82	0.07
10/21/76	2327	43073.685	16.86	0.10
12/18/76	1925	43131.517	16.93	0.06
12/18/76	1934	43131.524	16.83	0.07
9/22/77	0302	43408.835	16.94	0.13

Key to Fig. 12. Data points whose rms is less than or equal to 0.1 Mag. are shown by a circle. Points with an rms greater than 0.1 Mag. are shown by a cross. A point corresponding to the weighted mean is plotted for two observations on the same night. Error bars at the right represent the mean magnitude of the object $\pm 1 \sigma$.

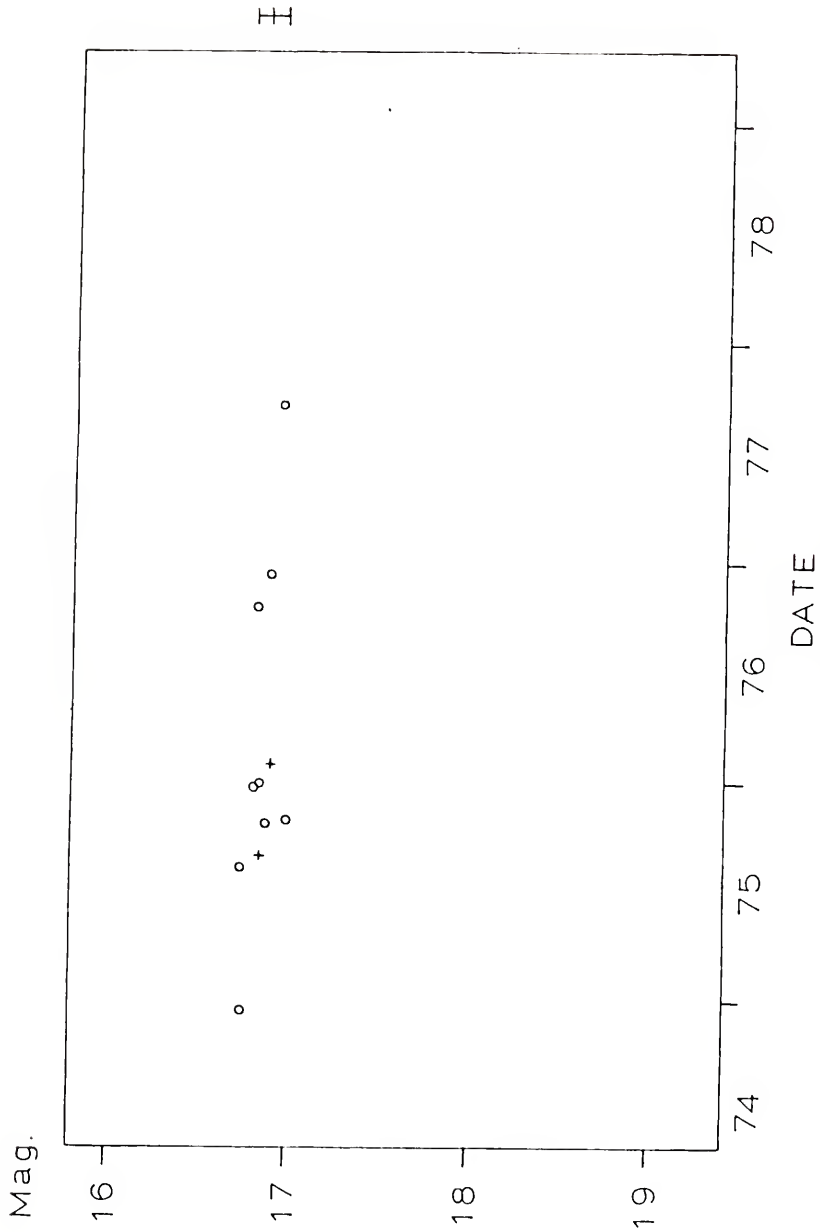


Fig. 12. Variation with Time of PHL 938.

PHL 3375

PHL 3375 is a blue star-like object located at $1^{\text{h}} 28^{\text{m}} 24^{\text{s}}$ and $+7^{\circ} 28'$ in the Palomar survey field of Haro and Luyten (1962). It was suggested as a QSO candidate by Sandage and Luyten (1967), who measured its magnitude ($V = 18^{\text{m}}.02$) and colors ($B - V = 0^{\text{m}}.29$, $U - B = -0^{\text{m}}.51$). Spectra by Burbidge (1968) showed emission lines of oxygen, magnesium and hydrogen at a redshift of 0.390. A radio survey by Fanti et al. (1977) found no radio emission at 1.4 GHz to the limit of the survey (10 mfu).

The comparison stars in the PHL 3375 field were calibrated by photographic transfer from SA 94 using an exposure of each field on a single plate taken on the night of December 31, 1975. These stars are identified in Fig. 13 and their magnitudes are listed in Table 6. Eleven observations of PHL 3375, including one pair taken one after the other, were made at Rosemary Hill Observatory. The coverage was somewhat hampered by Jupiter's passage through the field during August and September of 1975. The resulting magnitudes are displayed in Table 7. The variation of the object with time is shown in Fig. 14. PHL 3375 was slightly brighter in 1975 and $0^{\text{m}}.4$ dimmer in 1978. Statistics show that this object is probably variable (C.L. = 92%). It has a mean magnitude of $17^{\text{m}}.94$ with a range of $0^{\text{m}}.66$. The average rms scatter of the comparison stars was $0^{\text{m}}.11$ (Table 43).

TABLE 6
Comparison Stars for PHL 3375

Star	1	2	3	4	5	6	7	8	9	10	11	12
Mag.	17.87	17.69	18.42	17.80	17.76	15.93	17.41	18.30	18.32	17.84	16.43	18.49

Fig. 13. PHL 3375 Field (facing page). This photograph was reproduced from a plate taken at Rosemary Hill Observatory on the night of December 25, 1975. North is at the top and east is to the left. One minute of arc equals 7mm. The object is identified by two short perpendicular lines. The magnitudes of the comparison stars are given in TABLE 6 (above).

3
2
1
4
5
6
7
8
9
10
11
12

TABLE 7

B Magnitudes of PHL 3375

Date	EST	JD	Mag.	rms
12/17/74	2209	42399.631	18.03	0.09
10/12/75	0118	42697.762	17.96	0.07
11/ 1/75	2106	42718.587	17.95	0.09
12/24/75	1937	42771.526	17.71	0.23
12/25/75	2101	42772.584	17.79	0.08
12/31/75	2045	42778.573	17.85	0.09
2/18/76	2004	42827.544	17.78	0.14
10/21/76	2348	43073.700	17.90	0.13
10/21/76	2356	43073.706	18.12	0.11
11/ 7/77	2120	43455.597	17.92	0.09
11/ 3/78	2333	43816.690	18.37	0.12

Key to Fig. 14. Data points whose rms is less than or equal to 0.1 Mag. are shown by a circle. Points with an rms greater than 0.1 Mag. are shown by a cross. A point corresponding to the weighted mean is plotted for two observations on the same night. Error bars at the right represent the mean magnitude of the object $\pm 1 \sigma$.

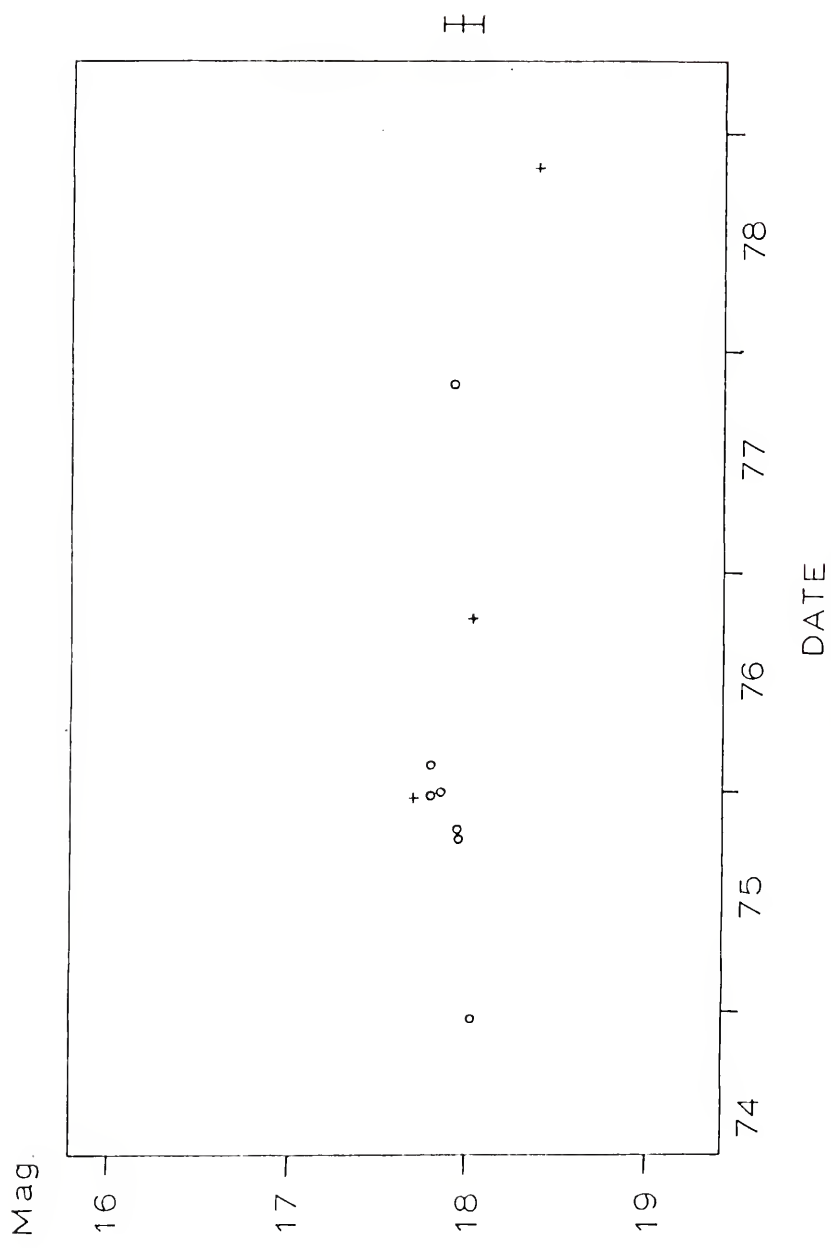


Fig. 14. Variation with Time of PHL 3375.

PHL 1027

Located at $1^{\text{h}} 30^{\text{m}} 30^{\text{s}}$ and $+3^{\circ} 22'$, PHL 1027 was a blue object on the Palomar survey plate studied by Haro and Luyten (1962). Photometry by Sandage and Luyten (1967) found colors suggestive of a QSO; $V = 17^{\text{m}}04$, $B - V = -0^{\text{m}}03$ and $U - B = -0^{\text{m}}77$. An emission line redshift of $z = 0.363$ based on neon, oxygen and hydrogen lines was determined by Burbidge (1968).

The comparison stars for PHL 1027 were calibrated by photographic transfer from SA 94, using a plate taken on the night of November 21, 1976. These stars are identified in Fig. 15 and their magnitudes are given in Table 8. The magnitudes from 13 observations of PHL 1027, including 2 pairs, are given in Table 9 and are plotted according to the date of observation in Fig. 16. The points scatter about a line and show no evidence of variation. The mean magnitude of PHL 1027 is $16^{\text{m}}83$, with a range of $0^{\text{m}}22$ compared with the average rms scatter of the comparison stars of $0^{\text{m}}09$ (see Table 43).

PHL 3632

PHL 3632 is listed at $1^{\text{h}} 39^{\text{m}} 54^{\text{s}}$ and $+6^{\circ} 10'$ by Haro and Luyten (1962). Sandage and Luyten (1967) obtained the following magnitude and colors: $V = 18^{\text{m}}15$, $B - V = 0^{\text{m}}13$ and $U - B = -0^{\text{m}}75$. Since its colors were in the QSO region of the color-color diagram (see Fig. 1), Burbidge (1968) took a spectrum of PHL 3632. Lines due to carbon implied a

TABLE 8
Comparison Stars for PHL 1027

Star	1	2	3	4	5	6	7	8	9	10	11	12
Mag.	17.50	16.09	16.09	15.09	15.80	17.93	18.02	17.49	16.55	17.81	17.55	16.00

Fig. 15. PHL 1027 Field (facing page). This photograph was reproduced from a plate taken at Rosemary Hill Observatory on the night of November 21, 1976. North is at the top and east is to the left. One minute of arc equals 7mm. The object is identified by two short perpendicular lines. The magnitudes of the comparison stars are given in TABLE 8 (above).

11

9

12

1' 2

3

4

5

6

8

17

10

TABLE 9
B Magnitudes of PHL 1027

Date	EST	JD	Mag.	rms
12/17/74	2234	42399.649	16.78	0.07
8/14/75	0238	42638.818	16.83	0.09
9/ 4/75	0249	42659.826	16.94	0.10
10/15/75	0417	42700.887	16.33	0.10
10/26/75	2117	42712.595	16.99	0.10
12/24/75	1959	42771.541	16.86	0.10
11/21/76	2151	43104.619	16.93	0.07
11/21/76	2200	43104.625	16.76	0.06
12/24/76	2205	43137.628	16.83	0.14
12/24/76	2214	43137.635	16.78	0.09
9/20/77	0230	43406.812	16.76	0.13
11/ 7/77	2132	43455.606	16.86	0.05
11/ 3/78	2321	43816.681	16.86	0.10

Key to Fig. 16. Data points whose rms is less than or equal to 0.1 Mag. are shown by a circle. Points with an rms greater than 0.1 Mag. are shown by a cross. A point corresponding to the weighted mean is plotted for two observations on the same night. Error bars at the right represent the mean magnitude of the object $\pm 1 \sigma$.

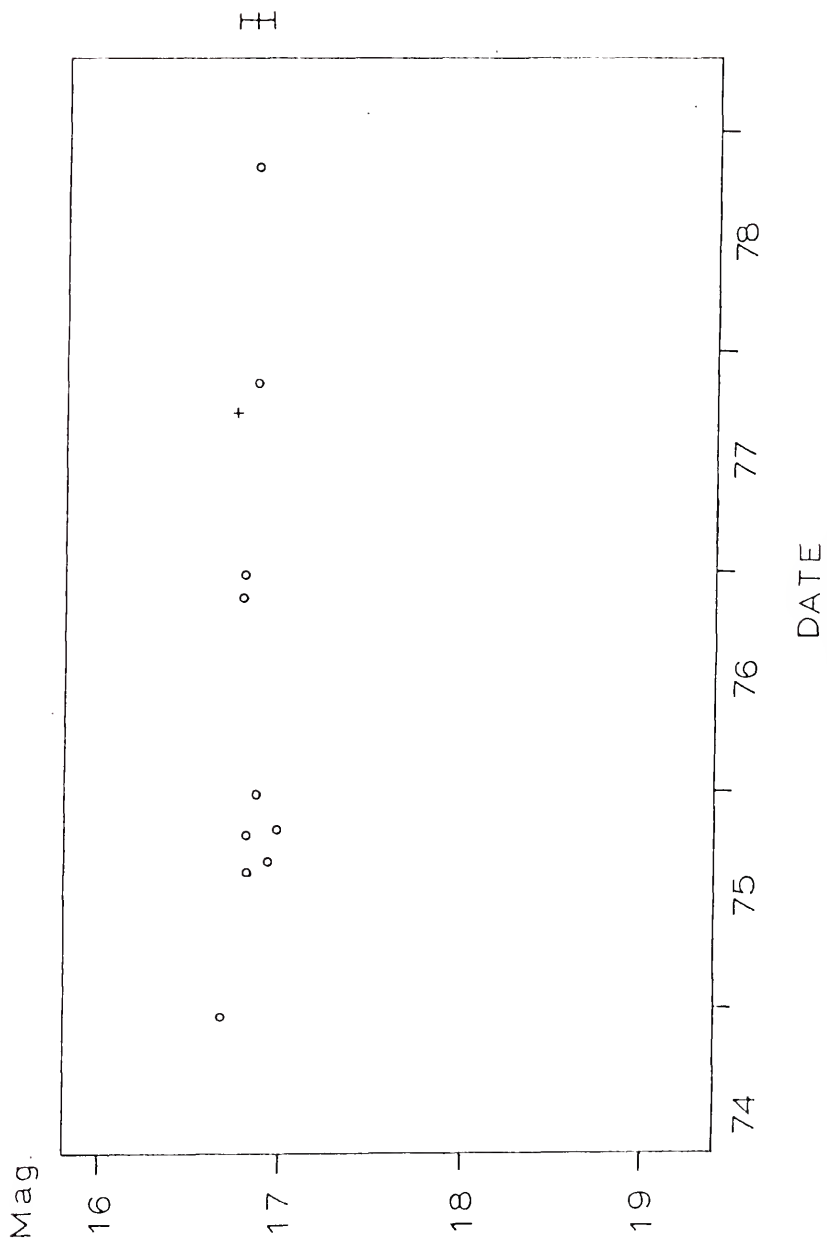


Fig. 16. Variation with Time of PHL 1027.

TABLE 10
Comparison Stars for PHL 3632

Star	1	2	3	4	5	6	7	8	9	10	11	12
Mag.	17.33	17.20	15.81	17.91	14.95	18.30	18.11	17.56	15.27	17.42	18.04	18.12

Fig. 17. PHL 3632 Field (facing page). This photograph was reproduced from a plate taken at Rosemary Hill Observatory on the night of November 18, 1976. North is at the top and east is to the left. One minute of arc equals 7mm. The object is identified by two short perpendicular lines. The magnitudes of the comparison stars are given in TABLE 10 (above).

12
10
9
8
7
6
5
4
3
2
1
11

TABLE 11

B Magnitudes of PHL 3632

Date	EST	JD	Mag.	rms
1/ 2/75	1930	42415.521	17.61	0.08
8/15/75	0227	42639.810	17.37	0.06
10/12/75	2131	42698.605	17.63	0.07
10/26/75	0132	42711.772	17.45	0.10
12/24/75	2016	42771.553	17.68	0.08
11/18/76	2139	43101.610	17.73	0.08
11/18/76	2148	43101.617	17.62	0.07
1/18/77	2122	43162.599	17.61	0.14
1/18/77	2131	43162.605	17.63	0.11
9/20/77	0345	43406.865	17.54	0.11
11/ 3/78	2207	43816.630	17.94	0.13

Key to Fig. 18. Data points whose rms is less than or equal to 0.1 Mag. are shown by a circle. Points with an rms greater than 0.1 Mag. are shown by a cross. A point corresponding to the weighted mean is plotted for two observations on the same night. Error bars at the right represent the mean magnitude of the object $\pm 1 \sigma$.

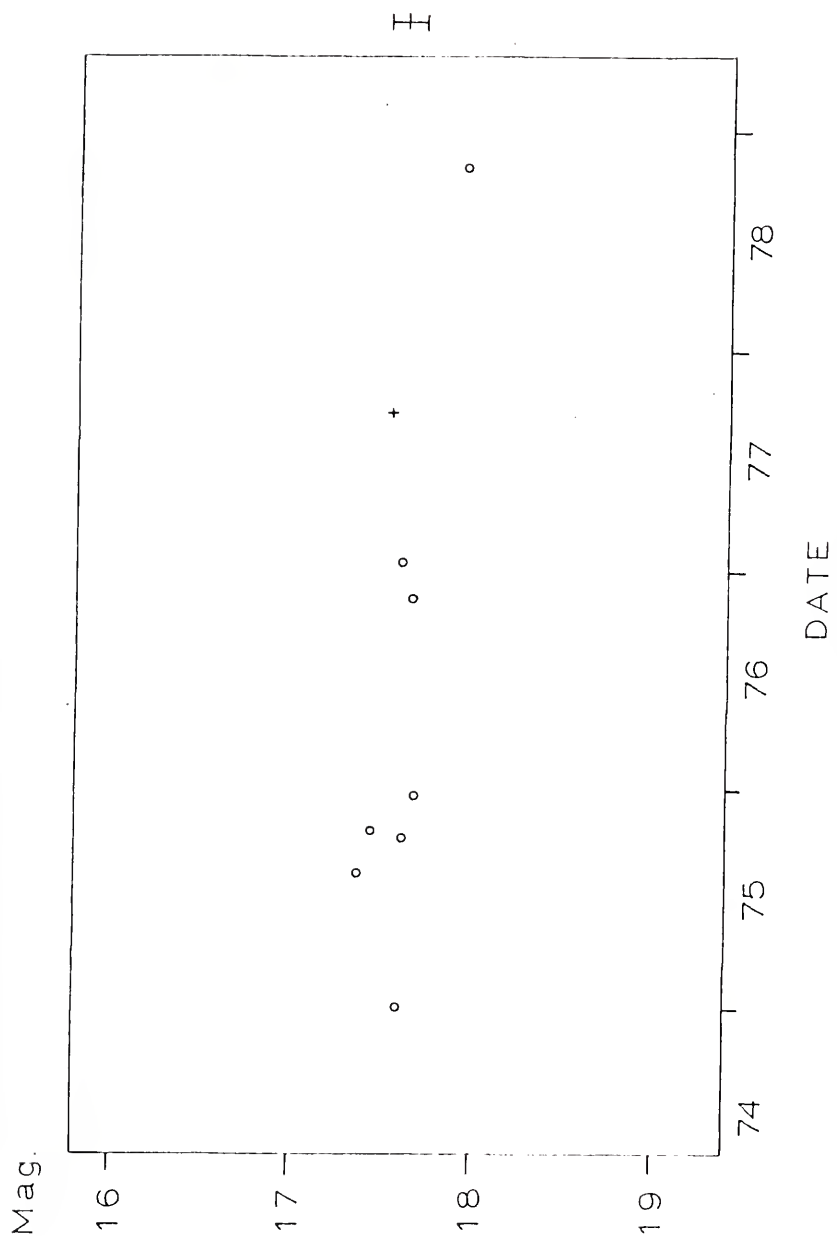


Fig. 18. Variation with Time of PHL 3632.

redshift of approximately 1.5. The object was definitely a QSO but the redshift was not as precisely measured as most of the others.

Comparison stars for PHL 3632 were calibrated by photographic transfer from SA 94, using a plate taken on the night of December 24, 1975. These stars are identified in Fig. 17 and the magnitudes are given in Table 10. The Florida results contain 11 observations of PHL 3632, including two pairs. These magnitudes are given in Table 11 and are plotted in Fig. 18. The object appeared brighter in 1975 and had faded in 1978. PHL 3632 has a mean magnitude of $17^m.59$, with a range of $0^m.57$ and an average scatter of the comparison stars of $0^m.08$. χ^2 statistics give a 98 percent confidence of variation (Table 43).

PHL 1186

PHL 1186 was a stellar object found in the Haro and Luyten (1962) survey because of its ultraviolet excess. Its position is $1^h 47^m 36^s$ and $+9^\circ 1'$. Burbidge (1967) gives its magnitude and colors as $V = 17^m.4$, $B - V = -0^m.02$ and $U - B = -0^m.83$. Emission lines of neon, oxygen and hydrogen show a redshift of $z = 0.270$ (Burbidge, 1968).

The comparison stars for PHL 1186 were calibrated by photographic transfer from SA 94, using a plate taken on the night of December 24, 1975. They are identified on Fig. 19 and their magnitudes are given in Table 12. Sixteen observations, including 4 pairs, were made at Rosemary Hill Observatory. The resulting magnitudes are given in Table 13. PHL 1186's variation with time is shown in Fig. 20. The object brightened between 1974 and 1975 and remained at the higher

TABLE 12
Comparison Stars for PHL 1186

Star	1	2	3	4	5	6	7	8	9	10	11	12
Mag.	17.85	16.23	17.20	15.44	17.61	16.32	15.96	17.36	18.06	17.37	17.84	17.75

Fig. 19. PHL 1186 Field (facing page). This photograph was reproduced from a plate taken at Rosemary Hill Observatory on the night of October 12, 1975. North is at the top and east is to the left. One minute of arc equals 7mm. The object is identified by two short perpendicular lines. The magnitudes of the comparison stars are given in TABLE 12 (above).

6¹²

7 8 9 10 5

4

3

1

11

2

TABLE 13
B Magnitudes of PHL 1186

Date	EST	JD	Mag.	rms
12/ 9/74	2329	42391.687	17.78	0.08
8/14/75	0358	42638.874	17.42	0.13
10/13/75	0267	42698.797	17.58	0.12
11/ 1/75	2106	42718.587	17.24	0.10
12/24/75	2203	42771.627	17.32	0.08
2/18/76	2019	42827.555	17.39	0.09
8/23/76	0232	43013.814	17.81	0.15
8/23/76	0241	43013.820	17.60	0.07
8/28/76	0308	43018.839	17.53	0.11
8/28/76	0317	43018.845	17.44	0.13
10/21/76	0019	43072.722	17.55	0.10
10/21/76	0028	43072.728	17.58	0.15
12/18/76	1957	43131.540	17.56	0.13
12/18/76	2004	43131.544	17.49	0.10
9/20/77	0315	43406.844	17.52	0.12
11/ 3/78	2223	43816.641	17.52	0.11

Key to Fig. 20. Data points whose rms is less than or equal to 0.1 Mag. are shown by a circle. Points with an rms greater than 0.1 Mag. are shown by a cross. A point corresponding to the weighted mean is plotted for two observations on the same night. Error bars at the right represent the mean magnitude of the object $\pm 1 \sigma$.

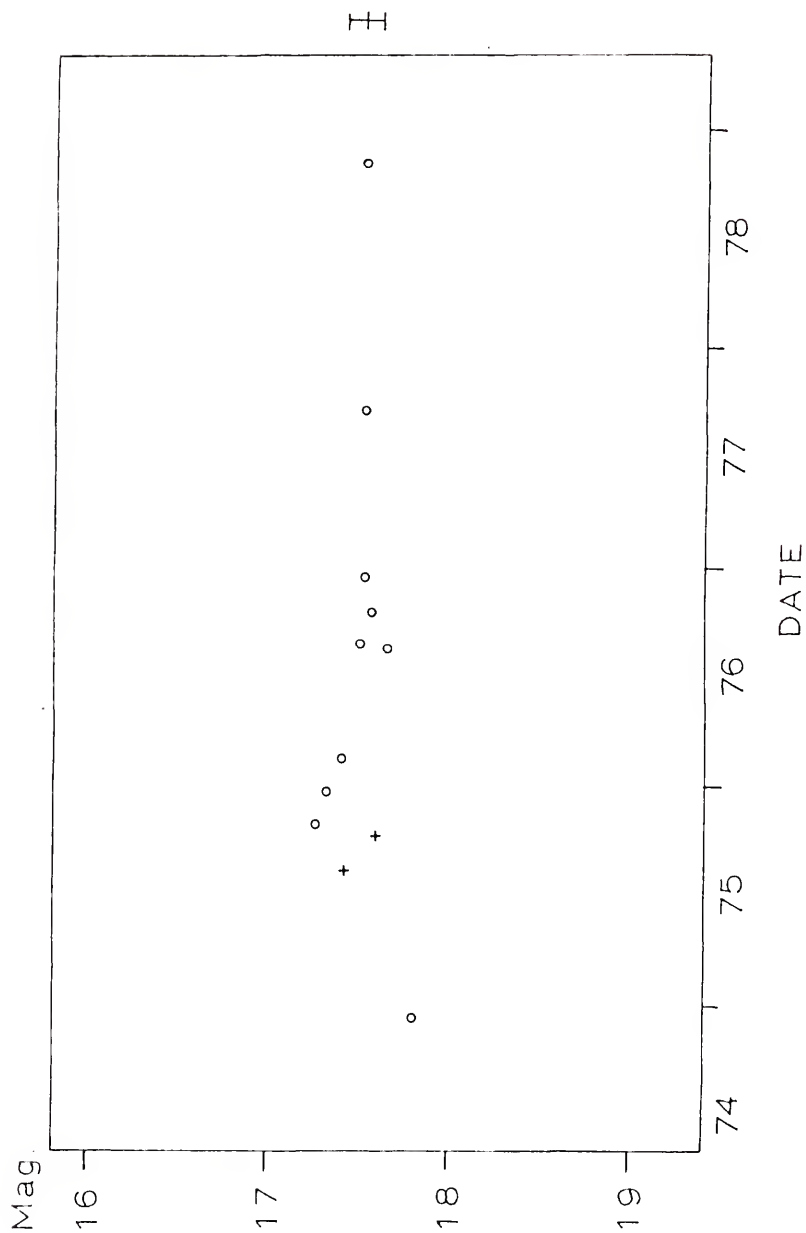


Fig. 20. Variation with Time of PHL 1186.

level. The mean magnitude was $17^m.51$, with a range of $0^m.54$ as compared to an average rms scatter of the comparison stars of $0^m.09$. The confidence level for variability is 98 percent (Table 43).

PHL 1194

Haro and Luyten (1962) list PHL 1194 at $1^h 48^m 42^s$ and $+9^\circ 2'$. This field and that of PHL 1186 overlap partially. The objects are 17 minutes of arc apart. Sandage and Luyten (1967) give $V = 17^m.5$, $B - V = -0^m.07$, $U - B = -0^m.85$ and $z = 0.298$. Spectra by Burbidge (1968) show emission lines of neon, oxygen and hydrogen at a redshift of $z = 0.299$ and an absorption line which is probably Ly_α but might be due to magnesium. A radio search by Fanti et al. (1977) at 1.4 GHz failed to detect a radio source at this position with a detection limit of 15 mfu.

Comparison stars for PHL 1194 were calibrated by photographic transfer from SA 94, using a plate taken on the night of December 9, 1974. These stars are identified in Fig. 21 and their magnitudes are given in Table 14. Results from 13 observations, including 3 pairs, are tabulated in Table 15. Variation is evident in Fig. 22. The graph shows PHL 1194 brightening over the period 1974 to 1977 and much fainter in 1978. The mean magnitude is $17^m.47$, with a range of $0^m.65$ and an average rms scatter of the comparison stars of $0^m.10$ (see Table 43). Statistics give a confidence level greater than 99.9 percent that this object is variable.

TABLE 14

Comparison Stars for PHL 1194

Star	1	2	3	4	5	6	7	8	9	10	11	12
Mag.	18.49	17.36	16.98	15.95	17.22	17.41	17.27	18.84	16.60	17.28	18.64	16.06

Fig. 21. PHL 1194 Field (facing page). This photograph was reproduced from a plate taken at Rosemary Hill Observatory on the night of November 1, 1975. North is at the top and east is to the left. One minute of arc equals 7mm. The object is identified by two short perpendicular lines. The magnitudes of the comparison stars are given in TABLE 14 (above).

4
3 2
1
5
12
11 6 7
10 9 8

TABLE 15
B Magnitudes of PHL 1194

Date	EST	JD	Mag.	rms
12/ 9/74	2231	42391.647	17.78	0.06
8/14/75	0333	42638.856	17.53	0.11
10/13/75	0142	42698.779	17.47	0.13
11/ 1/75	2150	42718.618	17.34	0.07
12/24/75	2213	42771.634	17.43	0.09
8/28/76	0245	43018.823	17.36	0.09
8/28/76	0254	43018.829	17.65	0.13
10/22/76	0052	43073.744	17.49	0.10
10/22/76	0044	43073.739	17.62	0.08
12/18/76	2022	43131.557	17.39	0.10
12/18/76	2031	43131.563	17.28	0.06
9/20/77	0328	43406.853	17.12	0.12
11/ 3/78	2233	43816.648	17.63	0.12

Key to Fig. 22. Data points whose rms is less than or equal to 0.1 Mag. are shown by a circle. Points with an rms greater than 0.1 Mag. are shown by a cross. A point corresponding to the weighted mean is plotted for two observations on the same night. Error bars at the right represent the mean magnitude of the object $\pm 1 \sigma$.

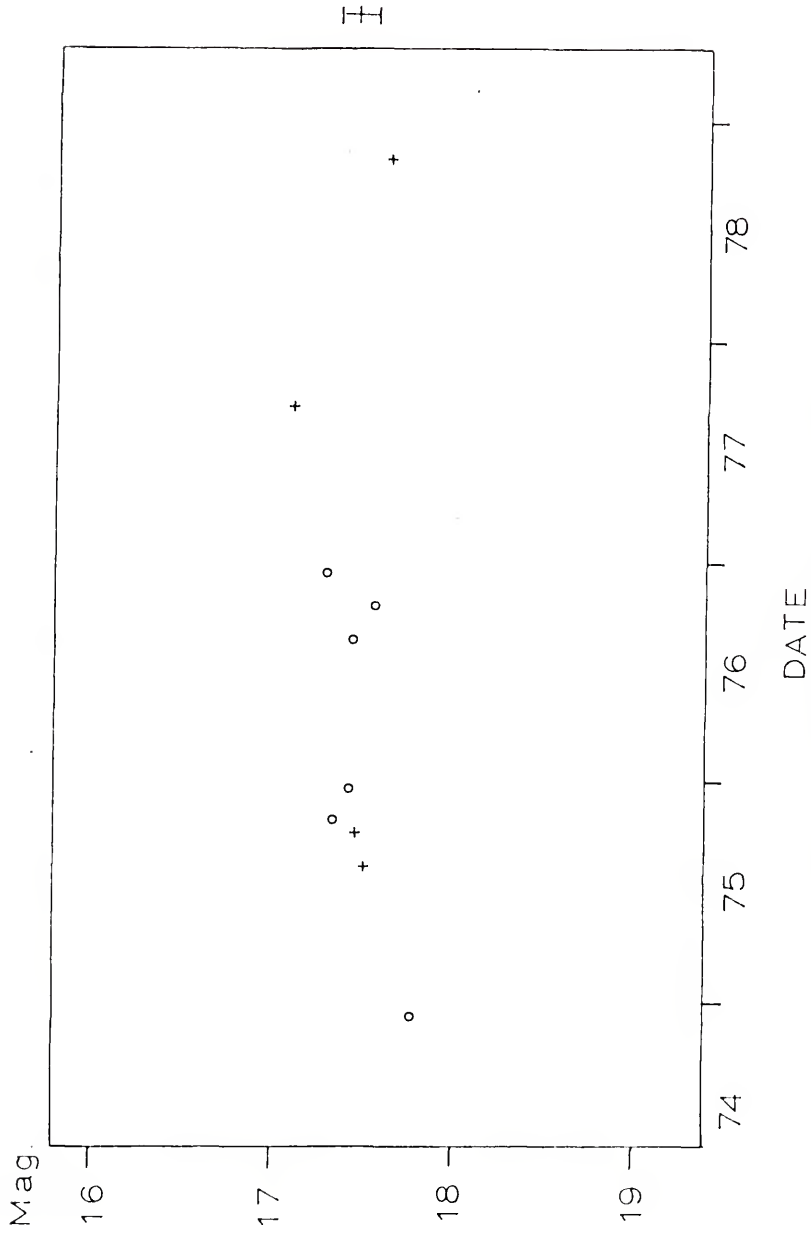


Fig. 22. Variation with Time of PHL 1194.

PHL 1222

PHL 1222, located at $1^{\text{h}} 51^{\text{m}} 12^{\text{s}}$ and $+4^{\circ} 48'$, was one of the blue objects found by Haro and Luyten (1962). Photometry by Sandage and Luyten (1967) gives a V magnitude of $17^{\text{m}}.63$, $B - V = 0^{\text{m}}.41$ and $U - B = 0^{\text{m}}.78$. Burbidge (1968) determined the emission line redshift to be 1.910. An absorption line, probably Ly_{α} , is also present. Fanti et al. (1977) detected no radio emission at 1.4 GHz greater than 20 mfu. The detection level here is somewhat larger due to the presence of a nearby radio source.

Comparison stars for PHL 1222 were calibrated by photographic transfer from SA 94, using a plate taken on the night of December 24, 1975. These stars are identified in Fig. 23 and their magnitudes are recorded in Table 16. Thirteen observations of PHL 1222, including 3 pairs, were made at Rosemary Hill Observatory. The resulting magnitudes are given in Table 17 and they are plotted against time in Fig. 24. The brightness of the object appears to be steady with a possible slight decline in 1978. No convincing evidence of variation is seen. The mean magnitude is $17^{\text{m}}.72$, with a range of $0^{\text{m}}.29$ and an rms scatter of the comparison stars of $0^{\text{m}}.07$ (Table 43).

PHL 1226

One of the objects found by the Haro and Luyten (1962) survey, PHL 1226 at $1^{\text{h}} 51^{\text{m}} 48^{\text{s}}$ and $+4^{\circ} 34'$, aroused extra interest due to its close proximity to a galaxy, IC 1746. Photometry by Sandage and Luyten

TABLE 16
Comparison Stars for PHL 1222

Star	1	2	3	4	5	6	7	8	9	10	11	12
Mag.	16.80	16.50	15.70	18.33	17.84	18.25	17.22	18.23	18.23	18.05	17.89	16.52

Fig. 23. PHL 1222 Field (facing page). This photograph was reproduced from a plate taken at Rosemary Hill Observatory on the night of November 21, 1976. North is at the top and east is to the left. One minute of arc equals 7mm. The object is identified by two short perpendicular lines. The magnitudes of the comparison stars are given in TABLE 16 (above).

10 18 7

12
11

3 1 2 9

4 5 6

TABLE 17

B Magnitudes of PHL 1222

Date	EST	JD	Mag.	rms
1/ 2/75	1959	42415.541	17.77	0.07
8/15/75	0316	42639.844	17.83	0.11
10/26/75	2224	42712.642	17.72	0.10
12/24/75	2232	42771.647	17.71	0.07
11/21/76	2153	43104.620	17.64	0.09
11/21/76	2201	43104.626	17.75	0.09
11/ 7/77	2159	43455.624	17.61	0.05
11/ 3/78	2347	43816.699	17.90	0.08

Key to Fig. 24. Data points whose rms is less than or equal to 0.1 Mag. are shown by a circle. Points with an rms greater than 0.1 Mag. are shown by a cross. A point corresponding to the weighted mean is plotted for two observations on the same night. Error bars at the right represent the mean magnitude of the object $\pm 1 \sigma$.

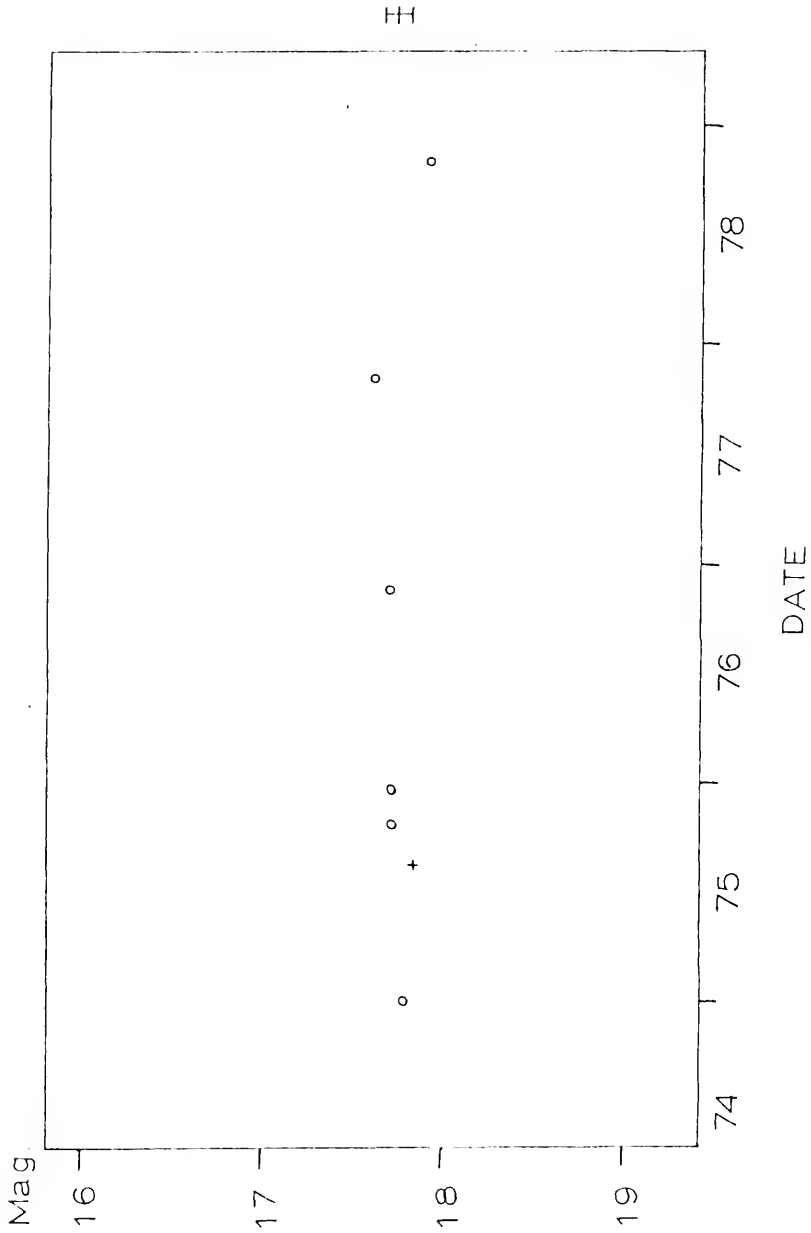


Fig. 24. Variation with Time of PHL 1222.

TABLE 18
Comparison Stars for PHL 1226

Star	1	2	3	4	5	6	7	8	9	10	11	12
Mag.	16.22	18.22	14.46	18.03	15.74	16.79	18.02	17.19	17.82	17.25	18.46	17.79

Fig. 25. PHL 1226 Field (facing page). This photograph was reproduced from a plate taken at Rosemary Hill Observatory on the night of January 1, 1976. North is at the top and east is to the left. One minute of arc equals 7mm. The object is identified by two short perpendicular lines. The magnitudes of the comparison stars are given in TABLE 18 (above).

.3 .5 .6

IC 1746

21 7 8 9 4
11 12

.10

TABLE 19
B Magnitudes of PHL 1226

Date	EST	JD	Mag.	rms
9/22/74	0301	42312.834	17.04	0.10
12/ 9/74	2329	42391.687	16.93	0.08
8/15/75	0323	42639.849	16.98	0.12
10/13/75	0217	42698.803	17.11	0.07
10/26/75	2238	42712.651	17.05	0.06
1/ 1/76	1914	42779.510	16.97	0.07
11/21/76	2258	43104.665	17.30	0.12
11/21/76	2306	43104.671	17.30	0.12
12/24/76	2238	43137.651	17.11	0.14
12/24/76	2247	42137.658	17.19	0.07
11/ 7/77	2150	43455.618	17.28	0.12
11/ 3/78	2356	43816.706	17.07	0.09

Key to Fig. 26. Data points whose rms is less than or equal to 0.1 Mag. are shown by a circle. Points with an rms greater than 0.1 Mag. are shown by a cross. A point corresponding to the weighted mean is plotted for two observations on the same night. Error bars at the right represent the mean magnitude of the object $\pm 1 \sigma$.

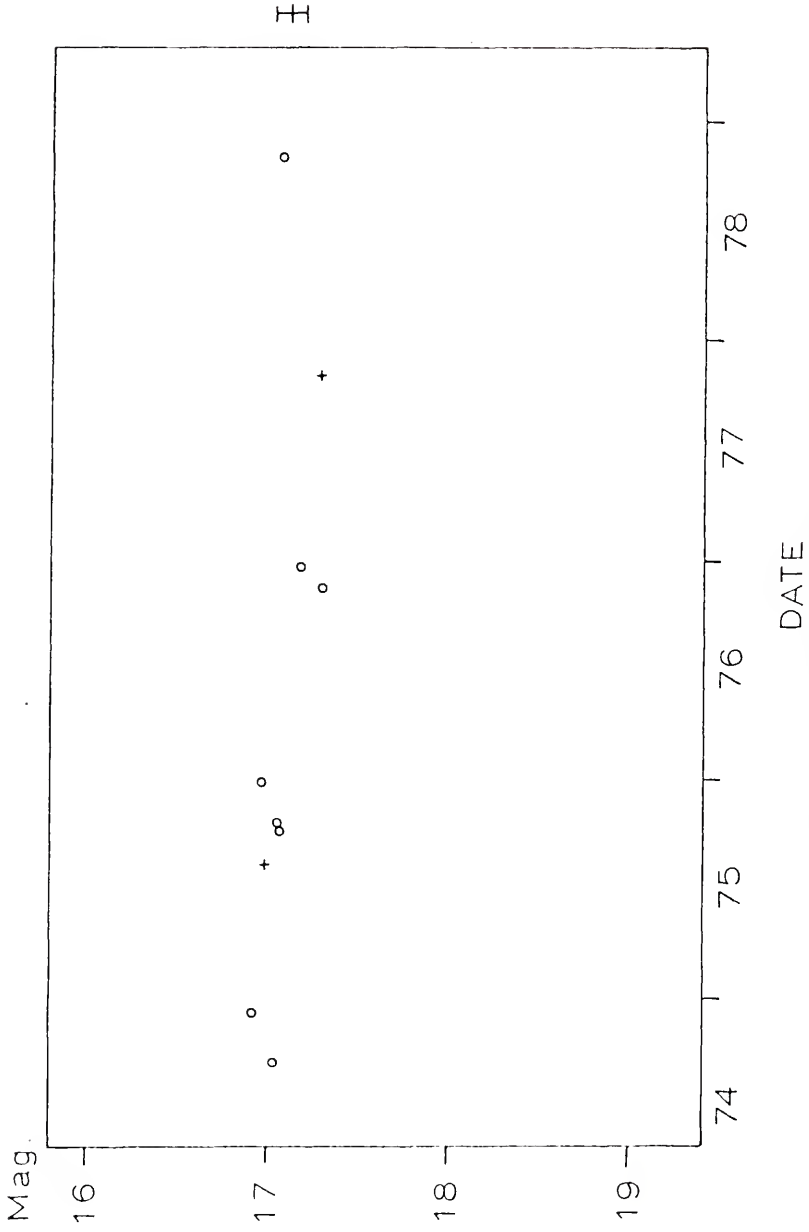


Fig. 26. Variation with Time of PHL 1226.

(1967) gave its magnitude at $17^m.5$ and its colors as $B - V = 0^m.04$ and $U - B = -0^m.72$. Burbidge (1968) measured its redshift as $z = 0.404$. Burbidge et al. (1971) reported the existence of a faint 19th-magnitude object between the QSO and the galaxy. This object proved to be transitory. A radio search by Fanti et al. (1977) at 1.4 GHz failed to detect any radio emission to the detection limit of 20 mfu.

The comparison stars for the PHL 1226 field were calibrated by photographic transfer from SA 94, using a plate taken on the night of January 11, 1976. These stars are identified in Fig. 25 and their magnitudes are given in Table 18. Twelve observations were made of PHL 1226, including 2 pairs. The resulting magnitudes are given in Table 19. Figure 26 shows the behavior of PHL 1226 with time. The object brightened in 1974 and declined from 1975 to 1977, possibly rising again in 1978. The mean magnitude is $17^m.12$, with a range of $0^m.36$ and an average rms scatter of the comparison stars of $0^m.08$. Statistics show a 98 percent confidence of variation.

On the night of November 7, 1977, a strange, possibly non-stellar object of approximately $18^m.7$ appeared near the QSO on the side opposite the galaxy. This object appeared only on this exposure and possibly, on the same night, at the edge of the field of PHL 1222, which overlaps PHL 1226.

Summary

This sample contains 7 objects from the Sandage and Luyten (1967) field at $1^h +6^o$ and one nearby object, PHL 938, with the same colors

(Table 1). These 8 objects have a spread in V magnitude from $17^m.04$ to $18^m.15$. Their B - V colors range from $-0^m.07$ to $+0^m.41$ and their U - B colors from $-0^m.51$ to $-0^m.88$. There are redshifts from $z = 0.27$ to $z = 1.93$.

Variability results are shown in Table 43. Three objects (PHL 938, PHL 1027 and PHL 1222) have shown no real evidence of variation during this time period. One object (PHL 3375) whose variability has a confidence level (C.L.) greater than 90 percent is probably variable, but variability is not usually considered established unless the confidence level exceeds 95 percent. Three objects (PHL 3632, PHL 1186 and PHL 1226) are variable (C.L. >95%) and one (PHL 1194) is strongly variable (C.L. >99%). No relation between variability and magnitude, color or redshift is apparent in this sample.

CHAPTER 5

FIELD AT $13^{\text{h}} +36^{\circ}$

M 3

The comparison stars for the RQOSOs in the Braccesi field at $13^{\text{h}} +36^{\circ}$ were calibrated using stars in M 3 located at $13^{\text{h}} 40^{\text{m}} +28.6^{\circ}$. A photoelectric sequence of outer stars in M 3 was published by Sandage (1970), giving V magnitudes and B - V and U - B colors. This allows calculation of B magnitudes for these stars. Eleven observations were made of the area of M 3. A sequence of 14 stars was read on each plate and the magnitudes were iteratively smoothed to give the best fit for this photographic system. These 14 stars are identified in Fig. 27. Their designation and magnitudes are listed in Table 20.

BSO 1

BSO 1 was one of the original blue "interlopers" found by Sandage (1965) and Sandage and Veron (1965). They reported a redshift of 1.241. Braccesi et al. (1968) measured its magnitude and colors, finding $V = 16^{\text{m}}98$, $B - V = 0^{\text{m}}31$, $U - B = -0^{\text{m}}78$, and infrared excess (Iex) of $-0^{\text{m}}30$. Absorption lines were also visible in the spectrum. Further photometry of this field was done by Braccesi et al. (1970). It is number 9 on that list. A more precise optical position is given by

TABLE 20

Standard Stars in M 3

Number	Designations*	Old B Mag.*	Smoothed B Mag.
1	II-18	15.05	15.09
2	II-6	15.69	15.73
3	II-13	15.85	15.82
4	II-4	15.94	15.96
5	II-11	16.10	16.13
6	I-27	16.12	16.03
7	I-56	16.21	16.21
8	I-47	16.27	15.81
9	F	16.58	16.58
10	II-9	17.45	17.54
11	II-29	18.04	17.99
12	F 1	18.45	18.45
13	F 2	18.98	18.99
14	F 3	19.10	19.05
15	F 5	19.29	
16	F 6	19.49	
17	F 7	20.11	

* Sandage, 1970.

NOTE: Stars 15, 16 and 17 were used to extend the sequences for B 234 and B 312.

Fig. 27. M 3 Field (facing page). This photograph was reproduced from a plate taken at Rosemary Hill Observatory on the night of April 28, 1976. North is at the top and east is to the left. One minute of arc equals 7 mm. The magnitudes of the standard stars are given in TABLE 20.

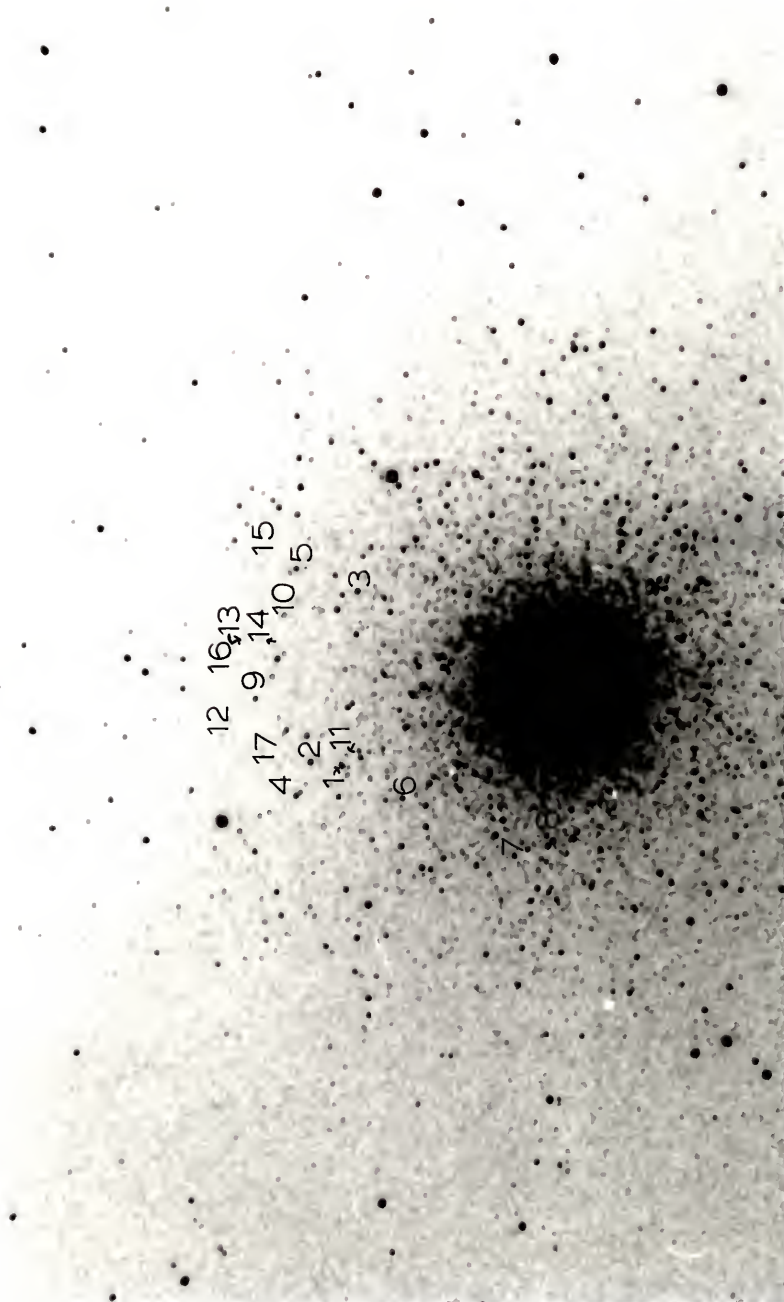


TABLE 21
Comparison Stars for BSO 1

Star	1	2	3	4	5	6	7	8	9	10	11	12
Mag.	17.18	17.57	17.35	16.08	16.36	17.48	18.37	16.62	14.72	17.91	16.60	16.45

Fig. 28. BSO 1 Field (facing page). This photograph was reproduced from a plate taken at Rosemary Hill Observatory on the night of January 25, 1976. North is at the top and east is to the left. One minute of arc equals 7mm. The object is identified by two short perpendicular lines. The magnitudes of the comparison stars are given in TABLE 21 (above).

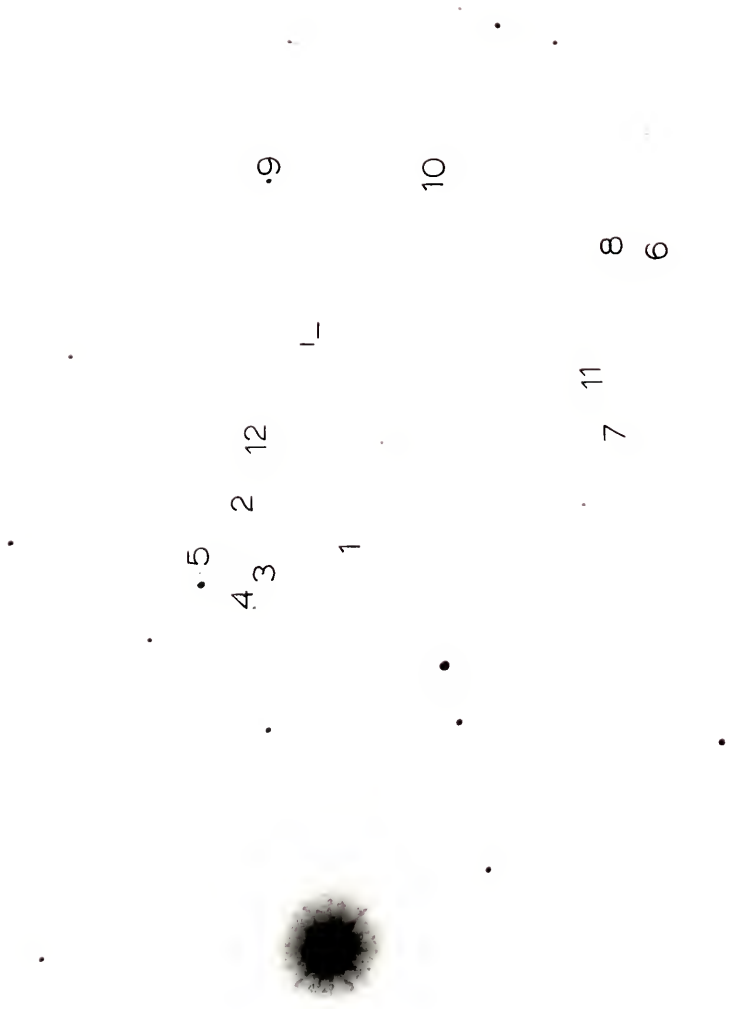


TABLE 22
B Magnitudes of BSO 1

Date	EST	JD	Mag.	rms
3/20/75	0312	42491.842	17.94	0.16
12/10/75	0531	42756.938	17.95	0.19
1/ 2/76	0503	42779.919	17.94	0.09
1/ 5/76	0503	42782.919	17.93	0.23
2/11/76	0402	42819.876	17.90	0.14
3/27 76	2128	42865.603	17.94	0.08
6/24/76	2314	42954.676	17.85	0.16
7/17/76	2153	42977.620	17.81	0.08
1/26/77	0514	42169.926	17.88	0.13
4/12/77	2312	43246.675	17.92	0.12
4/12/77	2318	43246.679	17.86	0.09
5/19/77	2314	43283.676	17.44	0.19
5/19/77	2321	43283.681	17.59	0.21
2/12/78	0315	43551.844	17.67	0.10
4/ 5/78	2240	43604.653	17.62	0.09
6/ 7/78	2250	43667.660	17.39	0.16
7/ 2/78	2208	43692.631	17.60	0.22

Key to Fig. 29. Data points whose rms is less than or equal to 0.1 Mag. are shown by a circle. Points with an rms greater than 0.1 Mag. are shown by a cross. A point corresponding to the weighted mean is plotted for two observations on the same night. Error bars at the right represent the mean magnitude of the object $\pm 1 \sigma$.

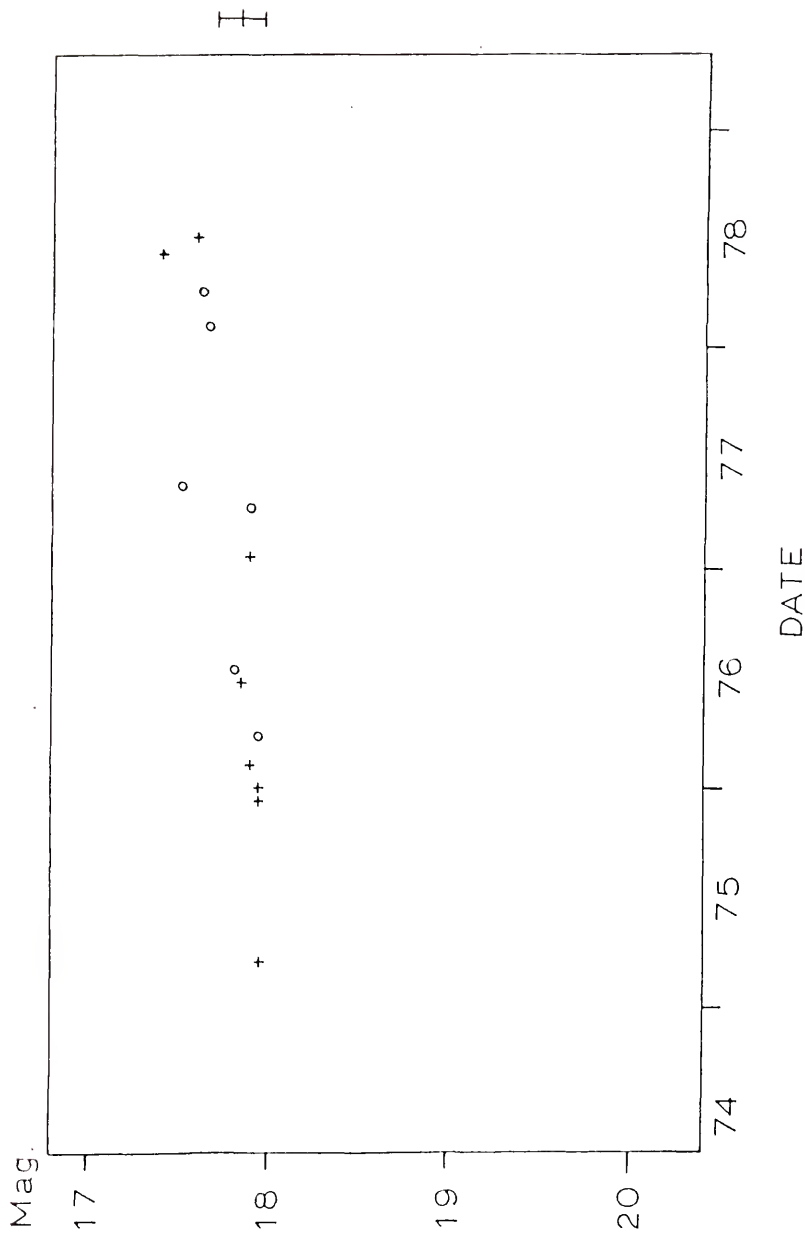


Fig. 29. Variation with Time of BSO 1.

Braccesi et al. (1973) as $12^{\text{h}} 46^{\text{m}} 28.7^{\text{s}}$ and $+37^{\circ} 46' 50''$. It was not detected in the radio by Katgert et al. (1973) with a detection limit of 10 mfu at 1.4 GHz.

Comparison stars for BSO 1 were calibrated by photographic transfer from M 3, using a plate taken on the night of January 25, 1977. The magnitudes of these comparison stars are given in Table 21 and they are identified in Fig. 28. Resulting magnitudes of 17 observations, including 2 pairs, are given in Table 22 and plotted in Fig. 29. BSO 1 has shown a slow, steady increase in magnitude over this 4-year period. The mean magnitude is $17^{\text{m}}80$, with a range of $0^{\text{m}}56$ compared to an rms scatter of the comparison stars of $0^{\text{m}}13$. (Since plate effects become more important for the fainter images, the average rms scatter of the comparison stars is expected to be greater in the fields of the fainter objects.) Statistics show BSO 1 to be variable at the 99 percent confidence level (Table 43).

B 46

Found by Braccesi et al. (1968), B 46 has a V magnitude of $17^{\text{m}}83$, B - V of $0^{\text{m}}36$, U - B of $-0^{\text{m}}87$ and Iex of $-1^{\text{m}}3$. Its redshift is 0.271. It is object AB 11 in the listing of Braccesi et al. (1970). A refined optical position of $12^{\text{h}} 46^{\text{m}} 29.6^{\text{s}}$ and $+34^{\circ} 40' 49''$ is given by Braccesi et al. (1973). It was not detected in the radio by Katgert et al. (1973) with a detection limit of 10 mfu at 1.4 GHz, or by Colla et al. (1970) with a limit of 20 mfu at 408 MHz.

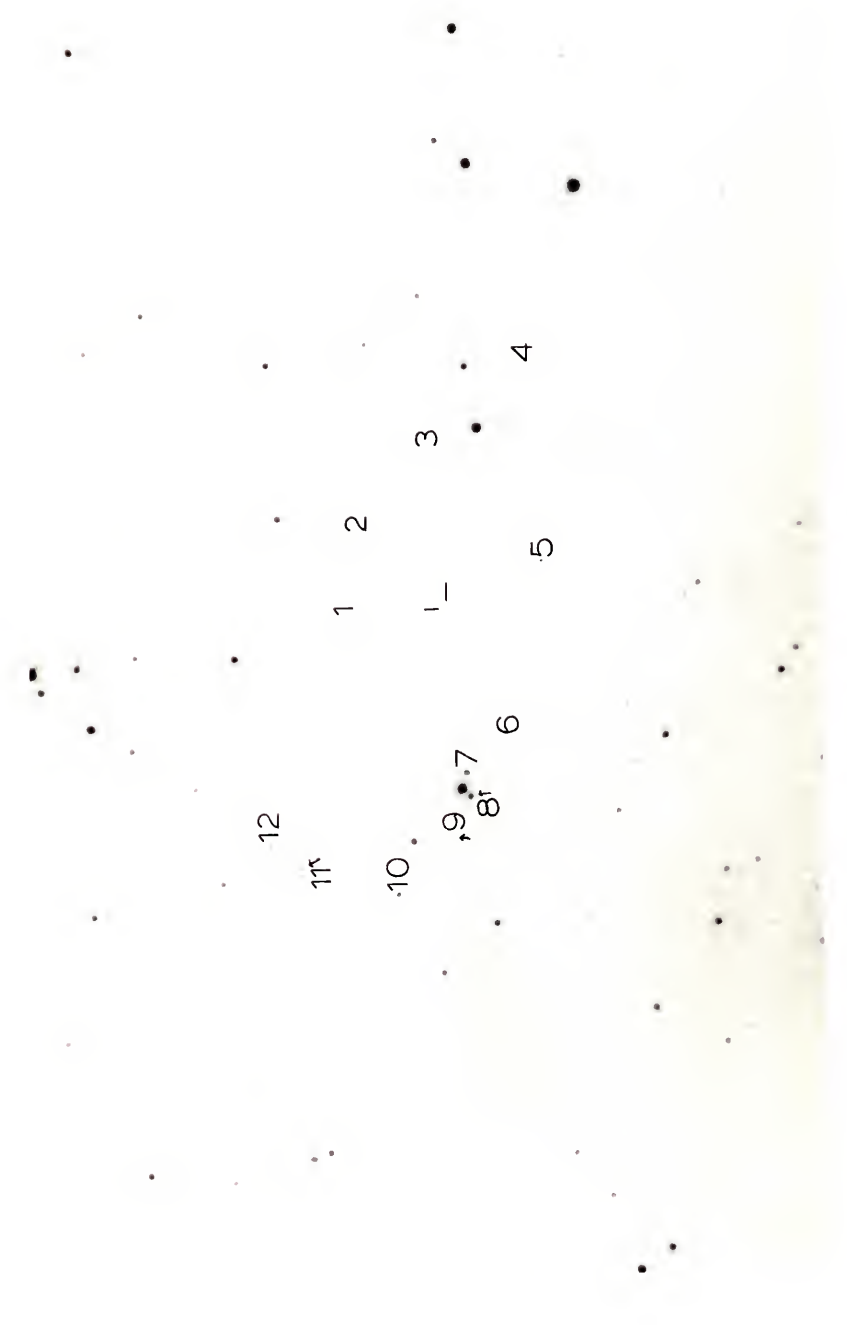
Comparison stars for B 46 were calibrated by photographic transfer from M 3 using a plate taken on the night of July 25, 1976. These stars

TABLE 23

Comparison Stars for B 46

Star	1	2	3	4	5	6	7	8	9	10	11	12
Mag.	17.00	18.44	17.41	17.17	17.10	17.69	15.70	14.82	18.07	14.63	16.87	17.12

Fig. 30. B 46 Field (facing page). This photograph was reproduced from a plate taken at Rosemary Hill Observatory on the night of April 21, 1976. North is at the top and east is to the left. One minute of arc equals 7mm. The object is identified by two short perpendicular lines. The magnitudes of the comparison stars are given in TABLE 23 (above).



12

11

10

9

8

6

1

2

3

4

5

TABLE 24
B Magnitudes of B 46

Date	EST	JD	Mag.	rms
5/11/75	2322	42544.682	17.76	0.11
1/ 2/76	0425	42779.911	17.80	0.06
3/27/76	2147	42865.616	17.83	0.07
4/21/76	2227	42890.644	17.82	0.08
4/21/76	2235	42890.649	18.04	0.09
7/17/76	2209	42977.631	17.97	0.18
7/25/76	2103	42985.585	18.03	0.15
2/25/77	0206	43199.796	18.24	0.13
2/25/77	0215	43199.802	18.31	0.10
4/12/77	2343	43246.697	18.19	0.12
4/12/77	2349	43246.701	18.16	0.13
5/19/77	2340	43283.694	18.19	0.12
5/19/77	2347	43283.699	18.23	0.12
2/12/78	0327	43551.852	17.92	0.11
4/ 5/78	2322	43604.682	18.32	0.08
6/ 7/78	2303	43667.669	17.90	0.08
7/ 2/78	2218	43692.637	18.27	0.16
7/10/78	2333	43700.690	18.32	0.15

Key to Fig. 31. Data points whose rms is less than or equal to 0.1 Mag. are shown by a circle. Points with an rms greater than 0.1 Mag. are shown by a cross. A point corresponding to the weighted mean is plotted for two observations on the same night. Error bars at the right represent the mean magnitude of the object $\pm 1 \sigma$.

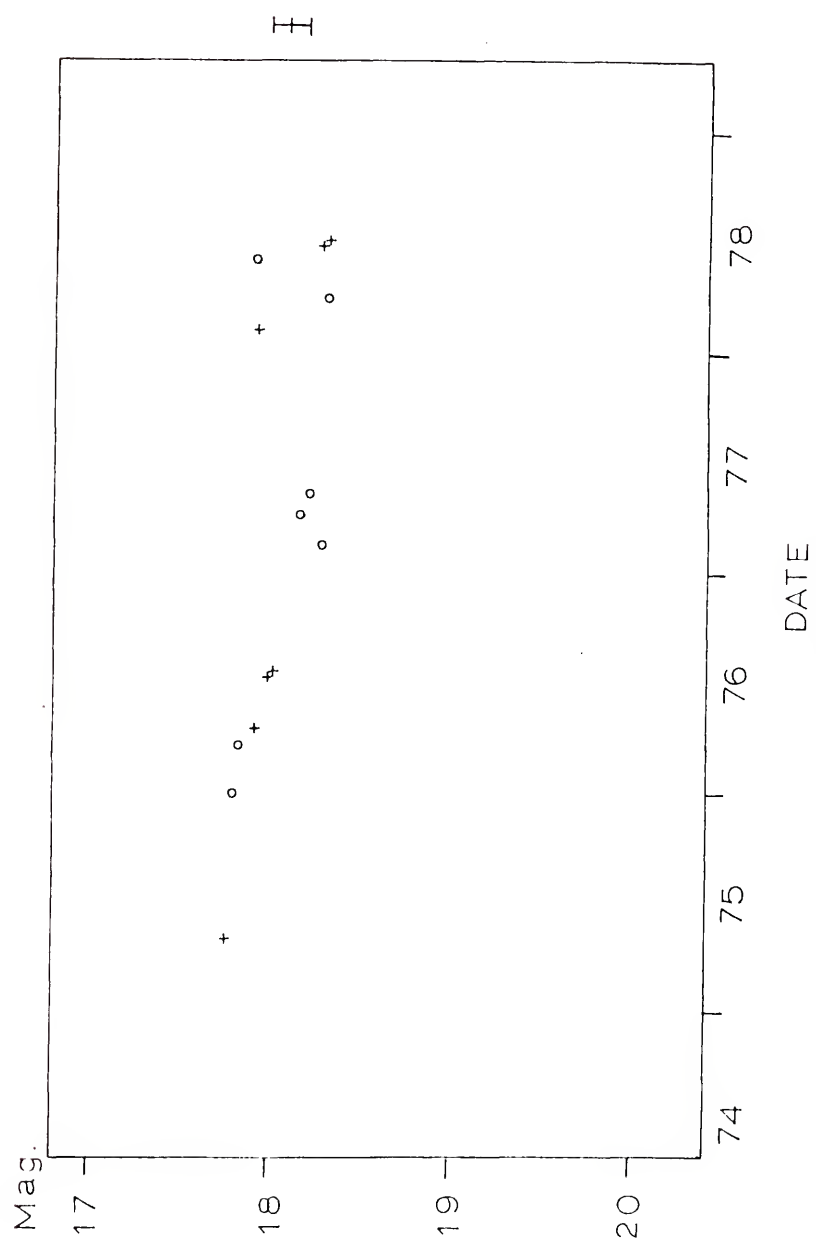


Fig. 31. Variation with Time of B 46.

are identified in Fig. 30 and their magnitudes are given in Table 23. Eighteen observations of B 46, including 4 pairs, were made at Rosemary Hill Observatory. The magnitudes were recorded in Table 24 and the variation with time is shown in Fig. 31. A decline over the period 1975-1977 is followed by activity in 1978 including higher points in February and June. This object is the most variable (C.L. > 99.9%) in this sample of RQOSOs (Table 43), and it shows two different types of variability. The mean magnitude is 18^m08 , with a range of 0^m56 compared to the average rms scatter of the comparison stars of 0^m10 .

BSO 2

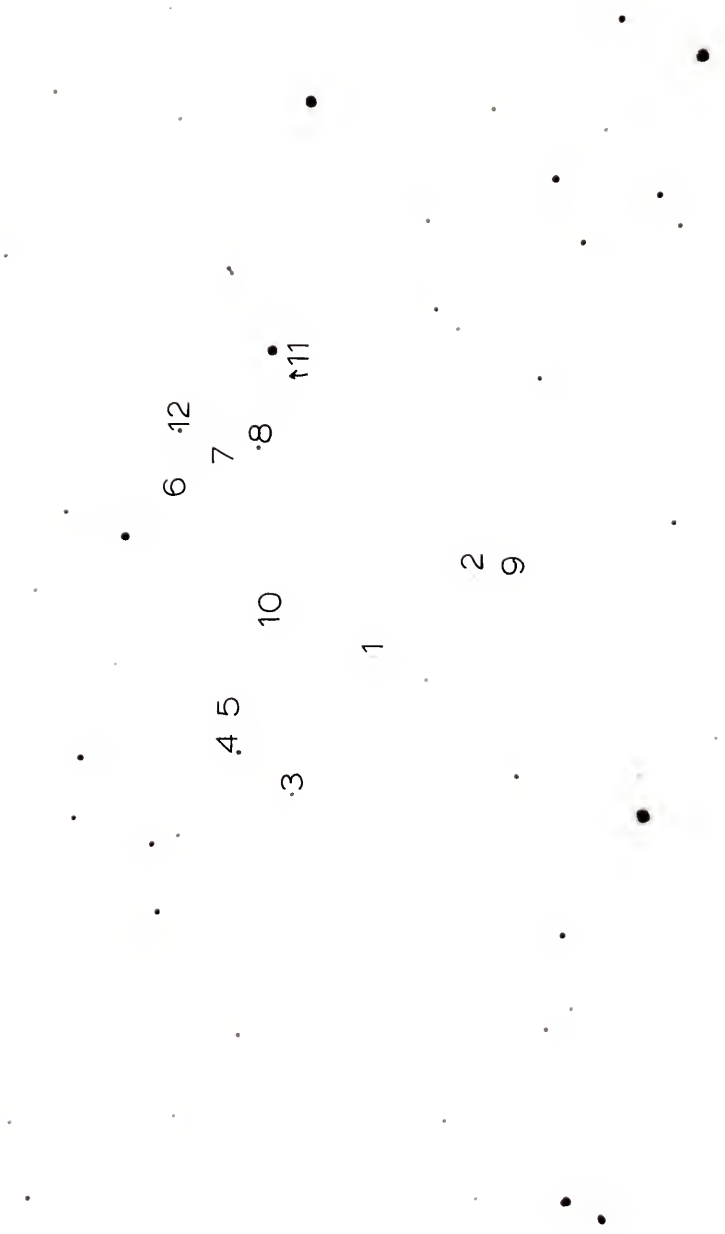
Sandage and Veron (1965) studied this object because of its strong ultraviolet image. Photometry by Braccesi et al. (1968) found a V magnitude of 18^m64 , B - V of 0^m28 , U - B of 0^m98 and Iex of -1^m6 . A redshift of 1.86 is based on two lines, tentatively identified with neon and oxygen. BSO 2 is the same as B 47 on their list, and it was later referred to as object AB 17 in the study by Braccesi et al. (1970). A refined optical position of $12^h 48^m 17.7^s$ and $+33^\circ 47' 11''$ was given by Braccesi et al. (1973). It was not detected in the radio by Katgert et al. (1973) with a detection limit of 10 mfu at 1.4 GHz, or by Colla et al. (1970) with a limit of 20 mfu at 408 MHz.

Comparison stars for BSO 2 were calibrated by photographic transfer from M 3 using a plate taken on the night of May 20, 1976. Their magnitudes are given on Table 25 and their positions are shown in Fig. 32. Twelve observations of BSO 2, including two pairs, were taken at Rosemary Hill Observatory. The magnitudes of BSO 2 are given in

TABLE 25
Comparison Stars for BSO 2

Star	1	2	3	4	5	6	7	8	9	10	11	12
Mag.	17.05	16.78	16.09	15.27	19.22	17.83	17.65	15.53	18.29	18.76	17.89	15.18

Fig. 32. BSO 2 Field (facing page). This photograph was reproduced from a plate taken at Rosemary Hill Observatory on the night of April 10, 1976. North is at the top and east is to the left. One minute of arc equals 7mm. The object is identified by two short perpendicular lines. The magnitudes of the comparison stars are given in TABLE 25 (above).



6 12

7

8

11

4 5

10

3

1

2

9

TABLE 26

B Magnitudes of BSO 2

Date	EST	JD	Mag.	rms
1/ 2/76	0524	42779.933	18.81	0.11
3/27/76	2209	42865.631	18.49	0.12
4/ 2/76	2231	42871.647	19.20	0.12
5/29/76	2126	42928.501	18.95	0.13
2/21/77	0420	43195.389	18.88	0.11
2/21/77	0429	43195.895	18.82	0.14
4/10/77	2241	43244.653	18.86	0.08
4/10/77	2234	43244.649	18.59	0.15
2/12/78	0344	43551.864	18.63	0.14
5/ 4/78	2326	43633.685	18.82	0/13
6/ 7/78	2319	43667.680	18.82	0.14
7/ 2/78	2234	43692.649	18.67	0.14

Key to Fig. 33. Data points whose rms is less than or equal to 0.1 Mag. are shown by a circle. Points with an rms greater than 0.1 Mag. are shown by a cross. A point corresponding to the weighted mean is plotted for two observations on the same night. Error bars at the right represent the mean magnitude of the object $\pm 1 \sigma$.

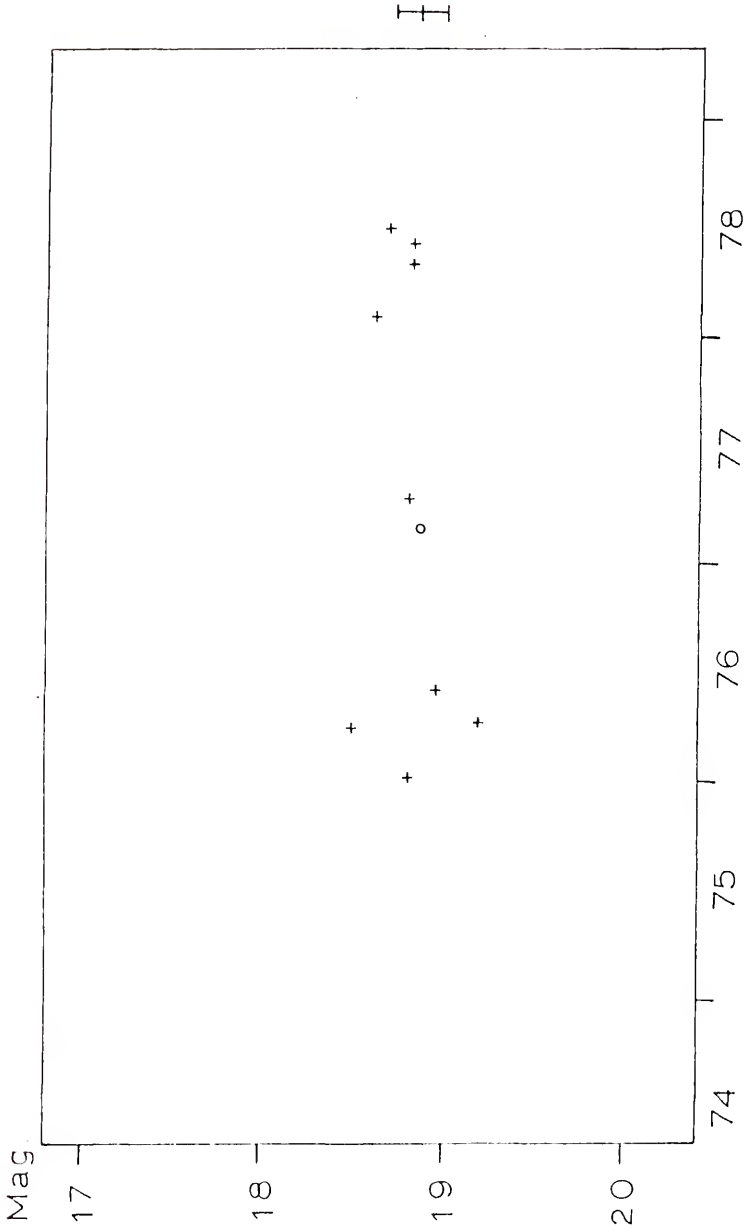


Fig. 33. Variation with Time of BSO 2.

Table 26, and they are shown graphically in Fig. 33. The object showed a sharp drop of $0^m.7$ over one week, March 27 to April 2, 1976. The mean magnitude is $18^m.83$, with a range of $0^m.71$ compared to an average rms scatter of the comparison stars of $0^m.12$ (Table 43). χ^2 statistics show that BSO 2 is probably variable (C. L. = 91%).

B 114

Braccesi et al. (1968) measured the V magnitude of B 114 as $17^m.92$, B - V as $0^m.08$, U - B as $-0^m.90$ and I_{ex} as $-1^m.2$. Its redshift is 0.221 based on lines of magnesium. Braccesi et al. (1973) list it as AB 47 at $12^h 52^m 57.9^s$ and $+33^\circ 35' 24''$. A radio survey at 1.4 GHz by Katgert et al. (1973) with a detection limit of 10 mfu, and one at 408 MHz by Colla et al. (1970) with a limit of 20 mfu, failed to find a source at this position.

Comparison stars for B 114 were calibrated by photographic transfer from M 3 using a plate taken on the night of July 25, 1976. These stars are identified in Fig. 34 and their magnitudes are listed in Table 27. Resulting magnitudes of twelve observations, including two pairs, are given in Table 28. The behavior with time is shown in Fig 35. B 114 shows a relatively steady decline over the entire 4-year period. It is $0^m.78$ fainter in 1978 than in 1975. B 114 is the second most variable object in this sample, with a confidence level greater than 99.9 percent (Table 43). The mean magnitude is $18^m.08$, with a range of $0^m.78$ compared to an average rms of the comparison stars of $0^m.10$.

TABLE 27

Comparison Stars for B 114

Star	1	2	3	4	5	6	7	8	9	10	11	12
Mag.	18.34	16.43	18.32	17.03	17.92	16.52	18.33	18.70	16.24	17.80	17.75	18.25

Fig. 34. B 114 Field (facing page). This photograph was reproduced from a plate taken at Rosemary Hill Observatory on the night of February 17, 1977. North is at the top and east is to the left. One minute of arc equals 7mm. The object is identified by two short perpendicular lines. The magnitudes of the comparison stars are given in TABLE 27 (above).

10
6 5
4 3
2
1 12
L
7
11
9
8

TABLE 28
B Magnitudes of B 114

Date	EST	JD	Mag.	rms
5/11/75	2353	42544.703	17.87	0.10
1/ 2/76	0524	42779.933	18.07	0.05
3/27/76	2305	42865.670	18.06	0.07
4/21/76	2302	42890.668	17.89	0.06
7/25/76	2137	42985.609	18.04	0.12
2/18/77	0416	43192.886	17.97	0.11
2/18/77	0424	43192.892	17.99	0.11
4/13/77	0002	43246.710	18.15	0.13
4/13/77	0008	43246.714	18.11	0.11
2/12/78	0416	43561.886	18.31	0.12
4/ 5/78	2322	43604.682	18.43	0.15
5/29/78	2234	43658.649	18.23	0.18
7/ 2/78	2246	43692.657	18.65	0.10

Key to Fig. 35. Data points whose rms is less than or equal to 0.1 Mag. are shown by a circle. Points with an rms greater than 0.1 Mag. are shown by a cross. A point corresponding to the weighted mean is plotted for two observations on the same night. Error bars at the right represent the mean magnitude of the object $\pm 1 \sigma$.

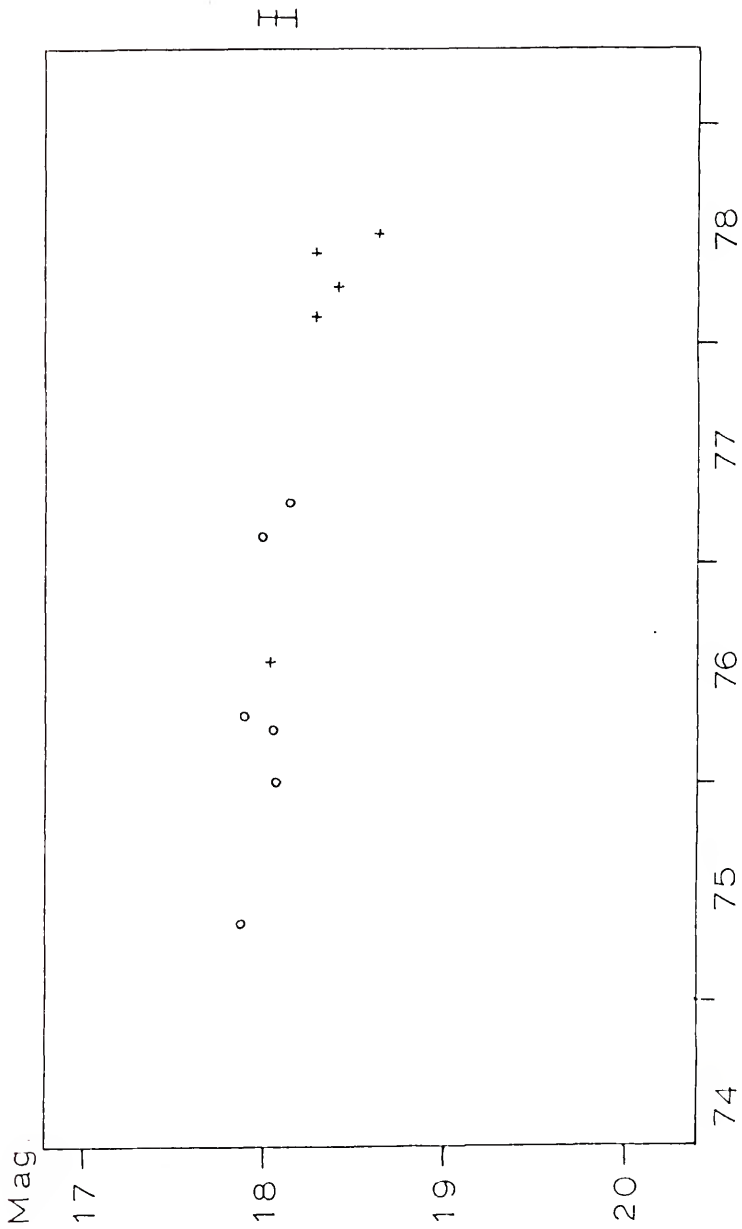


Fig. 35. Variation with Time of B 114.

B 154

Braccesi et al. (1968) found an 18^m56 (V) mag. object with appropriate colors of $B - V = 0^m32$, $U - V = 0^m70$ and $I_{ex} = -1^m2$. Its redshift of 0.183 is based on two oxygen lines. This is the same as object AB 64 on the list of Braccesi et al. (1973) at $12^h 55^m 2.1^s$ and $+35^\circ 21' 21''$. No radio source was found at this position by Katgert et al. (1973) at 1.4 GHz with a detection limit of 10 mfu, or by Colla et al. (1970) with a limit of 20 mfu at 408 MHz.

Comparison stars for B 154 were calibrated by photographic transfer from M 3 using a plate taken on June 19, 1977. These stars are identified in Fig. 36 and their magnitudes listed in Table 29. Thirteen observations, including 2 pairs, were made at Rosemary Hill Observatory. The magnitudes are given in Table 30. When these magnitudes are graphed versus time (Fig. 37) they show no secular change, but show a variation around the average magnitude. There was a sharp rise of 0^m49 in one month (May-June, 1978). The average magnitude is 18^m65 , with a range of 0^m78 compared to an average rms of the comparison stars of 0^m12 . Statistics show B 154 to be variable at the 97 percent confidence level (Table 43).

B 194

Braccesi et al. (1968) measured the magnitude of B 194 ($V = 17^m96$) and colors ($B - V = 0^m46$, $U - B = -0^m76$ and $I_{ex} = -1^m5$). Its redshift

TABLE 29
Comparison Stars for B 154

Star	1	2	3	4	5	6	7	8	9	10	11	12
Mag.	18.31	16.93	16.95	16.39	15.33	18.94	18.63	17.60	17.08	17.82	17.13	18.74

Fig. 36. B 154 Field (facing page). This photograph was reproduced from a plate taken at Rosemary Hill Observatory on the night of July 3, 1978. North is at the top and east is to the left. One minute of arc equals 7mm. The object is identified by two short perpendicular lines. The magnitudes of the comparison stars are given in TABLE 29 (above).

12

10

2

1

9 8

1-

3

4

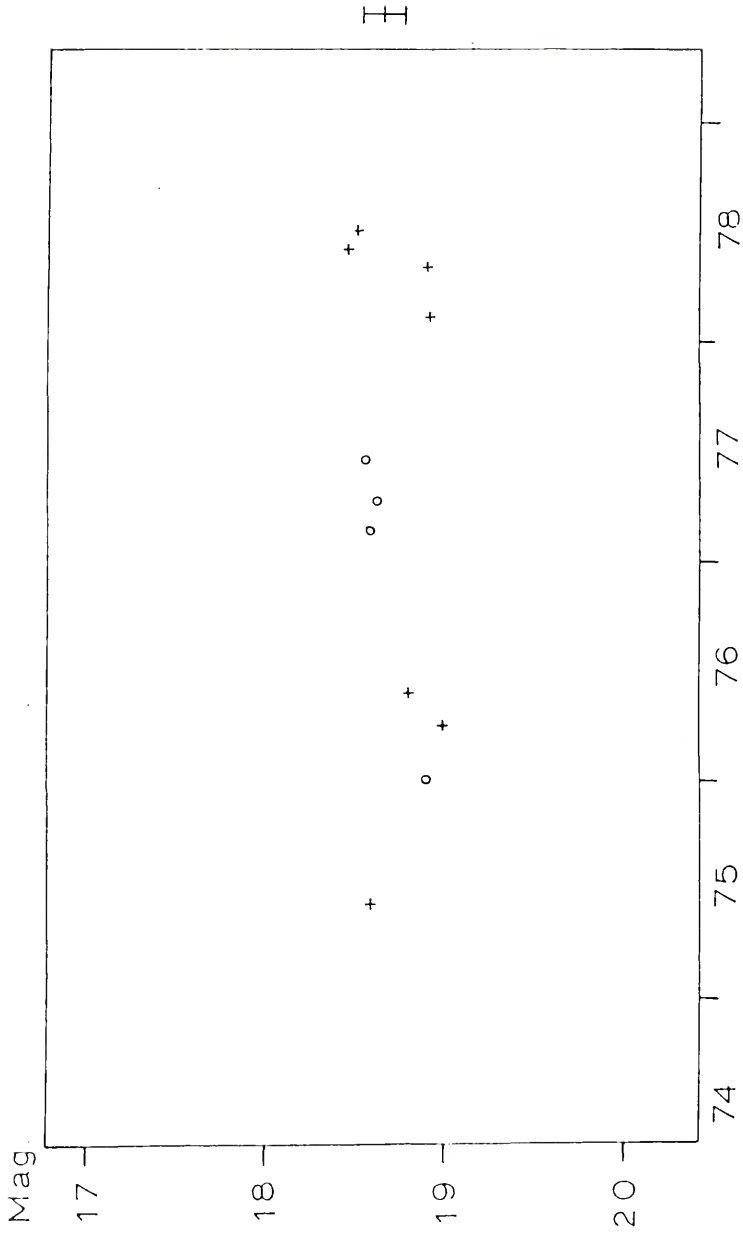
.5

6 11 7

TABLE 30
B Magnitudes of B 154

Date	EST	JD	Mag.	rms
6/11/75	2315	42575.677	18.58	0.14
1/ 2/76	0605	42799.962	18.89	0.10
4/ 2/76	2324	42871.683	18.98	0.14
5/29/76	2223	42928.641	18.80	0.14
2/25/77	0246	43199.824	18.60	0.13
2/25/77	0255	43199.830	18.54	0.12
4/10/77	2259	43244.666	18.62	0.06
4/10/77	2307	43244.672	18.57	0.13
6/19/77	2140	43314.611	18.54	0.10
2/15/78	0449	43554.909	18.90	0.13
5/ 4/78	2326	43633.685	18.91	0.13
6/ 7/78	2333	43667.690	18.46	0.16
7/ 3/78	2118	43693.596	18.50	0.14

Key to Fig. 37. Data points whose rms is less than or equal to 0.1 Mag. are shown by a circle. Points with an rms greater than 0.1 Mag. are shown by a cross. A point corresponding to the weighted mean is plotted for two observations on the same night. Error bars at the right represent the mean magnitude of the object $\pm 1 \sigma$.



DATE
Fig. 37. Variation with Time of B 154.

TABLE 31

Comparison Stars for B 194

Star	1	2	3	4	5	6	7	8	9	10	11	12
Mag.	15.29	14.89	16.10	17.05	16.93	14.46	17.27	17.48	16.51	18.49	18.78	15.76

Fig. 38. B 194 Field (facing page). This photograph was reproduced from a plate taken at Rosemary Hill Observatory on the night of February 10, 1976. North is at the top and east is to the left. One minute of arc equals 7mm. The object is identified by two short perpendicular lines. The magnitudes of the comparison stars are given in TABLE 31 (above).

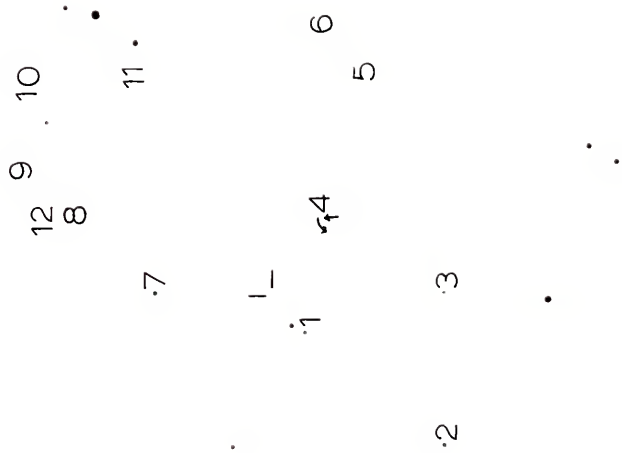


TABLE 32
B Magnitudes of B 194

Date	EST	JD	Mag.	rms
6/11/75	2251	42575.660	18.10	0.15
2/11/76	0422	42819.890	18.20	0.09
3/28/76	0039	42865.735	18.08	0.09
4/23/76	0031	42891.730	18.18	0.11
2/25/77	0311	43199.841	18.17	0.23
2/25/77	0320	43199.847	18.11	0.17
4/14/77	2344	43248.697	18.10	0.15
4/14/77	2352	43248.703	17.82	0.11
2/12/78	0427	43551.894	17.96	0.05
5/ 4/78	2339	43633.694	18.49	0.12
7/ 3/78	2132	43693.606	18.18	0.21

Key to Fig. 39. Data points whose rms is less than or equal to 0.1 Mag. are shown by a circle. Points with an rms greater than 0.1 Mag. are shown by a cross. A point corresponding to the weighted mean is plotted for two observations on the same night. Error bars at the right represent the mean magnitude of the object $\pm 1 \sigma$.

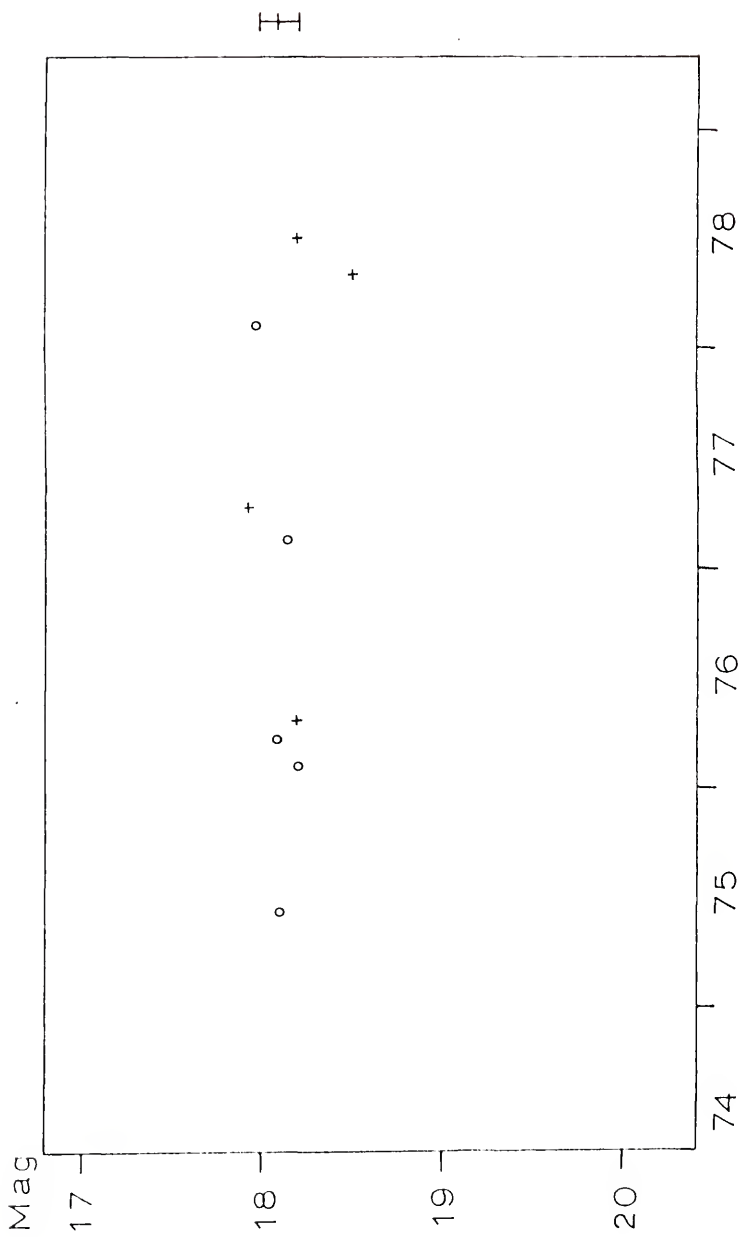


Fig. 39. Variation with Time of B 194.

of 1.864 is based on Ly_{α} , neon and carbon lines. Absorption lines are also present. B 194 is the same as AB 69 in the Braccesi et al. (1973) list. Its optical position is $12^{\text{h}} 56^{\text{m}} 7.8^{\text{s}}$ and $+35^{\circ} 44' 54''$. B 194 was detected in the radio by Katgert et al. (1973) at 1.4 GHz, and confirmed by Fanti et al. (1977) with a radio flux of 18 mfu. It could still be considered radio "quiet", although not radio "silent."

Comparison stars for B 194 were calibrated by photographic transfer from M 3 using a plate taken April 22, 1976, at Rosemary Hill Observatory. These magnitudes are given in Table 31. The stars are identified in Fig. 38. Results of 11 observations, including 2 pairs, are shown in Table 32. The behavior with time is shown graphically in Fig 39. Points are scattered about the mean except for a sharp drop in May 1978. B 194 is probably variable (C.L. = 94%). Its mean magnitude is $18^{\text{m}}09$, with a range of $0^{\text{m}}41$ and an average rms scatter of the comparison stars of $0^{\text{m}}11$ (Table 43).

B 201

B 201 had a V magnitude of $16^{\text{m}}79$, $B - V = 0^{\text{m}}26$, $U - B = -0^{\text{m}}82$ and $I_{\text{ex}} = -1^{\text{m}}0$ when it was studied by Braccesi et al. (1968). A redshift of 1.375 is based on two strong carbon lines. It is listed as object AB 78 by Braccesi et al. (1973), who give its position as $12^{\text{h}} 57^{\text{m}} 26.7^{\text{s}}$ and $+34^{\circ} 29' 31''$. B 201 was not detected by radio survey of Colla et al. (1970) at 408 MHz with a detection limit of 20 mfu, or by Katgert et al. (1973) with a limit of 10 mfu at 1.4 GHz.

TABLE 33

Comparison Stars for B 201

Star	1	2	3	4	5	6	7	8	9	10	11	12
Mag.	17.09	18.77	14.79	18.30	17.61	18.64	16.48	15.98	15.40	18.91	15.12	18.65

Fig. 40. B 201 Field (facing page). This photograph was reproduced from a plate taken at Rosemary Hill Observatory on the night of April 14, 1977. North is at the top and east is to the left. One minute of arc equals 7mm. The object is identified by two short perpendicular lines. The magnitudes of the comparison stars are given in TABLE 33 (above).

2 1 '9

L

3

4 10

8 12

5

6

7

11

TABLE 34

B Magnitudes of B 201

Date	EST	JD	Mag.	rms
3/ 4/76	0429	42841.895	17.15	0.24
3/27/76	2327	42865.685	16.97	0.14
4/23/76	0130	42891.771	17.21	0.10
7/17/76	2230	42977.646	17.18	0.11
2/18/77	0528	43192.936	17.28	0.12
3/28/77	0158	43230.790	16.95	0.07
3/28/77	0205	43230.796	17.13	0.11
4/15/77	0010	43248.715	17.12	0.11
4/15/77	0014	43248.718	16.99	0.18
2/12/78	0531	43551.938	17.59	0.16
4/ 6/78	0019	43604.722	17.57	0.16
5/29/78	2248	43658.658	17.31	0.12
7/ 2/78	2330	43692.687	17.25	0.17

Key to Fig. 41. Data points whose rms is less than or equal to 0.1 Mag. are shown by a circle. Points with an rms greater than 0.1 Mag. are shown by a cross. A point corresponding to the weighted mean is plotted for two observations on the same night. Error bars at the right represent the mean magnitude of the object $\pm 1 \sigma$.

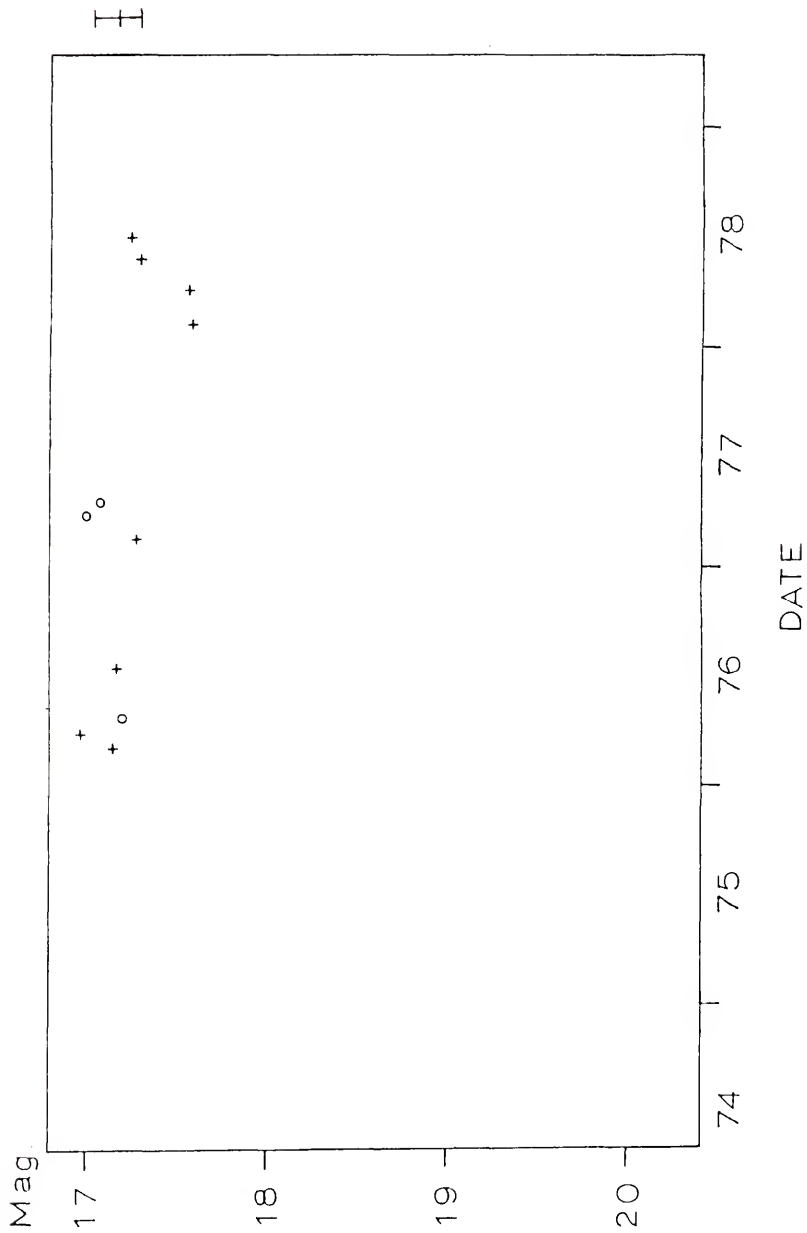


Fig. 41. Variation with Time of B 201.

Comparison stars for B 201 were calibrated by photographic transfer from M 3 using a plate taken on the night of April 14, 1977. The magnitudes of these stars are given in Table 33, and the stars are identified in Fig. 40. Thirteen observations of B 201, including 2 pairs, were taken. The magnitudes are shown in Table 34. The graph in Fig. 41 shows their distribution with time. B 201 appeared fainter in February and April 1978 and brighter in May and June of that year. This object is probably variable (C.L. = 94%). The mean magnitude is $17^m.17$, with a range of $0^m.62$ compared with an average rms scatter of the comparison stars of $0^m.13$ (Table 43).

BSO 6

The object referred to here as BSO 6 was identified by Sandage and Veron (1965). It is the same as B 243 in the list of Braccesi et al. (1968), who list its V magnitude as $17^m.67$, B - V as $0^m.05$, U - B as $-1^m.01$ and Iex as $-1^m.2$. The redshift of 1.956 is based on Ly_{α} , neon, silicon and carbon lines. Braccesi et al. (1973) refer to BSO 6 as AB 90 and give its location as $12^h 59^m 31^s$ and $+34^{\circ} 27' 19''$. No radio emission was detected at this position by Colla et al. (1970) at 408 MHz with a detection limit of 20 mfu, or by Katgert et al. (1973) with a limit of 10 mfu at 1.4 GHz.

Comparison stars for BSO 6 were calibrated by photographic transfer from M 3 using a plate taken on the night of April 28, 1976. These stars are identified in Fig. 42 and their magnitudes are given in Table 35. The resulting magnitudes from fourteen observations of BSO 6,

TABLE 35

Comparison Stars for ESO 6

Star	1	2	3	4	5	6	7	8	9	10	11	12
Mag.	18.06	17.32	17.71	14.27	18.44	18.40	17.77	16.50	18.44	18.21	17.72	17.25

Fig. 42. ESO 6 Field (facing page). This photograph was reproduced from a plate taken at Rosemary Hill Observatory on the night of April 28, 1976. North is at the top and east is to the left. One minute of arc equals 7mm. The object is identified by two short perpendicular lines. The magnitudes of the comparison stars are given in TABLE 35 (above).



TABLE 36

B Magnitudes of BSO 6

Date	EST	JD	Mag.	rms
5/12/75	0017	42544.720	18.22	0.13
3/ 6/76	0429	42843.895	18.01	0.13
3/28/76	0023	42865.724	18.16	0.08
4/28/76	2256	42897.664	18.35	0.11
2/18/77	0458	43192.915	18.42	0.12
2/18/77	0514	43192.926	18.30	0.09
3/28/77	0229	43230.812	18.03	0.08
3/28/77	0237	43230.817	18.40	0.12
4/13/77	0022	43246.724	18.47	0.12
4/13/77	0028	43246.728	18.20	0.09
2/12/78	0545	43551.948	18.05	0.14
4/ 5/78	2348	43604.700	18.28	0.12
5/29/78	2309	43658.673	18.17	0.08
7/ 2/78	2315	43692.677	18.15	0.20

Key to Fig. 43. Data points whose rms is less than or equal to 0.1 Mag. are shown by a circle. Points with an rms greater than 0.1 Mag. are shown by a cross. A point corresponding to the weighted mean is plotted for two observations on the same night. Error bars at the right represent the mean magnitude of the object $\pm 1 \sigma$.

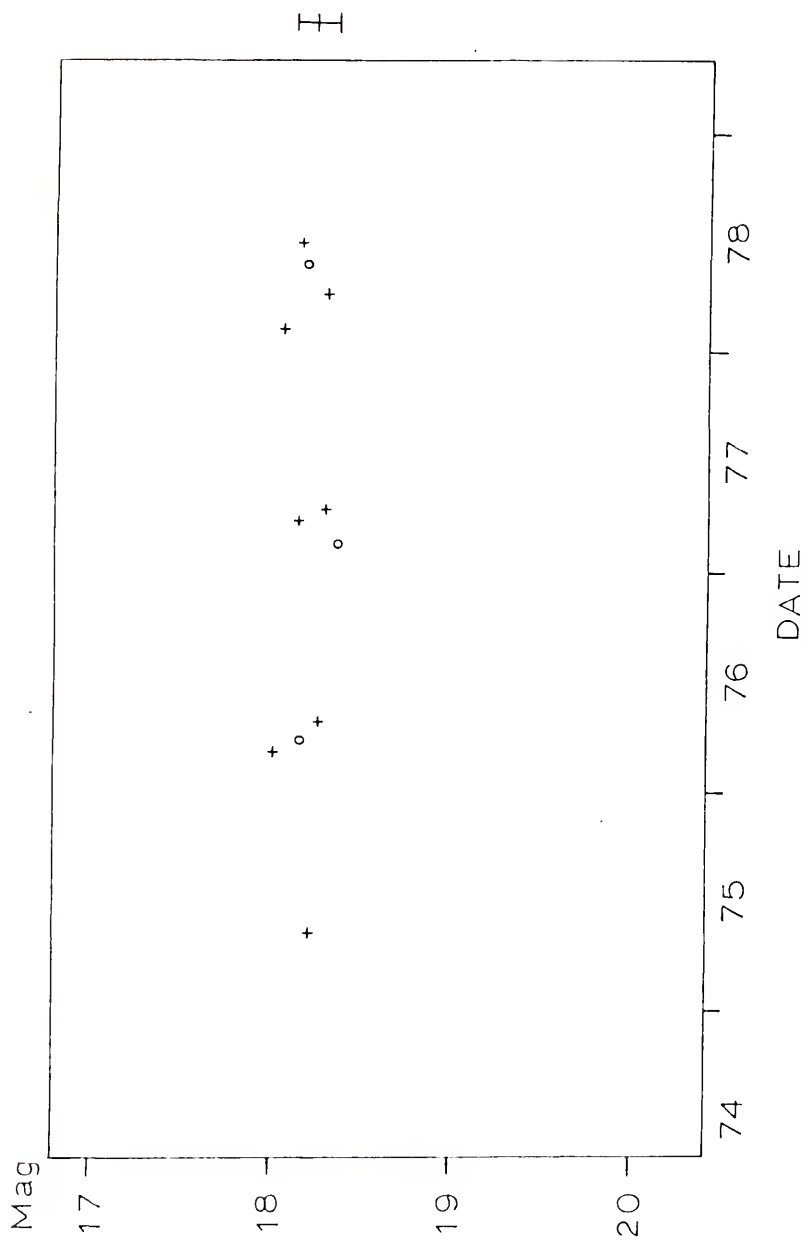


Fig. 43. Variation with Time of BSO 6.

including 3 pairs, are given in Table 36. Figure 43, a graph of magnitude versus time, shows only small scatter with no secular change. This object does not appear to be variable. The mean magnitude is $18^m.23$, with a range of $0^m.34$ compared to a $0^m.12$ rms scatter for the comparison stars (Table 43).

B 234

Braccesi et al. (1968) measured B 234's V magnitude as $17^m.52$, B - V as $0^m.86$, U - B as $-0^m.43$ and Iex as $-0^m.4$. A redshift of 0.060 is based on forbidden lines and Balmer lines of hydrogen. The widths of these lines are abnormally narrow in B 234. Braccesi et al. (1973) listed this object as AB 100 and gave its position as $13^h 0^m 42.5^s$ and $+36^\circ 7' 34''$. Radio surveys by Colla et al. (1970) at 408 MHz with a detection limit of 20 mfu, and Katgert et al. (1973) with a limit of 10 mfu at 1.4 GHz, failed to detect a radio source at this position.

Comparison stars for B 234 were calibrated by photographic transfer from M 3 using a plate taken at Rosemary Hill Observatory on the night of May 28, 1976. The magnitudes of these stars are given in Table 37 and their positions are shown on Fig. 44. Fourteen observations of B 234, including 3 pairs, were made. The magnitudes are given in Table 38. The graph in Fig. 45 shows scatter with a slight brightening over the period 1975-1977, followed by a sharp drop and rebound in 1978. This object is variable at a greater than 99 percent confidence level (Table 43). The mean magnitude is $18^m.48$, with a range of $0^m.77$ compared to an average rms of the comparison stars of $0^m.14$.

TABLE 37

Comparison Stars for B 234

Star	1	2	3	4	5	6	7	8	9	10	11	12
Mag.	19.06	18.26	17.63	15.59	19.30	17.31	17.47	19.35	17.91	19.57	16.54	18.80

Fig. 44. B 234 Field (facing page). This photograph was reproduced from a plate taken at Rosemary Hill Observatory on the night of July 3, 1978. North is at the top and east is to the left. One minute of arc equals 7mm. The object is identified by two short perpendicular lines. The magnitudes of the comparison stars are given in TABLE 37 (above).

12

11
10

6 7 8 9

5

4
10a 3
2-1
-1

TABLE 38
B Magnitudes of B 234

Date	EST	JD	Mag.	rms
6/ 9/75	2320	42573.681	18.71	0.09
4/21/76	2308	42890.672	18.23	0.16
4/28/76	2205	42897.628	18.57	0.10
4/ 8/77	2344	43242.697	18.30	0.16
4/11/77	0010	43244.715	18.22	0.15
4/11/77	0016	43244.719	18.35	0.15
5/16/77	2215	43280.635	18.64	0.19
5/16/77	2221	43280.640	18.38	0.09
2/15/78	0426	43554.893	18.56	0.18
5/29/78	2319	43658.680	18.56	0.16
7/ 3/78	2146	43693.615	18.91	0.29
12/10/78	0430	43852.896	18.66	0.17
12/10/78	0438	43852.901	18.54	0.16
12/31/78	0359	43873.874	18.14	0.12

Key to Fig. 45. Data points whose rms is less than or equal to 0.1 Mag. are shown by a circle. Points with an rms greater than 0.1 Mag. are shown by a cross. A point corresponding to the weighted mean is plotted for two observations on the same night. Error bars at the right represent the mean magnitude of the object $\pm 1 \sigma$.

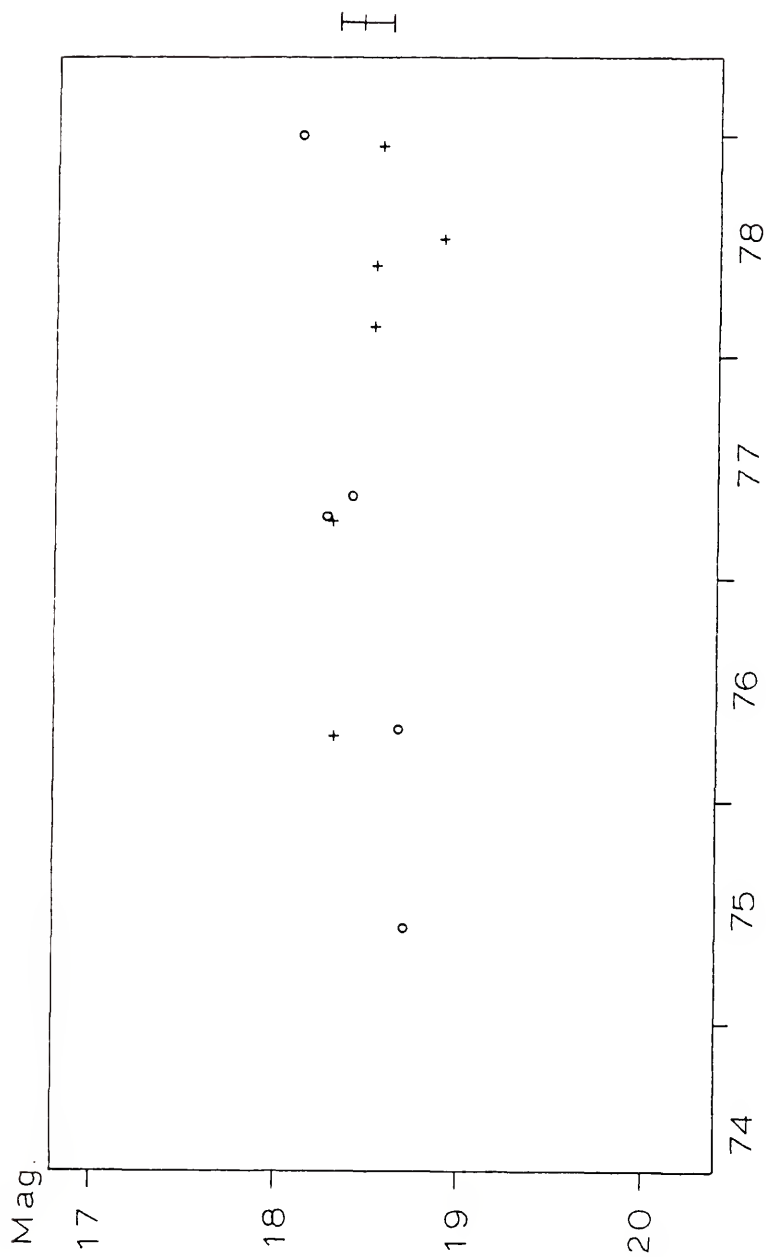


Fig. 45. Variation with Time of B 234.

B 312

Braccesi et al. (1968) listed the V magnitude of B 312 as 19^m08 , its B - V as 0^m14 , U - B as -0^m67 and Iex as -1^m5 . A redshift of 0.450 is given based on a strong magnesium line. Braccesi et al. (1973) list this object as AB 134 at $13^h 4^m 52.1^s$ and $+37^\circ 28' 38''$. No radio source was found at this position by Colla et al. (1970) at 408 MHz with a detection limit of 20 mfu, or by Katgert et al. (1973) with a limit of 10 mfu at 1.4 GHz.

Comparison stars for B 312 were calibrated by photographic transfer from M 3 using a plate taken on the night of June 19, 1977. These stars are identified in Fig. 46 and their magnitudes are given in Table 39. Resulting magnitudes from 10 observations of B 312, including 3 pairs, are given in Table 40. Figure 47 shows a sharp drop of 1 magnitude over a period of one month in May-June of 1977, followed by a slower rise to normal in 1978. B 312 is variable at a confidence level greater than 99 per cent (Table 43). The mean magnitude is 19^m24 , with a range of 1^m1 compared to an average rms scatter of the comparison stars of 0^m14 .

BSO 11

BSO 11 was studied by Sandage and Veron (1965) because of its strong ultraviolet image. It is the same object as B 416, for which Braccesi et al. (1968) gave $V = 18^m41$, $B - V = 0^m06$, $U - B = -0^m85$ and $I_{ex} = -1^m5$. A redshift of 2.084 is based on Ly_{α} and carbon lines.

TABLE 39

Comparison Stars for B 312

Star	1	2	3	4	5	6	7	8	9	10	11	12
Mag.	18.39	17.83	18.87	19.04	17.76	17.79	19.14	16.14	17.21	19.23	19.04	17.90

Fig. 46. B 312 Field (facing page). This photograph was reproduced from a plate taken at Rosemary Hill Observatory on the night of February 11, 1978. North is at the top and east is to the left. One minute of arc equals 7mm. The object is identified by two short perpendicular lines. The magnitudes of the comparison stars are given in TABLE 39 (above).

10

9

8

7

6

11

1

2

3

4

5

12

TABLE 40
B Magnitudes of B 312

Date	EST	JD	Mag.	rms
6/13/75	2244	42577.656	19.91*	0.18
4/ 2/76	2340	42871.694	19.41	0.28
4/10/77	2323	43244.683	19.14	0.06
4/10/77	2329	43244.687	19.11	0.18
5/16/77	2132	43280.606	19.34	0.16
5/16/77	2139	43280.610	19.17	0.22
6/19/77	2219	43314.638	19.90	0.12
2/12/78	0359	43551.874	19.26	0.12
5/ 5/78	0002	43633.710	19.09	0.15
7/ 3/78	2217	43693.637	18.81	0.20

* Faint end extrapolation, deleted from statistics.

Key to Fig. 47. Data points whose rms is less than or equal to 0.1 Mag. are shown by a circle. Points with an rms greater than 0.1 Mag. are shown by a cross. A point corresponding to the weighted mean is plotted for two observations on the same night. Error bars at the right represent the mean magnitude of the object $\pm 1\sigma$.

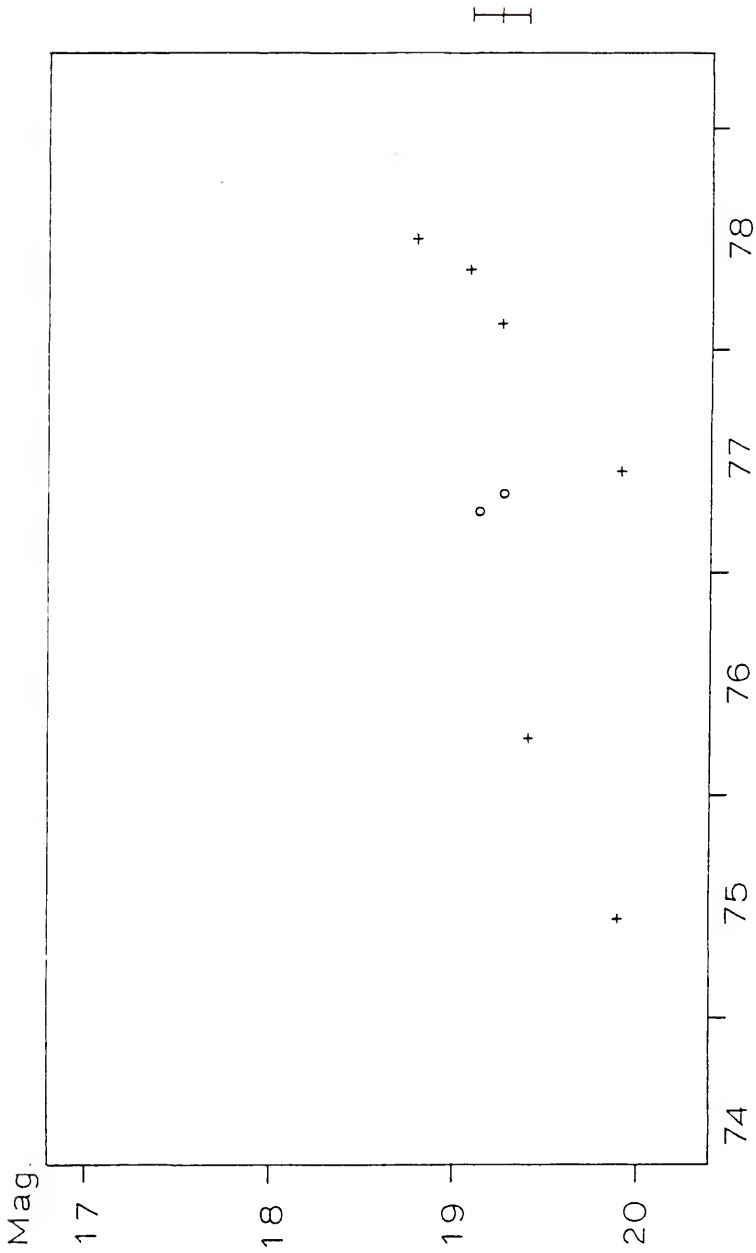


Fig. 47. Variation with Time of B 312.

TABLE 41
Comparison Stars for BSO 11

Star	1	2	3	4	5	6	7	8	9	10	11	12
Mag.	17.88	15.94	18.10	16.97	18.49	16.24	19.30	17.68	18.47	19.09	19.24	18.21

Fig. 48. BSO 11 Field (facing page). This photograph was reproduced from a plate taken at Rosemary Hill Observatory on the night of July 3, 1978. North is at the top and east is to the left. One minute of arc equals 7mm. The object is identified by two short perpendicular lines. The magnitudes of the comparison stars are given in TABLE 41 (above).

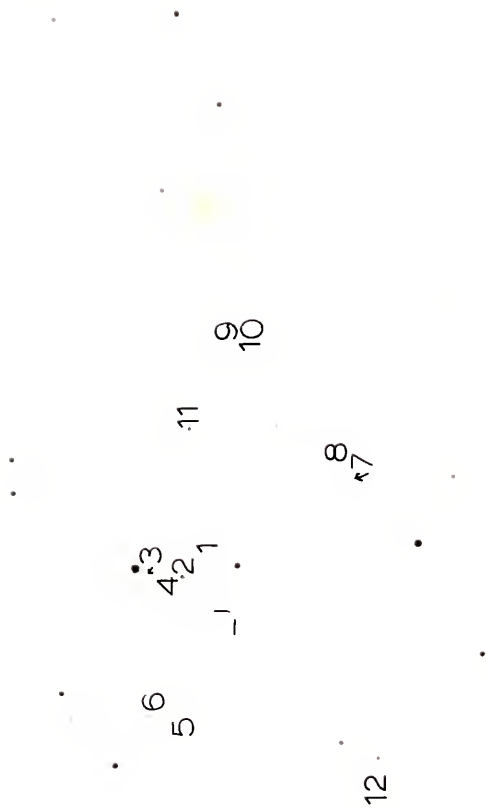


TABLE 42

B Magnitudes of BSO 11

Date	EST	JD	Mag.	rms
6/13/75	2305	42577.670	19.06	0.12
4/28/76	2319	42897.680	18.84	0.15
2/21/77	0342	43195.862	18.79	0.14
4/10/77	2346	43244.699	18.62	0.12
4/10/77	2351	43244.702	18.65	0.12
5/16/77	2154	43280.621	18.84	0.19
5/16/77	2201	43280.626	18.56	0.15
2/15/78	0514	43554.926	19.40	0.14
5/ 4/78	0017	43632.720	18.71	0.09
7/ 3/78	2201	43693.626	18.74	0.15

Key to Fig. 49. Data points whose rms is less than or equal to 0.1 Mag. are shown by a circle. Points with an rms greater than 0.1 Mag. are shown by a cross. A point corresponding to the weighted mean is plotted for two observations on the same night. Error bars at the right represent the mean magnitude of the object $\pm 1 \sigma$.

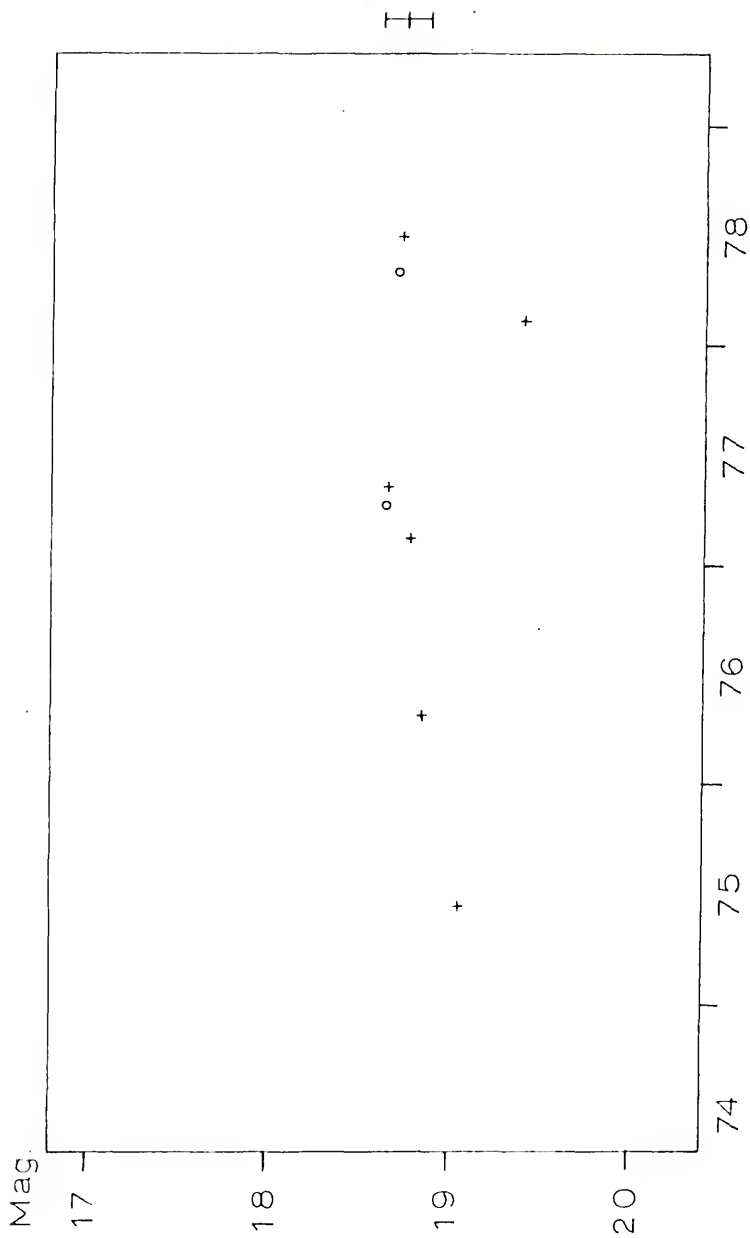


Fig. 49. Variation with Time of BSO 11.

Absorption lines may also be present. Braccesi et al. (1973) list BSO 11 as AB 168 and give its optical position as $13^{\text{h}} 11^{\text{m}} 19.5^{\text{s}}$ and $+36^{\circ} 15' 40''$. No radio source was found at this position by Colla et al. (1970) with a detection limit of 20 mfu at 408 MHz, or by Katgert et al. (1973) with a limit of 10 mfu at 1.4 GHz.

Comparison stars for BSO 11 were calibrated by photographic transfer from M 3 using a plate taken at Rosemary Hill Observatory on the night of February 20, 1977. These stars are identified in Fig. 48 and their magnitudes are listed in Table 41. Ten observations of BSO 11, including 2 pairs, were made. The resulting magnitudes are recorded in Table 42 and plotted versus the date of the observation in Fig. 49. BSO 11 showed a slow rise from 1975 to 1977 followed by a drop in February 1978, after which it began to rise again. BSO 11 is variable with a 99 percent confidence level (Table 43). The mean magnitude is $18^{\text{m}}.76$, with a range of $0^{\text{m}}.77$ compared to a $0^{\text{m}}.12$ rms scatter of the comparison stars.

Summary

Of the 11 objects in the $13^{\text{h}} +36^{\circ}$ field, two (B 46 and B114) are variable at a confidence level greater than 99.9 percent, and five more (BSO 1, B 154, B 234, B 312 and BSO 11) are variable at a confidence level greater than 95 percent. The three others (BSO 2, B 194 and B 201) whose confidence level is greater than 90 percent are probably variable, but variability is not usually considered to be convincing unless the confidence level exceeds 95 percent. One object, BSO 6, did

TABLE 43

Variability of the Sample of Radio-Quiet Quasi-Stellar Objects

OBJECT	NP	\bar{B}	ΔB	\overline{rms}	χ^2	df	C.L.%	V.I.
PHL 938	13	16.85	0.25	0.08	7.60	10	33	0.87
PHL 3375	11	17.94	0.66	0.11	15.33	9	92	1.38
PHL 1027	13	16.83	0.22	0.09	4.90	10	10	0.69
PHL 3632	11	17.59	0.57	0.08	18.46	8	98	1.61
PHL 1186	16	17.51	0.54	0.09	23.10	11	98	1.62
PHL 1194	13	17.47	0.65	0.10	35.00	9	999	2.30
PHL 1222	8	17.72	0.29	0.07	6.06	6	58	1.03
PHL 1226	12	17.12	0.36	0.08	20.61	9	98	1.65
BSO 1	17	17.80	0.56	0.13	31.52	14	99	1.80
B 46	18	18.08	0.56	0.10	75.63	13	999	3.58
BSO 2	12	18.83	0.71	0.12	15.40	9	91	1.38
B 114	12	18.08	0.78	0.10	46.06	9	999	2.68
B 154	13	18.65	0.78	0.12	20.22	10	97	1.55
B 194	11	18.09	0.41	0.11	14.26	8	94	1.39
B 201	13	17.17	0.62	0.13	17.91	10	94	1.44
BSO 6	14	18.23	0.34	0.12	8.59	10	43	0.93
B 234	14	18.48	0.77	0.14	24.43	10	99	1.75
B 312	9	19.24	1.10	0.14	20.26	6	99	1.87
BSO 11	10	18.76	0.77	0.12	20.65	7	99	1.81

not show evidence of variation during the period of this study.

Of the above group, two objects, B 46 and B 114, show secular declines and one, BSO 1, shows a secular rise. One object, B 154, shows a sharp rise, while four objects, B 194, B 234, B 312, and BSO 11, show sharp drops. Positive (fainter magnitude) excursions from the mean seem to be more common than are negative ones. This evidence is suggestive but not conclusive of any general trend.

These 11 objects have a spread in V magnitude from $16^m.79$ to $19^m.08$. Their B - V colors range from $0^m.05$ to $0^m.86$, their U - B colors from $-1^m.01$ to $-0^m.43$, and their Iex from $-1^m.6$ to $-0^m.03$. There are redshifts from $z = 0.060$ to 2.084 (Braccesi et al. 1968). No relation is apparent between V.I. and U - B, B - V, U - V, or Iex. There is a slight correlation between V.I. and the $v - i$ given by Braccesi et al. (1970). Both of the strongly variable objects (C.I. $> 99.9\%$) have rather low redshifts.

A discussion of the search for correlation between variability and the colors, redshifts and magnitudes of the total sample of RQSOs is given in Chapter 6.

CHAPTER 6

CONCLUSIONS

Florida ROOSO Results

Of the total sample of nineteen objects in the two fields studied ($1^{\text{h}} +6^{\circ}$ and $13^{\text{h}} +36^{\circ}$), three, PHL 1194, B 46, and B 114, are variable at a confidence level (C.L.) greater than 99.9 percent. Eight more objects, PHL 3632, PHL 1186, PHL 1126, BSO 1, B 154, B 234, B 312, and BSO 11, are variable with a confidence level greater than 95 percent. One of these objects, B 312, has shown a change in brightness greater than one magnitude on a time scale of months and may later prove to be an optically violent variable (OVV) when observed more often.

Four objects, PHL 3375, BSO 2, B 194, and B 201, with confidence levels greater than 90 percent but less than 95 percent, may vary but variability is not considered to be convincing until the confidence level exceeds 95 percent. Four more objects, PHL 938, PHL 1027, PHL 1222, and BSO 6, have not shown any real evidence of variability during this time.

In describing the types of variability exhibited by quasars observed at Rosemary Hill Observatory, McGimsey et al. (1975) have assigned each object to one of four subclasses. Subclass I objects show short term "flickering" about a mean magnitude. Subclass II contains objects with long term trends. Subclass III consists of objects with

approximately equal amounts of flickering and secular change. Subclass IV objects are episodic with periods of little variation interspersed with more active periods. These subclasses have been adequate to describe the behavior of both OVVs and less active quasars with no great concentration in any one subclass. These subclasses are used only to describe the current behavior. An object need not remain in the same subclass. Objects described by subclass IV may return to subclass I, II or III for long periods. Or an object of subclass I, II or III may suddenly act like a IV.

RQOSOs' behavior can also be described in this way. In this sample, three objects, PHL 1186, PHL 1226, and B 154, fall into subclass I (flickering) and two, PHL 3375 and B 201, into subclass II (secular). Three RQOSOs, PHL 3632, B 234 and B 114, show a mixture of flickering and secular drift (subclass III). BSO 1, B 312 and BSO 11 would be considered "episodic"; and three others combine episodic with flickering (PHL 1186), or with a slowly changing level (PHL 1194 and B 46).

The amplitudes of the variations observed in these objects are not as large as those seen in some quasars. The largest difference in magnitude was 1^m . The time intervals between consecutive observations were too long to allow classification of the RQOSO B 312 as an optically violent variable (OVV), a term used to describe objects with variations greater than one magnitude on a time scale of days or weeks, although it might have qualified if it had been observed that often.

The variability index (V.I.) described in Chapter 3 was used to allow mathematical and graphical comparison between the extent of

variability represented by V.I. and other properties of the radio-quiet quasi-stellar objects. Least squares lines were fitted in both variables ($y = mx + b$ and $x = m'y + b'$) and the linear correlation coefficient ($r = \sqrt{mm'}$) was determined in each comparison. These values are tabulated in Table 44. In the case of a tight relationship, the two lines will be essentially the same ($m' = 1/m$ and $r = 1$). When there is no dependence, the two lines will be nearly at right angles and r will be almost zero. When there is a lot of scatter in the data, a correlation coefficient nearly equal to one cannot be expected even if a strong relationship is present.

Since ΔB , the difference between the brightest and faintest magnitudes of the RQSO, is a different measure of the variation in the object, a correlation between V.I. and ΔB is to be expected. The two measures are not the same, however, because V.I. is dependent on the ratio of ΔB and rms and upon the frequency of excursions from the average magnitude. As seen in Table 44 the linear correlation coefficient between V.I. and ΔB is 0.46. In comparing V.I. and B_{\max} (faintest), B_{\min} (brightest) and \bar{B} (average), a similar correlation is seen in each instance and with a similar slope, in the sense that the fainter objects are slightly more variable. The correlation is slightly better for B_{\max} (faintest) than for \bar{B} (average) and somewhat worse for B_{\min} (brightest). This may be a reflection of the existence of more faint excursions from the mean magnitude.

Since these two samples of RQSOs were chosen on the basis of their colors, the spectral color differences, $U - B$, $B - V$ and $U - V$ are known for all of the objects in both fields and I_{ex} and $v - i$ are known for

TABLE 44

Linear Correlation Coefficients

V.I. vs	b	m	m'	b'	r
ΔB	0.92	1.33	0.16	0.29	0.46
\bar{B}	-3.24	0.27	0.29	17.45	0.28
B_{\max}	-2.99	0.25	0.36	17.65	0.30
B_{\min}	-2.30	0.22	0.21	17.34	0.22
U - B	1.51	-0.18	-0.01	-0.77	0.04
B - V	1.63	0.10	0.01	0.20	0.03
U - V	1.41	-0.24	-0.02	-0.97	0.07
I _{ex}	1.81	-0.02	-0.01	-1.14	0.01
v - i	1.44	0.62	0.13	0.40	0.28
z_{RQSOs}	1.99	-0.38	-0.49	1.71	0.43
z_{QSRSs}	3.19	-0.83	-0.13	1.41	0.33
z_{both}	2.79	-0.66	-0.13	1.33	0.29
$\log z_{RQSOs}$	1.51	-0.57	-0.27	0.20	0.39
$\log z_{QSRSs}$	2.09	-2.17	-0.08	0.09	0.41
$\log z_{\text{both}}$	1.91	-1.43	-0.08	0.03	0.33
B - 5 log z	-0.48	0.11	1.65	16.45	0.43

the objects in $13^h + 36^o$ field (Sandage and Luyten, 1967; Braccesi et al. 1968; and Braccesi et al. 1970). In figures 50 through 54, V.I. is plotted as the y coordinate and the color difference along the x coordinate. The circles denote the PHL objects and the crosses represent BSO or B objects. No relation is apparent in the graphs and the linear correlation coefficients are 0.04 for U - B, 0.03 for B - V and 0.07 for U - V.

Two additional color differences are known for the 11 objects in the field at $13^h + 36^o$. Iex is an estimate of the difference between the near-infrared magnitude of the object and the blackbody curve. The difference in magnitude of the object in the visual and near infrared photographic systems is denoted v - i. No relationship is seen between V.I. and Iex (correlation coefficient 0.01), but there is a slight correlation between V.I. and v - i in the sense that those objects with more positive v - i are somewhat more variable. These objects would be brighter in the infrared than the less variable objects. This may be the reason that the objects in the $13^h + 36^o$ field, which were selected for brightness in the infrared, are, as a group, more variable than the objects in the $1^h + 6^o$ field. That is, a blue stellar object which is strong in the infrared might not only be more likely to be a quasar, but also be more likely to vary.

Comparison of variability with redshift, and hence with age, assuming the redshift is cosmological, is complicated by the spread in intrinsic brightness. Figure 55 shows variability index (V.I.) versus $\log z$ for the RQSO sample. Redshift (z) is also marked along the horizontal axis. As is suggested by the graph, the more variable of the

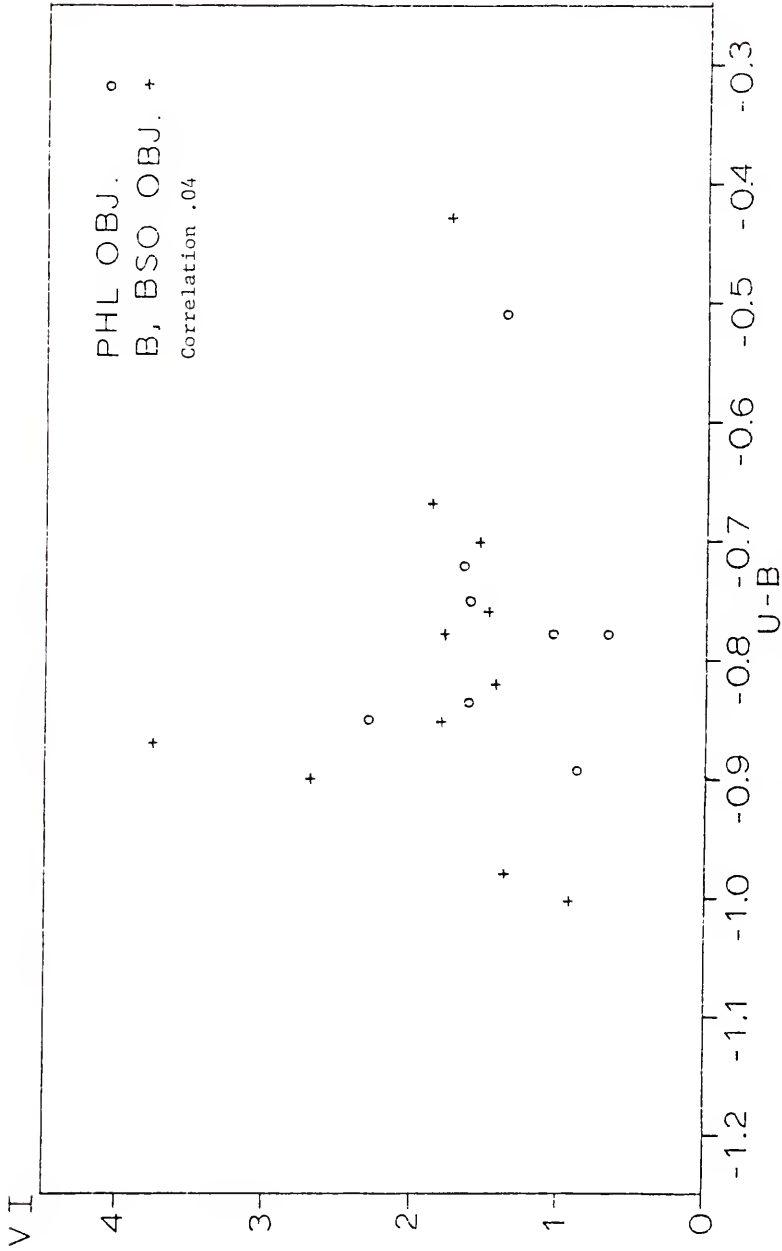
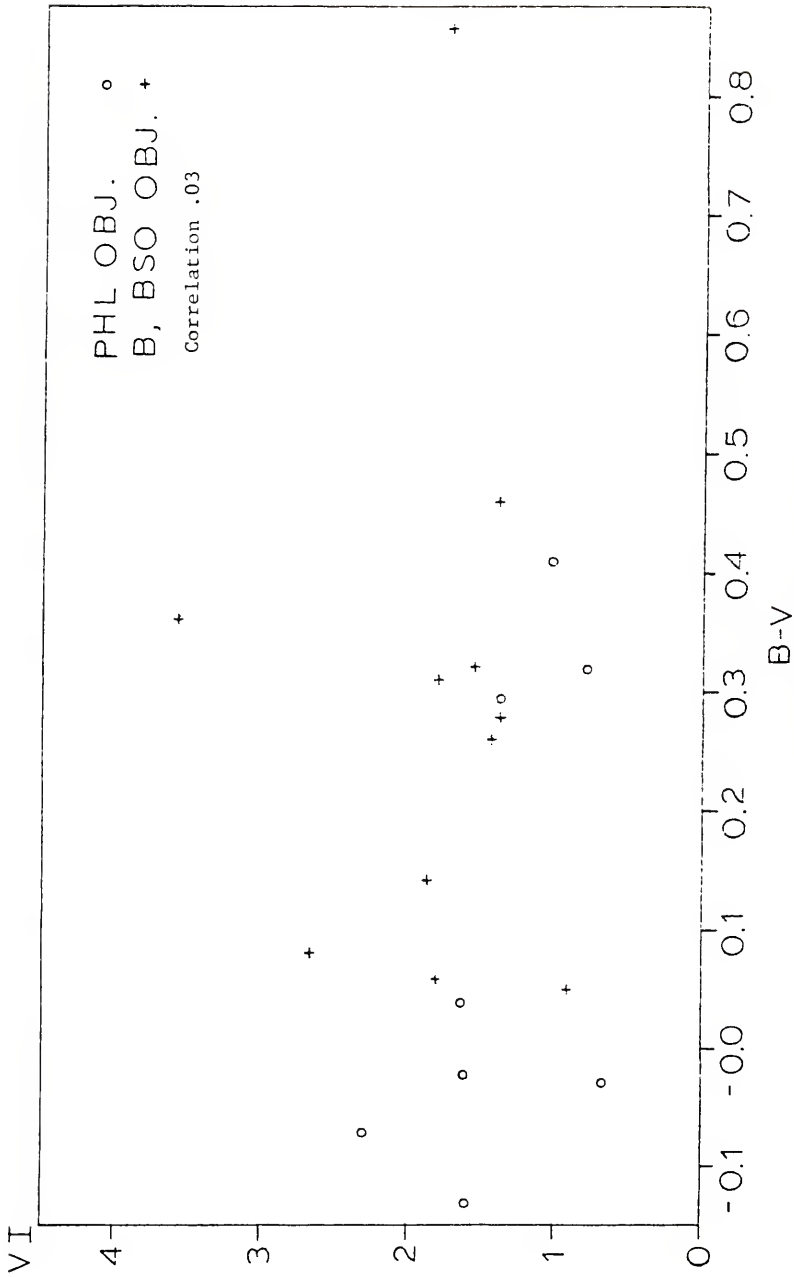


Fig. 50. Variability Index versus U - B.



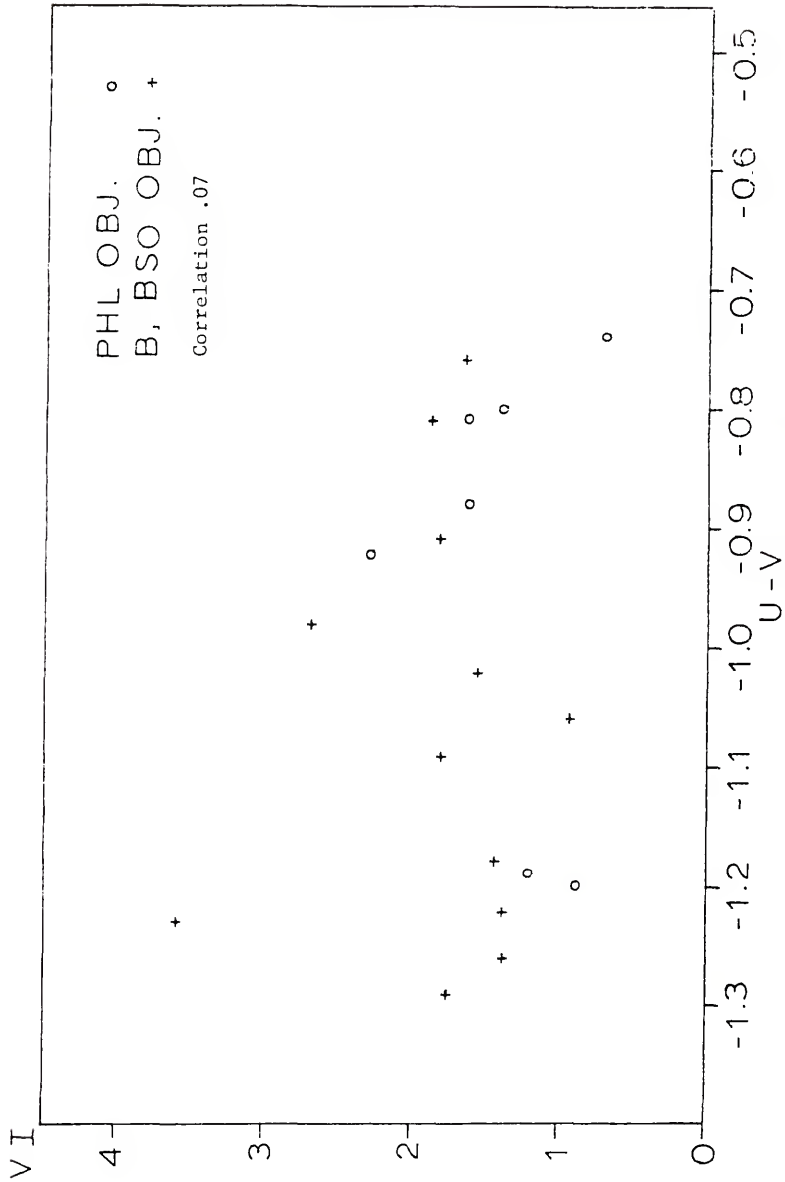


Fig. 52. Variability Index versus U - V.

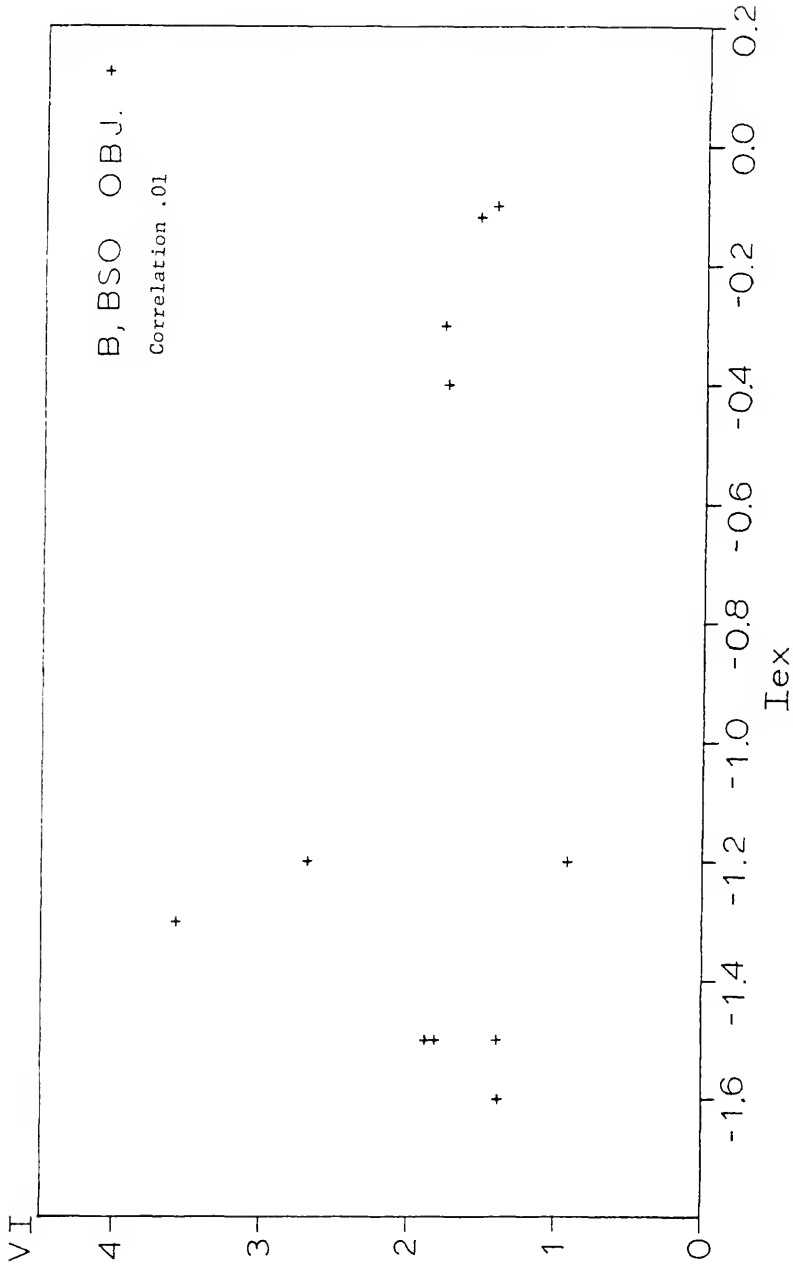


Fig. 53. Variability Index versus Iex.

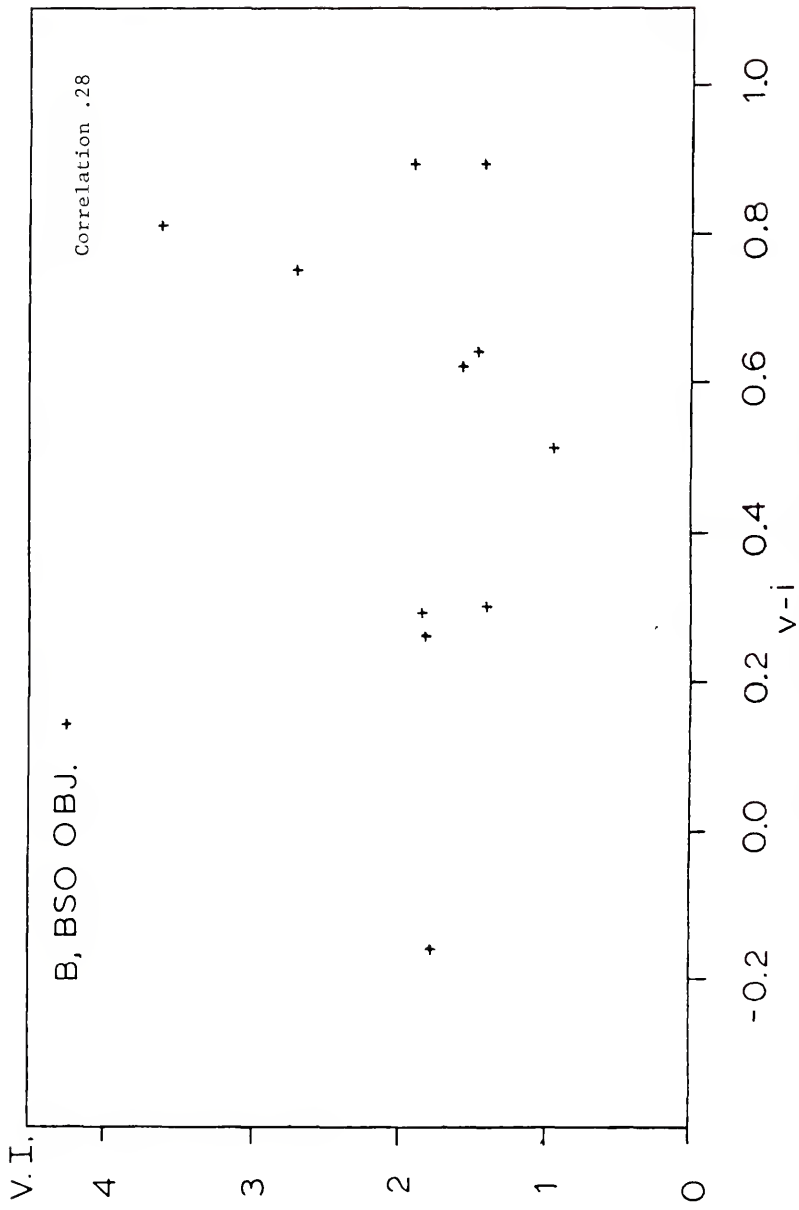


Fig. 54. Variability Index versus v - i.

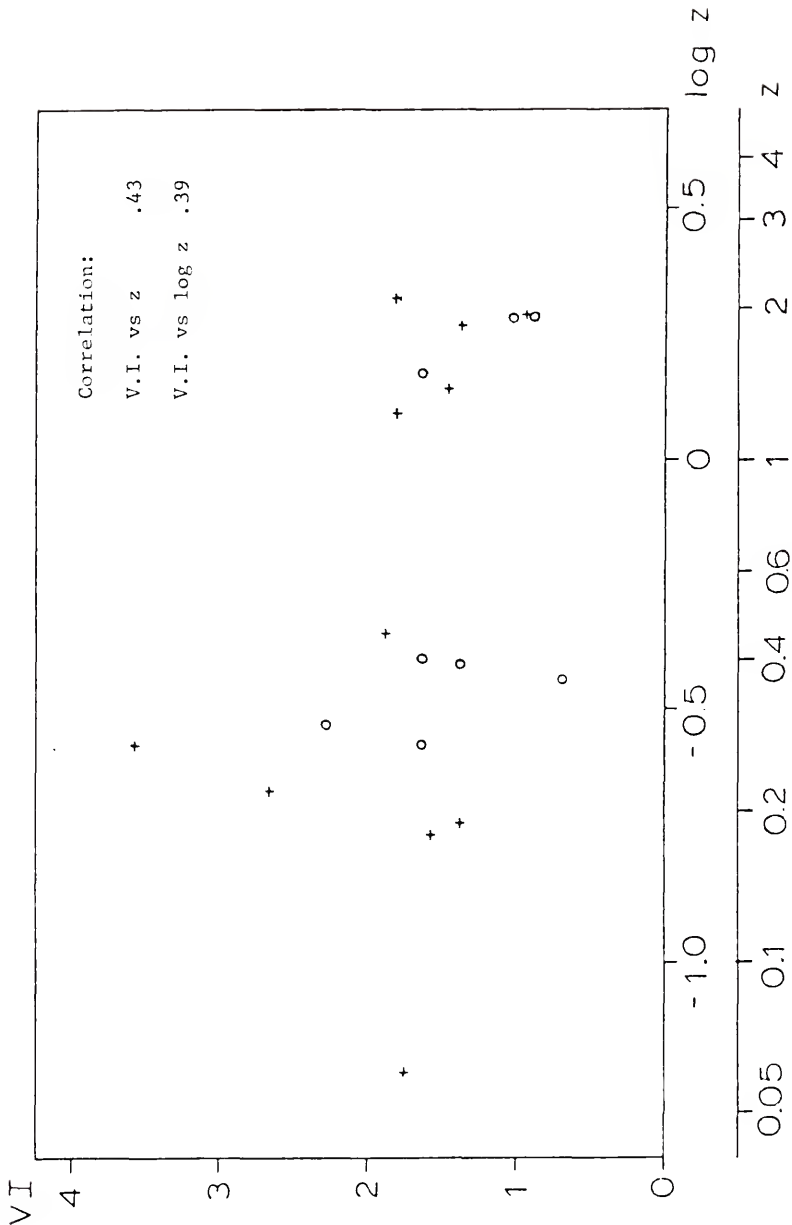


Fig. 55. Variability Index versus Redshift for the RQ90 Sample.

objects have low redshifts. The linear correlation coefficient is 0.43 for V.I. versus z and 0.39 for V.I. versus $\log z$. The closer RQSOs are more likely to be variable. If the redshift is cosmological, the closer RQSOs are also older and at a later stage in their evolution.

At low redshifts, objects can be observed which are fainter intrinsically than could be observed at greater distances. Since the correlation between V.I. and \bar{B} suggested that objects fainter in apparent magnitude, which might be expected to be more distant, were more likely to vary, a relative intrinsic brightness (R.I.B. = $\bar{B} - 5 \log z$) was computed to investigate the relation between variability and the intrinsic brightness of the object, in an attempt to separate faintness due to distance from intrinsic faintness. Figure 56 shows V.I. plotted along the vertical axis and relative intrinsic brightness plotted along the horizontal axis. The intrinsically fainter objects show greater extent of variability, with a linear correlation coefficient of 0.43.

Other Studies of RQSOs

In a study at Bologna covering the period 1967-1971, of 148 objects in the $13^h + 36^o$ field, Bonoli et al. (1979) found 89 objects to be variable at greater than 95 percent confidence levels. Because yearly averages are used to form their χ^2 statistic, this procedure is less likely to pick up flickering or bursting behavior. It is sensitive mainly to long-term secular changes.

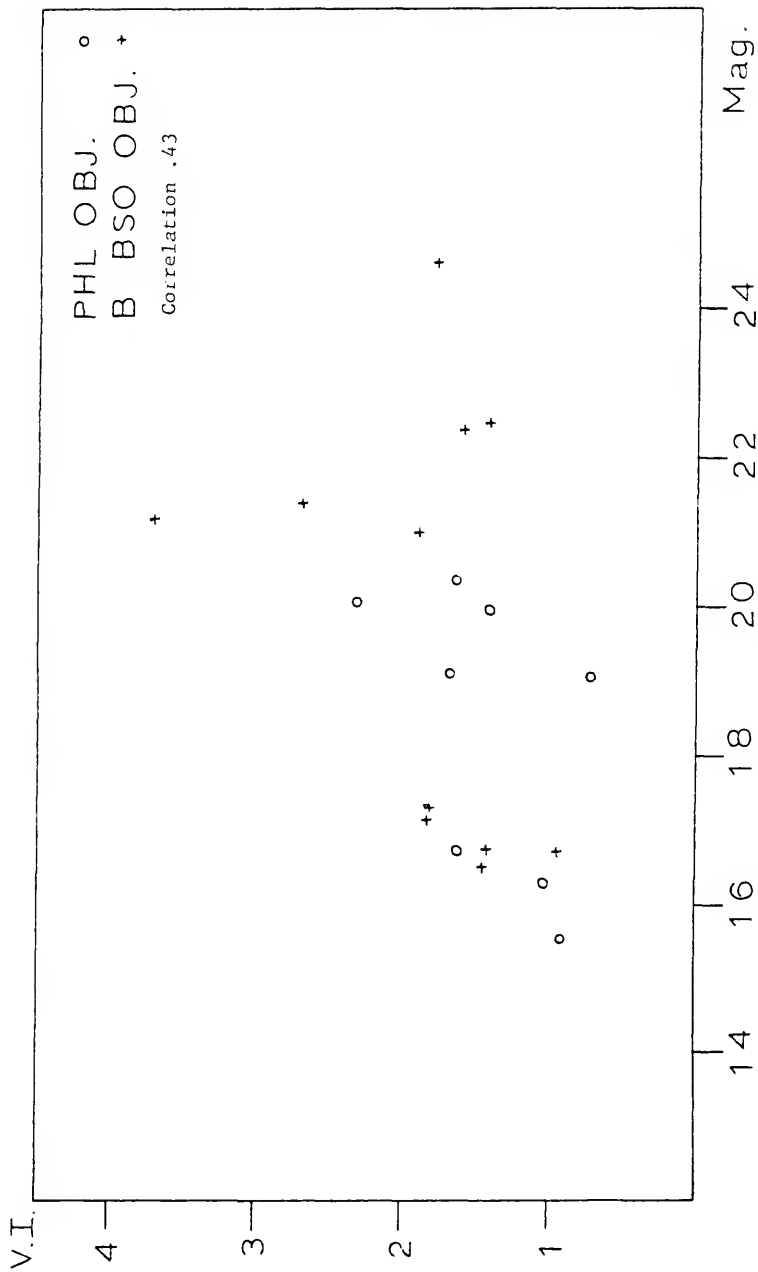


Fig. 56. Variability Index versus Relative Intrinsic Brightness.

For this reason, and because the Bologna and Florida observations cover different epochs, the variability found in the eleven objects common to both samples do not show close agreement. BSO 6 did not show variability (C.L. > 95%) in either study. B 234 was nonvariable (C.L. \approx 62%) during the period of the Bologna observations but became more active during the Florida observations, brightening during 1975-1977, then dropping sharply in 1978 and rebounding late in the year, resulting in a confidence level greater than 99 percent. B 154 (probably subclass I) was nonvariable according to Bonoli et al. (1979), but appears to be variable (C.L. = 97%) in the present work. B 46 is more convincingly variable (C.L. > 99.9%) in the Florida observation. Bonoli et al. (1979) suggested that OVV behavior occurs ten times less often in RQOSOs. The Florida RQOSRO results are consistent with this suggestion.

Studies of the field at $8^{\text{h}} 48^{\text{m}} +18^{\circ}$ (Usher, 1978) and the $15^{\text{h}} 10^{\text{m}} +24^{\circ}$ field (Usher and Mitchell, 1978) approached RQOSO variability from another direction. They proposed that, of the blue objects in the field, most of those which showed variability would prove to be quasi-stellar objects (QSOS) when their spectra were taken.

Usher (1978) used a combination of photoelectric and photographic observations to calculate three statistical indicators. One measures integrated variability by means of a chi square probability function. Another, the signal-to-noise ratio, is sensitive to large changes over short intervals of time, as in bursting behavior. The last indicator, which utilizes the photoelectric observations and averages of the

photographic magnitudes, can detect quite small secular changes in brightness. This technique can, by improving the odds for spectral confirmation, save telescope time and increase the number of known QSOs for number count and luminosity studies, and for extending the Hubble diagram. It does not prove what percentages of QSOs are variable.

Usher (1978) estimates that 60 percent of QSOs should be detected through variability at a confidence level > 97 percent. This figure is consistent with the 11 variables of 19 RQSOs in the Florida sample. On the basis of 22 QSOs in these two fields identified by Schmidt (1974), none of which has a confidence level of variability less than 80 percent in this survey, Usher and Mitchell (1978) suggest that the collection of all blue stellar objects which vary with C.L. > 80 percent should include almost all the QSOs. The Florida sample with similar coverage in which one-fifth of the RQSOs have a confidence level less than 80 percent, does not support this suggestion.

Usher (1975) suggested that QSOs at higher redshifts should vary more actively because they are seen at an earlier stage of their evolution. This is not borne out by the Florida RQSO results, in which the three very active objects all have low redshifts.

Comparison with QRS Variability

Of the 84 QSOs observed as part of the Florida quasar monitoring program that had enough data for analysis in 1976, half (Scott et al., 1976) were variable with a confidence level of 95 percent or more. Sixty-four percent of the quasars reported on by Pollock et al. (1979)

and by Pica et al. (1980) were variable at the 95 percent confidence level. Fifty-eight percent of the RQSO sample showed variability at this level. RQSOs show examples of each of the four types of variation described by McGimsey et al. (1975). OVVs comprise 10-20 percent of most quasar samples. OVV behavior could not have been readily detected in the RQSO sample since the time coverage of this study did not encourage such detection. Since only one RQSO had a change in brightness greater than one magnitude, it is probable that OVVs do not represent as large a proportion of the RQSOs.

Variations of up to 1^m were measured, but no strong flares were detected such as have been seen in the more violent quasars like NRAO 512 (McGimsey et al., 1975). "Anti-flares," sharp drops in magnitude, seemed to be more common in RQSOs. This judgment is mostly subjective. There were more extremes fainter than the mean magnitude than there were brighter ones, although the numbers are too few for statistical significance. Anti-flares have been observed in QSRs: e.g., 3C446 (Penston and Cannon, 1970). McCrea (1972) added unstable dark protostars to his quasar theory to provide such drops in brightness.

The RQSO sample suggests that, contrary to the suggestion by Usher (1975), the QSOs at small redshifts are more likely to be strongly variable than those at large redshifts. A sample of quasi-stellar objects studied at Rosemary Hill Observatory (Pica et al., 1980) for which redshifts were available also seems to suggest this (see Fig. 57). The variability indices of the QSRs and RQSO samples may not be directly comparable because of the different time spans of

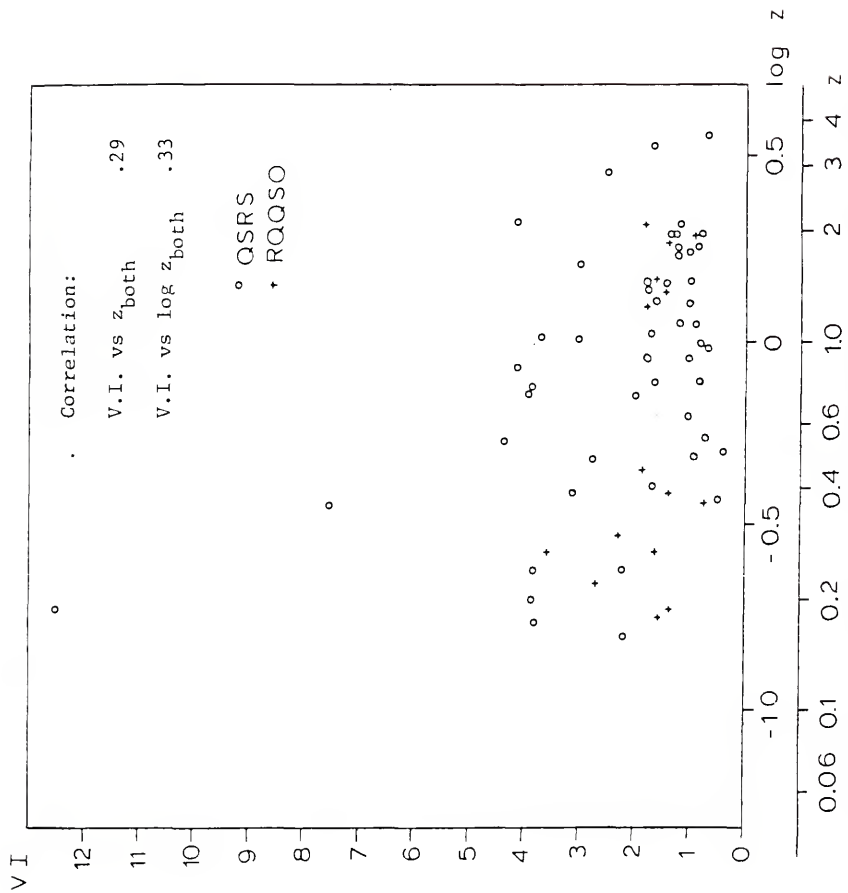


Fig. 57. Variability Index versus Redshift for QRSs and RQSOs.

observation, since, if objects are observed for a longer time, their variations are more likely to be detected.

The fainter RQSOs appear to be more variable. Pica et al. (1981) also find this to be the case for the larger sample of all quasars observed at Rosemary Hill Observatory.

In general, the RQSOs do not appear to be distinguishable from the QSRs (not including BL Lac type objects, which are a special class) by means of optical characteristics or by variability. As a group, they show a slightly lower amplitude of variation, but they are within the normal range of behavior of the QSRs.

Comparison with Quasar Models

Since neither the energy source nor the mechanism by which it varies is known, a broad range of theories and models for quasars have been proposed. Ames and Bahcall (1973) divided these theories into two general types: type I, those which assume a number of small independent sources; and type II, which predicate single large sources. These types would be expected to show different relationships between variability and optical luminosity. In type II, the larger, brighter sources would be expected to be more variable. For type I, the changes in relative brightness should be less for the larger, brighter aggregate sources.

The Florida RQSO results, showing some correlation between relative intrinsic brightness and variability index, suggest that the intrinsically fainter RQSOs are more variable. This seems to speak in favor of the type I sources, those which are made up of a group of

small, independently variable energy sources, and against the type II theories of single, large sources.

A correlation between variability index and redshift corresponds to a relation between variability and either greater age (if the redshift is assumed to be cosmological) or whatever other mechanism the theory suggests to provide the redshift. In the case of a cosmological redshift, some attempt should be made to separate correlation with relative intrinsic brightness from correlation with redshift. Even if there is no luminosity evolution, (Ames and Bahcall, 1973, do not find evidence for a relation between relative intrinsic brightness and redshift for quasars), the optical detection cut-off in apparent B magnitude couples the effects in these two variables, since intrinsically faint sources could not be detected at high redshifts.

Because of this coupling, it cannot be said definitely which of these variables is more primarily related to variability. Variability is enhanced in the case of either intrinsically fainter sources or older sources or both. Since the correlations for relative intrinsic brightness and for redshift are approximately equal, both for QSRSs and for RQOSOs, and since producing a correlation as large as 0.43 by transfer due to selection effects would require very strong correlation in one variable, it seems more likely that both relations exist.

The correlation between variability and redshift does not support suggestions that quasars should have been more active at an early period in their evolution (Usher, 1975).

Quasar models should not predict any strong dependence of variability on optical color differences $U - B$, $B - V$, or $U - V$. The

slight correlation between variability and $v - i$ does allow for some dependence on infrared brightness.

Summary

Radio-quiet quasi-stellar objects were originally found because their optical colors were like those of the known QRSs, and further identifications have been on this basis. The question was whether RQSOs also resembled QRSs in terms of their variability. Do RQSOs vary, and, if so, do they vary in the same manner as the QRSs? Is optical variability dependent on radio flux and/or radio variability? The answer is that RQSOs do vary in the same way that QRSs do. Slightly more than half are variable at a confidence level greater than or equal to 95 percent. The amplitude of variation may be somewhat less for RQSOs than for QRSs and optically violent variables are less common but the RQSO behavior is well within the normal range of behavior of the QRSs.

Since a numerical comparison between variability and other optical characteristics or redshift was greatly desired, a variability index ($V.I. = \chi^2 / df$ normalized to 30 degrees of freedom) was formed for the RQSO sample. Linear correlation coefficients of V.I. versus $U - B$, $B - V$, $U - V$, I_{ex} , $v - i$, average magnitude, redshift and relative intrinsic brightness were calculated. These results are shown in Table 44. No relation was found between V.I. and $U - B$, $B - V$, $U - V$, or I_{ex} . A slight correlation between variability and the $v - i$ given by Braccisi et al. (1970) for the B, BSO sample may suggest that variability is enhanced for objects which are brighter in the infrared.

There is a correlation between V.I. and magnitude and between V.I. and redshift, in the sense that the fainter and closer objects are more variable. These two variables are coupled through a selection effect due to the cut-off in apparent B magnitude, since the fainter RQOSOs can only be seen at low redshift. Thus, it is difficult to determine whether the increased variability is due to greater age or lower luminosity. This effect is also present in the quasar sample.

Further investigation of variability dependence on redshift, optical luminosity and brightness in the near-infrared would be very helpful. Near-infrared colors for quasars are needed in order to study this relationship further.

A normalized Chi Squared form is proposed to allow for graphical and numerical analysis of quasar variability and a line plus hyperbola is suggested as a mathematical form to fit the iris photometer iris reading/magnitude curve, giving the proper behavior at the sky limit while maintaining a linear form in the middle range even when only a limited number of comparison stars are available.

BIBLIOGRAPHY

- Aitken, A. C. (1952). Statistical Mathematics (Edinburgh: Oliver and Boyd, 7th Ed.).
- Ames, S., and Bahcall, J. N. (1973). Astrophys. Lett. 14, 199.
- Bonoli, F.; Braccési, A.; Federici, L.; and Zitelli, V. (1979). Astron. Astrophys. Suppl. 35, 391.
- Braccési, A. (1967). Nuovo Cimento 49B, 148.
- Braccési, A.; Formiggini, L.; and Gandolfi, E. (1970). Astron. Astrophys. 5, 264.
- Braccési, A.; Formiggini, L.; and Gandolfi, E. (1973). Astron. Astrophys. 23, 159.
- Braccési, A.; Lynds, C. R.; and Sandage, A. (1968). Astrophys. J. 152, L105.
- Brownlee, K. A. (1960). Statistical Theory and Methodology in Science and Engineering (New York: John Wiley & Sons, Inc.).
- Burbidge, E. M. (1967). Ann. Rev. Astron. Astrophys. 5, 399.
- Burbidge, E. M. (1968). Astrophys. J. 154, L109.
- Burbidge, E. M.; Burbidge, G. R.; Solomon, P. M.; and Strittmatter, P. A. (1971). Astrophys. J. 170, 233.
- Burbidge, E., M.; Lynds, C. R.; and Stockton, A. (1968). Astrophys. J. 152, 1077.
- Burkhead, M., and Seeds, M. (1971). AAS Photo-Bull. 3, 15.
- Cohen, H. L. (1980). Private communication.
- Colla, G.; Fanti, C.; Fanti, R.; Formiggini, L.; Gandolfi, E.; Grueff, G.; Lari, C.; Padrielli, L.; Roffi, G.; Tomasi, P.; and Vigotti, M. (1970). Astron. Astrophys. Suppl. 1, 281.
- Difley, J. A. (1968). Astron. J. 73, 762.
- Fanti, C.; Fanti, R.; Lari, C.; Padrielli, L.; van der Laan, H.; and de Ruiter, H. (1977). Astron. Astrophys. 61, 487.

- Feige, J. (1958). Astrophys. J. 128, 267.
- Folsom, G. H.; Smith, A. G.; Hackney, R.; and Hackney, K. (1971). Nature 230, 199.
- Greenstein, J., and Matthews, T. (1963). Nature 157, 1041.
- Hackney, K. R. (1973). Three-Color Photographic Photometry of Active Quasi-Stellar Radio Sources, Ph.D. dissertation, University of Florida.
- Haro, G., and Luyten, W. (1962). Bol. Obs. Tonantzintla y Tacubaya 3, 37.
- Hazard, G.; Mackey, M. B.; and Shimmins, A. J. (1963). Nature 197, 1037.
- Humason, M. L. and Zwicky, F. (1947). Astrophys. J. 105, 85.
- Iriarte, B. and Chavira, E. (1957). Bol. Obs. Tonantzintla y Tacubaya 2, 3.
- Katgert, P.; Katgert-Merkelijn, J. K.; Le Poole, R. S.; and van der Laan, H. (1973). Astron. Astrophys. 23, 171.
- Kinman, T. (1966). Astrophys. J. 14, 1232.
- Matthews, T. A. and Sandage, A. (1963). Astrophys. J. 138, 30.
- McCrea, W. H. (1972). In IAU Symposium No. 44, External Galaxies and Quasi-Stellar Objects, ed. D. S. Evans (Dordrecht: Reidel), 283.
- McGimsey, B. G.; Smith, A. G.; Scott, R. L.; Leacock, R. J.; Edwards, P. L.; Hackney, R. L.; and Hackney, K. R. (1975). Astron. J. 80, 895.
- Penston, M. V. and Cannon, R. D. (1970). R. Obs. Bull. 159, 85.
- Pica, A. J.; Pollock, J. T.; Smith, A. G.; Leacock, R. J.; Edwards, P. L.; and Scott, R. L. (1980). Astron. J., 85, 1442.
- Pica, A. J.; Smith, A. G.; and Pollock, J. T. (1981). In preparation.
- Pollock, J. T.; Pica, A. J.; Smith, A. G.; Leacock, R. J.; Edwards, P. L.; and Scott, R. L. (1979). Astron. J. 84, 1658.
- Purgathofer, A. (1969). Lowell Obs. Bull. 1, 98.
- Sandage, A. (1965). Astrophys. J. 141, 1560.
- Sandage, A. (1970). Astrophys. J. 162, 841.

- Sandage, A. (1972). Astrophys. J. 178, 25.
- Sandage, A. and Luyten, W. (1967). Astrophys. J. 148, 767.
- Sandage, A. and Veron, P. (1965). Astrophys. J. 142, 412.
- Schmidt, M. (1963). Nature 197, 1040.
- Schmidt, M. (1974). Astrophys. J. 193, 509.
- Scott, R. L.; Leacock, R. J.; McGimsey, B. Q.; Smith, A. G.; Edwards, P. L.; Hackney, K. R.; and Hackney, R. L. (1976). Astron. J. 81, 7.
- Scott, R. L. and Smith, A. G. (1976). AAS Photo-Bull. 12, 6.
- Usher, P. D. (1975). Astrophys. J. Lett. 198, L57.
- Usher, P. D. (1978). Astrophys. J. 222, 40.
- Usher, P. D. and Mitchell, E. J. (1978). Astrophys. J. 222, 1.

BIOGRAPHICAL SKETCH

Patricia Louise Edwards was born September 22, 1949, in Richmond, Virginia. After her junior year in high school she took part in a NSF Summer Program in 1966. She graduated from Highland Springs High School in 1967. She received a Bachelor of Arts Degree in Physics from Carleton College in 1971. During this period she took summer classes at the University of Richmond (1968) and the University of Minnesota (1970).

She enrolled in graduate school at the University of Florida in the Department of Physics and Astronomy, receiving a Graduate School Fellowship, 1971-72. She held teaching assistantships, 1972-75 and 1976-77, and a research assistantship in 1975. In 1972 she was Secretary-Treasurer of the newly formed Florida Amateur Astronomical Society.

I certify that I have read this study and that in my opinion it conforms to acceptable standards of scholarly presentation and is fully adequate, in scope and quality, as a dissertation for the degree of Doctor of Philosophy.

Alex G. Smith

Dr. Alex G. Smith, Chairman
Professor of Astronomy

I certify that I have read this study and that in my opinion it conforms to acceptable standards of scholarly presentation and is fully adequate, in scope and quality, as a dissertation for the degree of Doctor of Philosophy.

Thomas D. Carr

Dr. Thomas D. Carr
Professor of Astronomy

I certify that I have read this study and that in my opinion it conforms to acceptable standards of scholarly presentation and is fully adequate, in scope and quality, as a dissertation for the degree of Doctor of Philosophy.

Howard L. Cohen

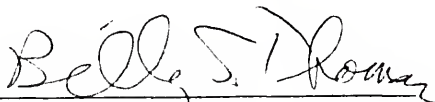
Dr. Howard L. Cohen
Associate Professor of Astronomy

I certify that I have read this study and that in my opinion it conforms to acceptable standards of scholarly presentation and is fully adequate, in scope and quality, as a dissertation for the degree of Doctor of Philosophy.

Guy C. Omer, Jr.

Dr. Guy C. Omer, Jr.
Professor of Astronomy

I certify that I have read this study and that in my opinion it conforms to acceptable standards of scholarly presentation and is fully adequate, in scope and quality, as a dissertation for the degree of Doctor of Philosophy.



Dr. Billy S. Thomas
Associate Professor of Physics

I certify that I have read this study and that in my opinion it conforms to acceptable standards of scholarly presentation and is fully adequate, in scope and quality, as a dissertation for the degree of Doctor of Philosophy.



Dr. Robert E. Wilson
Professor of Astronomy

This dissertation was submitted to the Graduate Faculty of the Department of Astronomy in the College of Liberal Arts and Sciences and to the Graduate Council, and was accepted as partial fulfillment of the requirements for the degree of Doctor of Philosophy.

March 1981

Dean, Graduate School

UNIVERSITY OF FLORIDA



3 1262 08553 1605